University of Naples Federico II

Department of Electrical Engineering and Information Technologies

Guido d'Alessandro

Ph.D. in Electrical Engineering

Enabling Technology for Wireless Power Transmission Supply to Remote Equipment in Critical Logistic Scenarios.

Tutor prof. Mauro D'Arco.

Table of Contents:

Introduction.

Electricity, in everyday society, has played and plays a key role in the development of mankind and of the entire planet, for as we know it today. Electricity contributed to the most important inventions and discoveries, marked progress and civilization, modifying, in its entirety, the idea and the structure of the social system in which we live, making it impossible to even imagine that, today, human society can do without employment and electricity use.

As a result, and with the evolution of technology, telecommunications have marked a step almost as important as the advent of electricity. Since the invention of the Telegraph, on wired systems, at first communications over the air without the use of wired infrastructure, as the first radio communications. Now, therefore, the possibility to remove hard links, referring to telecommunications, made perceive horizons of exploration, at the time and still today, unthinkable.

Think of the evolution that the Telegraph and radio have had, such as the mobile phone, television, current radio communications on the planet that interplanetary space. Wireless technology, today, is present in all areas of application. The reliability of such a solution is always growing and are innumerable domestic and industrial systems that use this technology.

Although it is natural to think of a data transfer system, free of physical links, appears much more difficult the idea that electrical energy can be transferred from one point to another without the need for connecting cables, but employing wireless systems, which, using different strategies, offer the possibility to transfer certain amounts of energy from one point to another more or less distant and with more or less efficiency, depending on the technology used.

Chapter 1: Transfer and storage of electrical energy.

Electricity is one of the most versatile forms of energy, prone to multiple applications. This is borne out by the evidence that electricity is used in a large number of applications and processes, ranging from domestic to industrial field. Electricity is used in households for the operation of household appliances, heating and cooling of rooms, leisure facilities and lighting. In the industry, electricity plays a key role, both in manufacturing plants, both in production plants. Today the car industry sees the growing use of electricity for traction purposes. This is evidenced by the increasing number and the entry into production of cars and hybrid vehicles, as well as totally electric vehicles.

Not to be forget the role that electricity reserve for lighting, whether for the home, both for architectural lighting, whether for public address. If focused on, in fact, the whole social system and the current state of the art is deeply and fundamentally linked to the use of electricity.

Although electricity is one of the most used forms of energy, it has a fundamental prerogative, which constrains the operating modalities relating thereto and the systems and infrastructure for it and developed.

Unlike other forms of energy, such as fossil fuels that can be used in motor systems, internal or external combustion, electricity storage is difficult. In other words, the storage or accumulation of electrical energy in special accumulators, simple case known as batteries, but in more complex systems like storage facilities such as pumping or basins, inertial systems of mechanical type, it is possible, but somewhat cumbersome and inconvenient in terms of performance and cost.

For this reason, electricity cannot be stored and must be consumed at the time of production. In other words, when a certain amount of electricity is produced, at the same time, it must be consumed, i.e., must be present at that precise moment that user needs. In other words, the production of electricity, moment

by moment, is tied to an electricity demand and is produced only after a request from a user or set of users who constitute the system load.

For this reason, the electric energy system of a country or a group of countries is considerably complex, and its management based on the planning, management and operation of the electrical system is a real discipline of electrical engineering. For this reason the transfer system of electricity is very complex and the distribution of electrical energy, from production to delivery to the end user, through a diversity of complex systems and equipment and highly sophisticated.

1.1 The electric energy in wireless critical logistic scenarios.

It is therefore necessary to have an electrical system that can produce, deliver, adapt and distribute electricity to a wide range of users, spread over a very wide and complex territory, such as that of a country or a nation, facing all the problems that may encounter, in the act of planning and realization of the wired systems that are needed.

In principle the system consists of electric power generation facilities from traditional sources, where the energy stored inside of raw materials, such as fossil fuels, recycled materials or nuclear fuels, is converted into thermal energy to be used inside special motor plant, to produce mechanical energy, which is suitably converted into electricity by means of electrical machines.

Additional electricity supply to the system is given by manufacturing plants from renewable sources, in which the energy stored inside of the wind, solar radiation, tides and geological gas is converted into electric power, through appropriate transformations. Finally there is the so-called accumulation energy, stored in the basins of production and pumping, in static accumulators and in rotating masses.

Such energy is adjusted, in terms of the electrical parameters, transmitted through electrical machines known as transformers, over long distances, and adapted to the different users, through to delivery, through the distribution

system, to the end user. All producing exactly energy demand, moment by moment. It is extremely clear that the inability to store the electricity involves a wide range of technical issues, widespread and debated. It is also evident that the need for wired systems for electricity transmission, involves a big burden, both in terms of accomplishment that in terms of Reconfigurability of the system.

Certainly, the latter, if intended for the transmission and distribution System implies a certain constraint, but if imagined for the small local system, begins to be much heavier. What is sure is that the possibility of reducing the wired systems and the ability to store energy so that they can be used in conditions easier is quite desirable.

In this work, that wants to collect the search path, a new technology is presented, which both in reference to some current and potential applications, both in relation to applications and scenarios, sets the stage for the reduction of wired systems in relation to the electricity transport, by facilitating the use of electrochemical devices such as batteries and storage sources. Surely, in reference to wired systems, relating to high-voltage electricity transmission, removal or reduction of physical infrastructure, would have an advantage, but it would be rather difficult, considering the involved powers, in the light of what you will be present in later chapters. As regards, however, the scope of the small powers, domestic and industrial applications of low power, the removal of infrastructure and physical connections appears obviously desirable, both in economic terms, both in practical terms, both in reference to the versatility and Reconfigurability of systems. Particularly in reference to that last attitude of systems, Reconfigurability of an apparatus is very welcome feature in the home, but even more so in reference to industrial and professional applications.

Chapter 2: Mutually Coupled Systems.

2.1 Coupled mode theory.

With CMT can be analyzed the exchange of energy between two resonating objects, as two resonant LC circuits. In this specific case means two resonant coils. Such a system is shown in Figure 2.1.

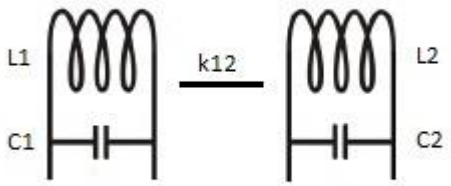

Figure 2.1: Resonant system made up of two mutually coupled LC circuits, and coupling factor k_{12}

Let be $a_1(t)$ and $a_2(t)$ the amplitudes of the fields applied to the coils, and expressed in the time domain. Labelled d_{12} the distance between the centers of two coils, the amplitudes of the fields applied can be expressed as follows.

$$\frac{da_1(t)}{dt} = -(j\omega + \Gamma_1)a_1(t) + jk_{12}a_2(t) + F_s(t) \tag{2.1}$$

$$\frac{da_2(t)}{dt} = -(j\omega + \Gamma_2 + \Gamma_L)a_2(t) + jk_{12}a_1(t) \tag{2.2}$$

where: ω è la pulsazione di risonanza delle due bobine.

ω is the resonance pulsation.

Γ_1, Γ_2 e Γ_L are reflection coefficients.

$F_s(t)$ is excitation applied at the first coil.

k_{12} is the coupling factor.

In steady state, and in the case of sinusoidal forcing $F_s(t) = A_s e^{-j\omega t}$, fields on two coils have a sinusoidal shape, $a_1(t) = A_1 e^{-j\omega t}$ and $a_2(t) = A_2 e^{-j\omega t}$.

It is possible to obtain the ratio of the amplitudes of two sinusoids from the equation below.

$$\frac{A_2}{A_1} = \frac{jk_{12}}{\Gamma_2 + \Gamma_L} \tag{2.3}$$

Now can be calculated the power absorbed by the coils and the power transferred to the load. These are respectively $P_1 = 2\Gamma_1 |A_1|^2$, $P_2 = 2\Gamma_2 |A_2|^2$, $P_L = 2\Gamma_L |A_2|^2$. Neglecting the power wasted in the near field the total power, PTOT is the sum of these three contributions and the efficiency of power transfer, for a 2 coils system, is given by (2.4).

$$\eta_2 = \frac{P_L}{P_{TOT}} = \frac{1}{1 + \frac{\Gamma_2}{\Gamma_L}\left[1 + \frac{k_{12}}{\sqrt{\Gamma_1 \Gamma_2}}\left(1 + \frac{\Gamma_L}{\Gamma_2}\right)^2\right]} \tag{2.4}$$

The equations for a pair of coils can be extended to the case of m coils, where all resonate at the same frequency. The first of the m coils is fed by a source, the last feeding the load. For simplicity is neglected the coupling between not neighboring coils. The amplitudes of the fields, in the time domain, on each coil, is expressed in (2.5).

$$\frac{da_i(t)}{dt} = -(j\omega + \Gamma_i) a_i(t) + jk_{i-1,i} a_{i-1(t)} + jk_{i,i+1} a_{i+1}(t) \tag{2.5}$$

The (10) is applied for fields on all coils except the first and last, that can be calculated using the (2.1) and (2.6).

$$\frac{da_m(t)}{dt} = -(j\omega + \Gamma_m + \Gamma_L)a_m(t) + jk_{m-1,m}a_{m-1}(t) \tag{2.6}$$

If a sinusoidal input signal is applied, as in the case of two coils, the amplitudes of the fields can be considered as $a_i(t) = A_i e^{-j\omega t}$. Similarly to the case of two coils, combining previous relation is obtained:

$$\begin{aligned} &\Gamma_i A_i - jk_{i-1,i}A_{i-1} - jk_{i,i+1}A_{i+1} = 0 \\ &(\Gamma_m + \Gamma_L)A_m - jk_{m-1,m}A_{m-1} = 0 \end{aligned} \tag{2.7),(2.8}$$

Solving these equations are calculated all the values A_i and from these we get the power on the various coils. The power absorbed by the i-th coil is $P_i = 2\Gamma_i |A_i|^2$, the power transferred to the load it is $P_L = 2\Gamma_L |A_L|^2$, and the total power will therefore be $P_{TOT} = \sum_{i=1..m} P_i + P_L$. Therefore the efficiency for a system of m reels can be expressed as in (2.9).

$$\eta_m = \frac{P_L}{P_{TOT}} = \frac{2\Gamma_i |A_m|^2}{\sum_{i=1..m} 2\Gamma_i |A_i|^2 + 2\Gamma_L |A_m|^2} = \frac{\Gamma_L}{\sum_{i=1..m-1} \Gamma_i \frac{|A_i|^2}{|A_m|^2} + \Gamma_m + \Gamma_L} \tag{2.9}$$

Is now analyzed the case of a power transfer system consisting of 4 coils, Fig. 2.2. The coils L_2 and L_3 are the real responsible for the power transmission, whereas the coil L_1 and L_4, of minor radius, are used for the impedances adaptation and are coplanar to L_2 and L_3.

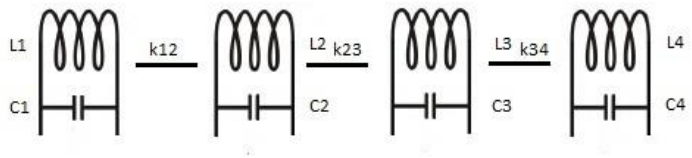

Figure 2.2 Resonant system made up of four mutually coupled LC circuits, and three coupling factor k_{ij}

For equation (2.7) and (2.8), for m = 4, is possible to determine A_1, A_2 e A_3 functioning of A_4:

$$\frac{A_3}{A_4} = \frac{\Gamma_4 + \Gamma_L}{jk_{34}} \tag{2.10}$$

$$\frac{A_2}{A_4} = \frac{\Gamma_3(\Gamma_4 + \Gamma_L) + k_{34}^2}{k_{34}k_{23}} \tag{2.11}$$

$$\frac{A_1}{A_4} = -\frac{\Gamma_2\Gamma_3(\Gamma_4 + \Gamma_L) + k_{34}^2\Gamma_2 + k_{23}^2(\Gamma_4 + \Gamma_L)}{jk_{12}k_{23}k_{34}} \tag{2.12}$$

In this analysis it was considered only the coupling between adjacent coils while were neglected the coefficients k_{13}, k_{14}, k_{24} relating to non-adjacent coils. If the distance d_{23} is not too small, this is a good approximation. Locate the amplitudes of the fields, you can evaluate the performance of the connection, combining (2.10), (2.11) and (2.12) with (2.9), obtaining (2.13).

$$\begin{cases} \eta_4 = \dfrac{k_{12}^2 k_{23}^2 k_{34}^2 \Gamma_L}{DEN} \\ DEN = \Gamma_1\left[\Gamma_2\Gamma_3(\Gamma_4 + \Gamma_L) + k_{34}^2\Gamma_2 + k_{23}^2(\Gamma_4 + \Gamma_L)\right]^2 + k_{12}^2\Gamma_2\left[k_{34}^2\Gamma_3(\Gamma_4 + \Gamma_L)\right]^2 + \\ + k_{12}^2 k_{23}^2\Gamma_3(\Gamma_4 + \Gamma_L)^2 + k_{12}^2 k_{23}^2 k_{34}^2(\Gamma_4 + \Gamma_L) \end{cases} \tag{2.13}$$

2.2 Reflected Load Theory.

In this case, is examined the condition of two resonant coils. In the following a four coil setup is considered. A two coils system can be modelled as shown in Figure 2.3. The two LC circuits must be tuned at the same resonate frequency.

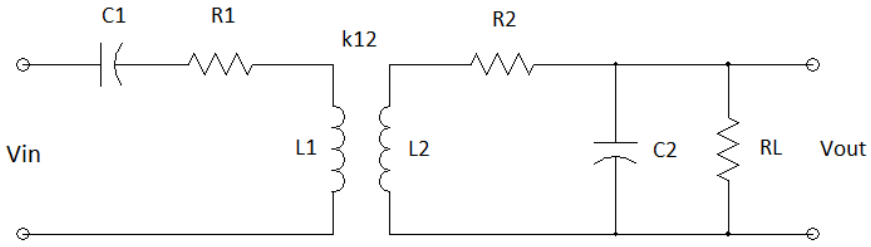

Figure 2.3: circuit diagram of a two coils resonant system.

The parameters that affect the performance are the coupling coefficient, k_{12}, and merit factors Q_1 and Q_2. According to the RLT the second circuit is reflected, which is connected to the load R_L, on first getting a circuit as shown in Figure 2.4. The parameters of this new equivalent circuit are calculated in (2.14) and (2.15).

$$R_{ref} = k_{12}^2 \left(\frac{L_1}{L_2} \right) R_p = k_{12}^2 \omega L_1 Q_{2L} \tag{2.14}$$

$$C_{ref} = \left(\frac{L_2}{L_1} \right) \left(\frac{C_2}{k_{12}^2} \right) = \frac{1}{\omega^2 L_1 k_{12}^2} \tag{2.15}$$

where: $R_{p2} = \frac{Q_2^2}{R_2}$, $R_p = \frac{R_{p2}}{R_L}$, $Q_{2L} = \frac{R_p}{\omega L_2}$

At the resonant frequency, C_{ref} resonates with $k_{12}^2 L_1$, $k_{12}^2 L_1$ resonates with C_1. Therefore, all incoming power is divided between R_1 and R_{ref}. Then, for the calculation of efficiency, the equivalent circuit to consider is the one shown in Figure 2.5.

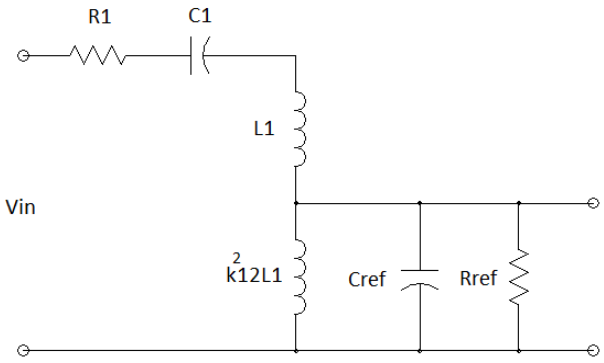

Figura 2.4: circuito equivalente tramite RLT

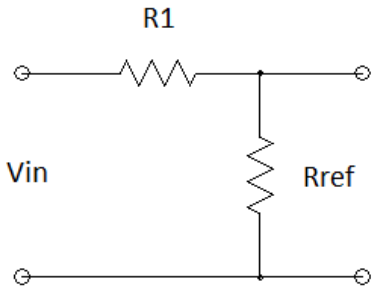

Figura 2.5: equivalent circuit while resonace mode is enabled.

The power absorbed by R_1 is dissipated as heat from the first coil. The power supplied to R_{ref}, i.e. the power transferred to the second coil, is shared between R_2 and R_L. The efficiency of the link can then be calculated with the help of the (2.16).

$$\eta_{12} = \frac{R_{ref}}{R_1 + R_{ref}} \frac{R_{p2}}{R_{p2} + R_L} = \frac{k_{12}^2 Q_1 Q_{2L}}{1 + k_{12}^2 Q_1 Q_{2L}} \frac{Q_{2L}}{Q_L} \qquad (2.16)$$

where: $Q_L = \frac{R_L}{\omega L_2}$, $Q_{2L} = \frac{Q_2 Q_L}{Q_2 + Q_L}$

If instead of having only two coils a system consisting of m coils is analyzed, the reflex load to the coil *i + 1* to the coil *i*, can be calculated by the Formula (2.17).

$$R_{refi,i+1} = k_{i,i+1}^2 \omega L_i Q_{(i+1)L} \qquad \text{con } i=1\ldots m-1 \tag{2.17}$$

Where $k_{i,i+1}$ is the coupling coefficient between windings *i* and *i + 1*, while $Q_{(i+1)L}$ is the quality factor of the load on the coil *i + 1*, and can be estimated (2.18).

$$Q_{iL} = \frac{\omega L_i}{R_i + R_{refi,i+1}} = \frac{Q_i}{1 + k_{i,i+1}^2 Q_i Q_{(i+1)L}} \qquad i=1\ldots m-1 \tag{2.18}$$

For the calculation of the quality factor of the load on the last coil which is connected in series with the load R_L is used instead (2.19).

$$Q_{mL} = \frac{\omega L_m}{R_m + R_L} \tag{2.19}$$

Determined the load values reflected on the coils, and quality factors, ignoring the inductive coupling between non-adjacent coils, the efficiency of the connection between the *i-th* coil and coil *(i + 1)-th* is obtained by (2.20).

$$\eta_{i,i+1} = \frac{R_{refi,i+1}}{R_i + R_{refi,i+1}} = \frac{k_{i,i+1}^2 Q_i Q_{(i+1)L}}{1 + k_{i,i+1}^2 Q_i Q_{(i+1)L}} \tag{2.20}$$

Therefore, the total power transfer efficiency, for a system with m coils, is obtained operating the product between the relative contributions to individual links and the term $\frac{Q_{mL}}{Q_L}$ as shown in (2.21).

$$\eta_{m-bobine} = \prod_{i=1}^{m-1} \eta_{i,i+1} \frac{Q_{mL}}{Q_L} \tag{2.21}$$

Therefore, the efficiency of an induction power transmission system, made of four resonant coils, Figure 2.6, through the RLT is calculated from (2.20) and (2.21). Again, this was ignored the coupling between the coils, and the result is shown by means of (2.22).

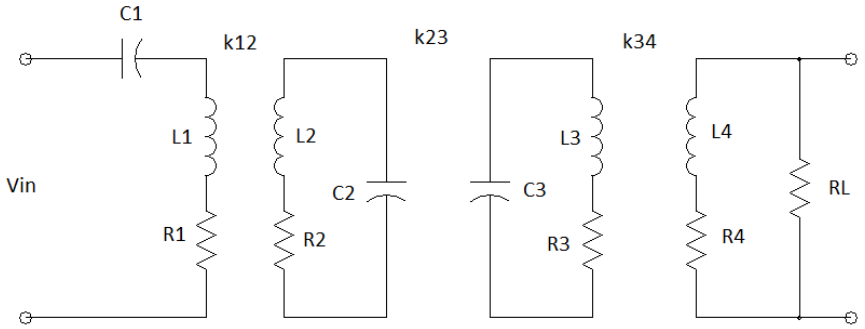

Figure 2.6: circuit diagram of a four coil resonant system.

$$\begin{cases} \eta_4 = \dfrac{N}{D}\dfrac{Q_{4L}}{Q_L} \\ N = \left(k_{12}^2 Q_1 Q_2\right)\left(k_{23}^2 Q_2 Q_3\right)\left(k_{34}^2 Q_3 Q_{4L}\right) \\ D = \left[\left(1+k_{12}^2 Q_1 Q_2\right)\left(1+k_{34}^2 Q_3 Q_{4L}\right)+k_{23}^2 Q_2 Q_3\right]\left[1+k_{23}^2 Q_2 Q_3+k_{34}^2 Q_3 Q_{4L}\right] \end{cases} \quad (2.22)$$

Chapter 3: State of the art of WPT technology.

The transmission of power or energy without the use of physical links, is the transmission of electricity from one source to one or more loads without the use of power cables or without the use of any type of physical structure both in small or long distances.

Although today the term wireless is very used in the communications sector, where the system of information transfer, more and more consolidated and becomes reliable, energy transmission, however, differs from simple wireless data communication, whereby signals need only maintain a high enough power to save itself intelligible, because the main purpose is established instead on high efficiency and integrity of the message exchanged. Consequently also systems and technology adopted are really different one each other.

As we learn from the scientific literature on the subject, the first experiments were conducted in the second half of the last century. If you stop to reflect with some attention, wireless technology was conceived some time ago.

The first who began to imagine that energy could theoretically be sent in free space, was the mathematical physicist James Clerk Maxwell, the author of the equations still at the base of the studies on electromagnetism, in his "Treatise on Electricity and Magnetism" of 1873.

The first to make a real project, at the beginning of the 20th century, was Nikola Tesla, the brilliant scientist responsible for Polyphase electricity system still in use. The ambitious and pioneering Tesla project consisted of a system that would allow to send energy on a global scale, but it never find fulfillment for lack of funds and to the technological limitations of the time.

As is often the case with regard to technological progress and to the advancement of scientific research, the main motive which gave rise to the first steps in development and application of wireless power transmission technology, was the war. Leading the most ambitious and most expensive

experiments belong to the period of World War II, during which has been explored mainly the approach involving microwaves as a vehicle of transmission.

In the past, three main approaches to transmit power without cable connections have been investigated. The first one exploits inductive principles whereas the second one relies on the use of microwave channels, the last experienced and the third approach recurs to laser beam technology.

The approach based on inductive principles employs a couple consisting of a source and a receiving station. The whole system can nearly be considered an air-gap transformer, where the primary circuit is into the source and the secondary circuit into the receiving station. The two circuits, essentially two windings, are electromagnetically coupled to each other; the effectiveness of the coupling largely depend on their mutual distance: it is weak when the circuits are at a distance, while becomes relevant when they approach each other. The power transfer becomes effective when the distance between source and receiving stations allows a relevant coupling. This technology is characterized by low power transfers, low efficiency at high distances but very high efficiency for narrow coverage, and short distance coverage. It is typically employed in portable devices battery charging applications, or home applications in which the coupling is obtained throughout an air-gap standing between sources and receivers which can be movable within a small area. The second approach pays attention to high power and long distances transmission. It has been considered in the scientific literature since the second half of the last century and goes under the name of wireless power transmission (WPT).

Research in this field have been abandoned until 1964, when, thanks to developments achieved in the field of microwave and wireless communication, after several years of studies the engineer William C. Brown, completed a project where was developed a mini helicopter powered by means of a radiative technology. Although this, the system cost prohibitive and appeared impractical, in order to be used in common applications. Brown continued however

searching until, in 1994, they 30 kW of power were transferred at more than a kilometer away, with an efficiency of 84%.

The generation system was formed by a magnetron coupled to a parabolic antenna that concentrated the necessary energy in a microwave beam. The transmitted energy was received by an on board rectenna array, working both as a receiving antenna and a rectifier to convert the microwave power to DC power. Since that experience, it was understood that the crucial element of the system was the rectenna.

Between 1969 and 1974 at the NASA's Marshall Space Craft Center a series of experiments were conducted with the aim of producing an extremely light rectenna to be used in space station in low earth orbit. The most interesting result of that series of experiments was the realization of a high efficiency rectenna, which allowed the set-up of a DC to DC transmission system with an overall efficiency of 26%.

Successively the efficiency of the rectenna was also improved by placing the rectenna elements closer to each other and by using a Gaussian beam horn to keep the transmitted power focused upon the rectenna itself. The overall DC to DC efficiency was increased up to 39%. Up to 1975 the use of vacuum tubes, although specifically designed for WPT applications, kept the overall performance of the system still rather lower than the expectations. A huge step was therefore made when Schottky barrier diode rectifiers were deployed to reach an overall DC to DC efficiency equal to 48%. However, even if solid state components have definitely replaced high-frequency vacuum tubes, the rectenna is still the bottleneck for the system performance.

Another milestone is represented by the demonstration project carried out in 1975 in the Mojave desert at JPL's Goldstone Facility. It consisted in the transmission of 30 kW power over a distance of 1600 meters; for this demonstration a 4x7 meters rectenna was used. This was one of the most important experiments realized up to now both in terms of transferred power and covered distance.

Further advancements were obtained in 1983 when for the first time in WPT context the thin-film technology was used to realize a high-efficiency reduced-size low-weight rectenna. The rectenna was attached to a 1.2 m experimental airplane wing. In fact, this type of antenna, thanks to the small size and weight, much lower than that of the previous dipole antennas, and to the superior robustness and reliability, could be mounted on aircrafts or space vehicles surfaces.

In 1991 a microwave power rover was powered by a 3 kW source operating at 5.86 GHz; 500 W DC was recovered to operate the test device.

In 1994 near Osaka, Japan, Prof. Kaya of Kobe University conducted its first ground to ground test transmitting 10 kW power at 2.45 GHz.

In 1995, an additional experiment was conducted at Kobe where a small helicopter flying at 50 meters of altitude was powered through a 10 kW parabolic antenna operating at 2.43 GHz frequency; the helicopter hosted a rectenna over the airship.

In 2007 an off-road, microwave powered demonstration vehicle was developed by Kyoto University. The system worked at 2.45 GHz and was driven by a 26 W 24 V DC motor.

In 2008 in Hawaii a long distance low power transmission experiment was conducted. The point to point distance was about 148 km and the test frequency chosen was 2.45 GHz. Anyway, up to now, the research and development efforts of the last decades have not triggered many prototyping actions, therefore the state-of-art induction WPT technologies are still far from pervading service applications.

3.1: The available technologies.

At present, some pioneering applications of energy transmission by means of inductive coupling and WPT, still at prototype stage, can be found in home automation or power sensor networks scenarios, in which cable connections are avoided.

At the present, the main attention is dedicated to two relevant applications in which energy is transmitted from sources to equipment deployed in rooms, areas, or territories where physical connections to energy sources are unfeasible or not convenient . Sometimes there is a strong need to avoid the disposal of cables or time constraints impede to wait for setting up a connection to the nearest power grid, and the deployment of a mobile local power source to be used as electrical generator is not possible.

With more emphasis to wireless measurement stations and similar applications, the first application consists in the total removal of cables needed both to power-on and control measuring instrumentation and sensors. Induction or radiative wireless power transmission can simplify both test configuration and improve its effectiveness by avoiding the problems related to cable intersections. In the practice, cable intersections significantly slow down the initial configuration of measurement stations as well as the running of the test; sometimes they are even responsible of more undesired effects compromising the outcomes of the test. Moreover cable connection may be an obstacle and prevent the control of climatic rooms in which measurement operations are performed, as well as, whenever they do not compromise the control of the environment itself, they can make the wiring operations extremely complex and expensive.

The second application consists in supplying remote equipment hosting diagnostic devices to perform periodical auto-test operations. Such equipment are often located in high critically places, and supplying them appears a non-trivial task, for which it is necessary to establish a point to point long distance and high power microwave connection channel [8]. In

particular, shelters hosting measurement stations that are located at a distance of about 10 km from the power source and need less than 100 kW, are considered. The shelter also houses the staff needed for its use, which includes the common energy services such as lighting and air-conditioning.

3.2 Induction Technology.

Mutual coupling mechanisms have been intensively studied in the past and are the basic operation principle of the power transformers utilized in the transmission and distribution energy networks.

Transformers can be described as static electrical machines that perform power transmission upon very short distances between a primary and a secondary circuit, fig 3.1. The primary circuit produces a magnetic flux by injecting current into a winding; the flux is concatenated by a second winding, which is part of the secondary circuit, that reacts producing an opposite magnetic flux. A ferromagnetic core bounds the magnetic flux within a limited volume, thus making the amount of dispersed flux negligible. This structural arrangement grants perfect coupling between the primary and secondary circuit, and assures very high efficiency values in power transmission, which for very large size transformers are superior to 99%. If the ferromagnetic core would be removed and the primary and secondary windings moved faraway form each other, the efficiency of the electrical system would be significantly lowered. Nonetheless, sufficient power could still be transmitted to the secondary circuit by increasing the current intensity in the primary winding, and admitting that only a part of the available power would be really picked up by the secondary circuit. Such a system is the kind of wireless power transmission system based on a magnetic induction approach that is nowadays gaining more and more attention.

In particular, relevant efforts are today oriented at improving the overall efficiency of magnetically coupled WPT systems, by employing resonant structures in place of transformers' windings. Specifically, LC structures characterized by identical resonant frequencies are formed by connecting a capacitor to each winding. The strength of the magnetic field produced by the primary circuit, which assures the power transmission, is thus improved thanks to the high intensity reactive currents that are not derived from the primary source, but are exchanged between inductors and capacitors. The connection to the grid is necessary to compensate both the power consumption due to the

absorption of the secondary circuit, typically connected to a power demanding load, and the losses of the non-ideal system components. It is worth noting that the possibility of non-intentional parasitic absorption by other systems is very unlikely because, in nature, except for ferromagnetic or dissipative loop-shaped objects, there are no widespread systems that can couple to magnetic sources. Moreover, the secondary circuit has to be finely tuned to the same oscillating frequency of the primary circuit; solutions that realize self-tuning systems should be considered when there is no control of the geometry of the system and its position in the environment, which as well known has a relevant impact on the resonant frequency of the system.

Induction technology is intended to serve in domestic or industrial environments. Typical low power applications involve sensor networks, which can be ordinarily located in areas more or less crowded by people.

For modern companies that need to dynamically reorganize their own departments, the inherent flexibility of the induction technology at supplying electrical facilities, as well as measurement and control equipment, appears very attractive.

The chief limit of the induction technology consists in the dependence of the power amount that can be transferred on the distance between source and load: poor coupling prevent form high power transfer. In other terms, the transmission efficiency strongly depends on the distance, geometry, and materials that surround the source and load.

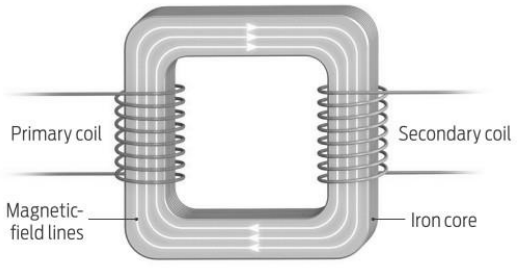

Fig.3.1: Schematic illustration of an electromagnetic transformer. Primary and secondary windings around a guiding structure for this stream are shown.

To improve the transmission efficiency, resonance coupled transformers are normally used. They are typically realized with the insertion of series or parallel capacitors within the primary and secondary windings of the air-gap transformer. In this way, the primary and secondary windings, that play the role of transmitting and receiving coils, actually act as a system made up of mutually coupled LRC circuits tuned at a resonant frequency. Fig. 3.2 shows a block diagram of an induction power transmission system.

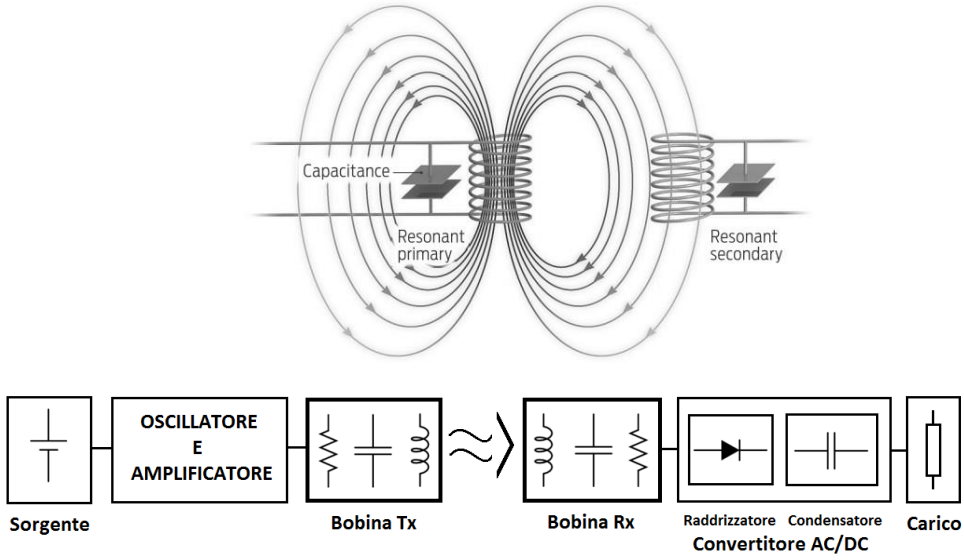

Fig. 3.2: resonant inductive system for wireless power transmission. At the top, the resonant transformer stripped of ferromagnetic core and by adding of capacitors. At the bottom a block diagram.

The induction technology, could be applied in somespecific applications where the electromagnetic coupling between source and load can be ensured in a very reliable way and with small air gaps. One possible application of power induction technology appears to be the battery charging of electric vehicles. For such application an high instantaneous power transfer is requested. The primary winding position can take place in special platforms in parking areas or stop

charging services, while the secondary winding, equipped with the necessary power electronics and control circuitry, on the vehicle itself.

In order to transfer energy on the base of an electromagnetic induction principle the coils should be set at a distance which is less than a third of the field wavelength: the attention has in fact to be paid mainly to the near-field magnetic component than to the far-field electrical one.

Therefore, given the distance at which the power has to be transferred, a first estimation of the operating frequency can be performed using equation (3.1)

$$f = \frac{c}{\lambda} \tag{3.1}$$

where c is the light speed and λ the wavelength. Frequencies in the range of units of MHz are adequate to transfer power in the range of some meters. The electrical parameters constituting the *LRC* system have to satisfy the constraints given as specifications at the design stage both in terms of resonance frequency f, and merit factor Q; the latter is related to the frequency-selectivity of the system. For an *LRC* system, the aforementioned quantities are given by equations (3.2) and (3.3):

$$f = \frac{1}{2\pi\sqrt{LC}} \tag{3.2}$$

$$Q = \frac{1}{R}\sqrt{\frac{L}{C}} \tag{3.3}$$

Unfortunately the accurate value of the parameters equivalent to R, C and L in (3.2) and (3.3) is not straightforward, since it involves a thorough study of the geometry of the system, in terms of coils sizes and distance between them. In the practical implementations, it is usually preferred to have the possibility of performing adjustments by means of suitable controls and accurately refine the tuning according to the needs. In fact, the results obtained at the design stage could be unreliable since the influence of the environment hosting the system as

well as the knowledge about the values of the parasitic effects is never sufficiently accurate. Furthermore, due to the very high reactive currents that usually take place in *LRC* circuits at resonance, the cross-section of the coils conductors, above all of the transmitting coil, have to be correctly chosen. Actually, if an RF operating frequency is adopted, the use of copper tubes rather than massive conductors is convenient to save materials and costs: the current density is negligible in the core of a massive conductor because of the skin effect. Similarly, the choice of the capacitors is connected to the issues related to high currents and frequency. The power source of the system can be a classic Colpitts or Hartley oscillator including an appropriate amplifier. Moreover resonant zero voltage switching ZVS and resonant zero current switching ZCS push pull inverter can be used to pilot the front end primary coil. To ensure that the energy collected by the receiver coil is adequate to power-on ordinary facilities, a first AC/DC conversion is necessary. If the load requires a secondary DC/AC conversion, an inverter has to be deployed. The rectifier stage appears to be the more critical of the two conversion stages, since it has to work at RF frequencies, and could require the employment of fast Schottky diodes.

3.3 Radiative Technology:

Pioneering WPT applications are much less than those recognized for induction technology. In fact, the deployment of WPT appliances needs a meticulous study of several items involving the power source, the transmitting devices, the microwave link features, which impact on the selection of the frequency band, and the receiving apparatus, made up of

antenna and power conversion equipment.

A pilot action can be the design and implementation of a small-scale experiment to perform microwave energy transmission from a radiating source to a receiver, and to convert microwave energy to low frequency energy, according to the requirements of the equipment to be supplied. The basic elements to be designed and assembled are: a microwave source, a high-directivity transmitting

antenna, a rectifying antenna (rectenna) made up of an antenna and a rectifier stage capable of functioning at microwave frequencies. In the following several details related to the necessary step that lead to a WPT experimental set-up are discussed. Concerning the power source, different types of microwave sources, such as magnetron, klystron and gyrotron, are available. For resonant cavity magnetron microwave generators consolidated design methodologies exist, and commercial solutions can be found on the market. High power microwave sources can be realized by deploying an array of magnetrons, to be suitably designed and implemented.

In the experimental setup it would be convenient to have a variable frequency microwave source to facilitate tuning operations and optimize the choice of the system operating frequency; standard resonant cavity sources unfortunately do not easy allow this kind of operation.

The field generated by the magnetron must be routed to a high directivity parabolic reflector by means of a waveguide horn antenna. The use of a parabolic reflector is necessary because horn antennas are not capable of ensuring sufficient directivity to confine the microwave energy in a collimated beam; power leakage would be in contrast to safety of persons and could also cause electromagnetic compatibility issues for sensitive equipment in the vicinity.

Also in point to point long distance transmission applications an extremely collimated beam able to concentrate the microwave energy in a focused receiving area is important.

The beam should have a power density as uniform as possible, starting from its center to the outer periphery, so as to optimize the receiving elements array. The main issue is containing the electromagnetic power dispersion as much as possible, avoiding above all the reflections by the same rectenna. The greatest difficulties in the realization of a microwave

power link is the conversion of the microwave energy stored in the high frequency field in a form usable for power supply applications. It is required that

the microwave energy is collected by a receiving antenna and converted to DC power, or, at least, at a frequency that will permit the energy transit into a common electrical cable. The device which performs this function takes the name of rectenna. A rectenna design that takes into account aspects such as the conversion efficiency, the overall dimensions of the device and its weight, is necessary. The need to reduce size and weight is very critical when the devices must find place on airship, or in space applications such as photovoltaic geostationary orbiting stations. The design includes custom realization of several devices: an array of in-air or thin-film integrated dipole antenna, a matching network, fast Schottky diodes rectifiers, capacitive filters, and so on. Parallelization is a key concept to make high power handle feasible.

In particular, a rectenna is essentially composed by an antenna and a static energy conversion stage. There are two different types of antenna that could be used: the dipolar type and the printed circuit board thin film type. It is remarkable that the power density that can be obtained from a single element of an array antenna is quite poor; hence large dimensions for the detector device are necessary, which represent a limiting factor in applications where size and weight play a fundamental role. Furthermore, in the case of high power microwave links the receiving equipment occupies a large area: every single dipolar item is accompained by a matching network and a rectifier stage. Although the first does not present special features, the rectifier stage appears quite delicate, in relation to the high frequency values. For this reason, the optimal choice of the Schottky type rectifier diode, in terms of final performance, is a key point. In terms of alignment, the rectenna array does not bring any problems because each individual array element has a DC power output, so no phase offset problems occur.

Concerning the frequency choice, a lower frequency limit can be considered the value 1 GHz. In theory, as regards the upper limit, it would be possible to use even optical or low infrared frequencies. Since the characteristics size of the devices is proportional to the wavelength of the radiated power, and

interconnections between space stations orbiting into vacuum, benefit from very short wavelength because propagation undergoes minimal losses, the choice of very high frequencies seems preferable.

On the counterpart, the physical realization of micrometer antennas is very difficult, and in the presence of a transmission means, such as the atmosphere, the propagation at lower frequencies is more convenient: the Friis equation shows in fact that the power received by an antenna, P_r, is directly proportional to the square of the wavelength, λ, while it is inversely proportional to the square of the distance, R, between transmitter and receiver according to equation (3.4).

$$P_r = P_t G_t G_r \left(\frac{\lambda}{4\pi r} \right)^2 \tag{3.4}$$

where G_t, and G_r, are respectively the transmitting and receiving gains.

The frequency considered for pilot experiments involving point to point connections through the atmosphere should be in the frequency interval between 2 and 3 GHz, which is the best compromise between the attenuation phenomena and the size of the antennas.

In the perspective of microwave links between orbiting stations or solar factory orbiting station links, higher operating frequency between 30 and 35 GHz are more appropriate, since the atmosphere exhibits a notch for the absorption rate at those frequencies.

More complex appears the frequency selection item in case of links connecting orbiting stations and ground equipment were the items of size and weight reduction and the presence of the atmosphere have to be considered.

Power transmission by means of induction or energy radiation mechanisms can be hazardous to people, flora and fauna, and can lead to failure or malfunctioning susceptible equipment.

The bio-effects of electric and magnetic fields can be classified as thermal and non-thermal. Thermal effects are associated with the absorption of the energy

contained in the magnetic field, dissipated in the form of heat, by the tissues and organs. With regard to these effects the organs most affected are the least vascularized, such as the lens.

As regards the non-thermal effects, research has hypothesized that long-term effects can be reported on the nervous system and possible mutations could involve the cells; in particular an increased permeability of the cell membrane could appear.

Still at the level of assumption, some studies have been started to demonstrate a potential change to the cardiovascular system.

Current researches are aimed at demonstrating effects on the behavior and/or damages for the orientation ability of people and animals in the presence of microwave and radiofrequency fields. There is a suspect that prolonged exposure to electric and magnetic fields alters the cognitive abilities of some insects or birds.

In case of long distance connections by a microwave link, the effects upon birds that could be wounded by the high energy beam, have to be taken into account. On the other hand their passage might cause problems on the microwave channel link; acoustic countermeasures could be considered to deter birds from flying in that zone.

Similarly the case of an aircraft crossing the microwave beam, which is not easy detectable, should not be jeopardized. It would be advisable to visually delineate the presence of the beam with suitably prepared laser signals. At the same time having a radar system that intercepts the presence of approaching aircrafts and, in case of danger, interrupts the microwave transmission, also seems to be an interesting solution, even if such a strategy would still require an auxiliary uninterruptible power supply for critical loads.

3.4 *Laser Technology:*

The principle of operation of a power transmission system using laser is very similar to that of solar power plants used for the conversion of stored energy in

solar radiation into electrical energy, converting it through photovoltaic panels. In this case, however, the energy is transmitted in the form of laser light, monochromatic and coherent, to photovoltaic panels optimized for the particular wavelength used. Laser light is much more intense than that of the Sun, and is collimated into a narrow beam. Can be transmitted in the desired direction, covering long distances due to the narrowness of the beam and the high collimation, which allow even a concentration of energy and more security than the microwave. Moreover, unlike the latter, the risk of interference with electronic equipment and radio waves is minimal.

The system uses an energy source and converts it into monochromatic light via laser diode arrays. The beam can be shaped by optical mirrors and directed towards the photovoltaic cells or the receiver photodiode. The latter deal with the conversion of optical energy into electricity, to be supplied to the devices to power, preferably by converters and power regulators.

To ensure proper functionality and safety of the system, it is appropriate to foresee the inclusion of thermal heat sinks and sensor with control circuits, especially for long distance applications. The sensors are meant to detect foreign objects that block the beam transmitted and allow the immediate shutdown of laser diodes. Connection and tuning between transmitter and receiver can be adjusted via the main laser.

Heat sinks are important because the lasers and photovoltaic panels are sensitive to changes in temperature, so heat accumulation is likely to seriously affect the efficiency of the whole system. Fig 3.3 shows, in principle, a transmission system using optical technology.

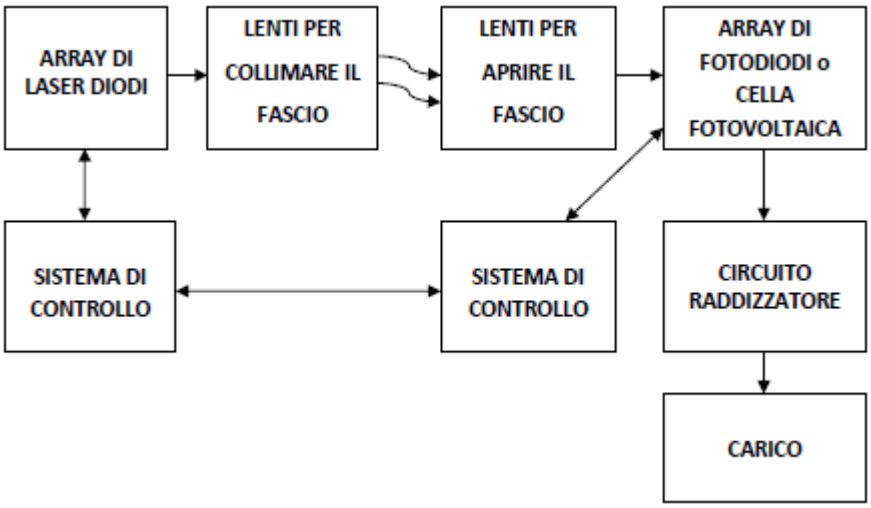

Fig.3.3: Diagram of a wireless power transmission system that uses optical technology, through the use of laser diodes, as transmission components and photodiodes or photovoltaic cells, as receive organs.

3.5 Main goal of the research activity:

The main issues of this work is to investigate and obtain results related to the delivery of appliances supplied by means of induction or radiation and optical mechanisms.

From the analysis of the possibility and feasibility, it is mainly chosen to investigate the inductive technology and specifically, the resonant one. This is because the technology is the most versatile in reference to light duty applications, with no excessive distances. On the other account, given the frequencies involved, appears easier prototyping and experimental uses of technology, without the need of special precautions. The same applies with regard to test environments and equipment necessary. Future pilot experiments aimed at strengthen wireless power transmission technologies have also been envisaged.

The main goal of the research activities is exploring solutions to make battery-less equipment operate in wastelands or desert zones in which connections to the grid are unreliable or missing, or in situations in which the main grid is intentionally shut down. Oppure applicazioni per le quali la possibilità di non

dover ricorrere a sistemi cablati o quanto meno, dotati di backup batteries appare auspicabile.

The motivations of the work have to be found in the problems experienced in supplying equipment employed in critical scenarios in which on-site powering is precarious or unreliable.

The advancement in WPT technologies would give the possibility of supplying also installations like measurement stations for which the realization of a physical connection would be costly in terms of time, or could represent an obstacle for the same measurement purpose, thereby affecting the measurement outcome. For this type of application much lower power and distance as tens of meters and few power is required.

Mature technologies solution would have relevant side effects.

For instance, they could offer the possibility of removing all cables both needed to supply instrumentation and equipment under test, and to connect instruments and equipment between each other as required by the test. In particular test conditions, in which cable intersections could

compromise the operation of the measurement task, or slow down the pre-arranged configuration, the aforementioned possibility is greatly valued.

Chapter 4: Resonant wireless power transmission technology.

The induction mechanism is the prevalent magnetic phenomenon observed in the presence of low frequency field variations, whereas it becomes very feeble at radio frequencies. In fact, induction systems rely on the magnetic component of a quasi-evanescent but not radiating field.

The coupling can be realized by means of coils of size comparable to the wavelength of the induction field. The operating frequencies can be between 10 kHz and 1 MHz, which are typical of circuits including coil inductors. The distance at which the power can be transmitted is a function of several parameters, some of which are related to the geometry, mutual position, and consistency of the coils, such as radius, mutual distance, alignment, number of turns, others depend on the circuitry parameters such as inductance and capacitance values.

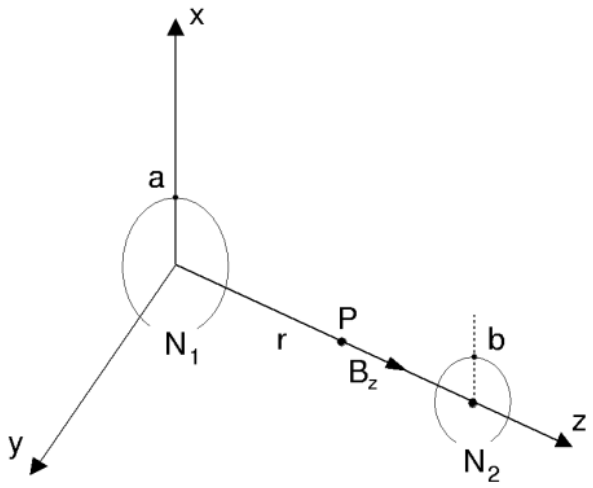

In formulas, the field produced by a planar coil with radius *a* at a distance *r*, is characterized by a normal component to the plane of the coil given by:

$$B_z = \frac{\mu_0 I_1 N_1 a^2}{2\sqrt{\left(a^2 + r^2\right)^3}} \tag{4.1}$$

where μ_0 is the magnetic permittivity of the vacuum, I_1 is the *rms* value of the electrical current in the coil, N_1 the number of turns, and *r* is the distance from the plane hosting the coil measured along the axis of the coil. Equation (4.1) shows that the strength of the normal component of the induction field decreases according to the third power of the distance. Equation (4.1) therefore makes sense for the possibility of transmitting power by the induction mechanism just upon short or medium distances, but discourages the use of the same mechanism to transfer power at long distances.

If a portion ψ of the induction flow is captured by a secondary coil made up of N_2 turns, an induced electromotive force:

$$E_2 = -j\omega_0 N_2 \psi \tag{4.2}$$

ω_0 being the angular frequency of the field, can be measured at the terminals of the coil, where the considered portion is given by:

$$\psi = \int_S \left(\vec{B} \cdot \vec{n} \right) ds \tag{4.3}$$

being *S* any surface bordered by the secondary coil. By combining equations (4.1), (4.2) and (4.3), the electromotive force induced at the terminals of the secondary coil can equivalently be expressed according to:

$$E_2 = -j\omega_0 M I_1 \tag{4.4}$$

in which the parameter *M* represents the mutual inductance of the coupled coils. The mutual inductance *M* depends on the physical and geometrical properties of the system. For a couple of coaxial coils at a distance *r* parallel to each other:

$$M = \frac{\mu_0 N_1 N_2 a^2 \left(\pi b^2\right)}{2\sqrt{\left(a^2 + r^2\right)^3}} \tag{4.5}$$

being *b* the radius of the secondary coil.

The power transfer actually occurs when a load is connected to the terminals of the coil to form a closed secondary circuit. It can be easy shown that the transmitted power includes both an active and a reactive component even if the load is a mere resistor. In fact, the secondary circuit is characterized by an inherent auto-inductance, which is responsible of an opposite reaction to the magnetic induction produced by the primary circuit. If the load is characterized by a resistance *RL* and the current flowing through the secondary circuit is I_2, equation (4.4) has to be rewritten as:

$$j\omega_0 M I_1 = \left(R_L + j\omega_0 L_2\right) I_2 \tag{4.6}$$

To obtain the maximum power transfer the secondary circuit has to be arranged in order to annul the whole reactance or susceptance. To this end the series or parallel insertion of a capacitor between the coil and the load shows to be effective, provided that its capacitance satisfies:

$$C_2 = \frac{1}{\omega_0^2 L_2} \tag{4.7}$$

For instance, in the case of series insertion equation (4.6) becomes:

$$j\omega_0 M I_1 = \left[R_l + j\left(\omega_0 L_2 - \frac{1}{\omega_0 C_2}\right)\right] I_2 = R_L I_2 \tag{4.8}$$

that shows how series configurations allow to annul the reactance of the secondary circuit; they are suggested to feed high impedance loads working with

low level currents. Parallel configurations annul the susceptance of the circuit and are suitable to feed low resistance loads working with high currents.

In several applications, especially when the coils are not immobilized, the auto and mutual inductance parameters can change. In this cases to preserve efficiency in the power transfer it is necessary to implement suitable control strategies to keep equation (4.7) valid. For instance, an electronically controlled variable capacitor, the capacitance of which is adaptively varied for tracking the maximum power transfer, could be used in the secondary circuit. The control strategy would require a wattmeter to monitor any power reductions and change the capacitance accordingly for restoring the most favorable operation. Otherwise a feedback could be forwarded to the primary circuit that could react by means of frequency adjustments.

The solution adopted by the proposed system avoids the use of the aforementioned cumbersome control strategies by deploying a Royer oscillator in the primary circuit. The Royer oscillator is capable of continually auto-tuning the frequency of the system in order to maximize the power transfer efficiency without neither requiring active driving of the frequency nor variable capacitors in the secondary circuit. For other solutions in which the primary circuit is driven by a sinusoidal current source, any tuning mismatch of the secondary circuit would lead to efficiency losses in power transfer system.

The system includes a primary circuit magnetically coupled to a secondary circuit that has to be remotely energized. The primary circuit is essentially a Royer oscillator made up of a resonant tank, realized connecting a capacitor C_r and a centered-tapped coil L_r. The secondary circuit has a front-end made up of a second coil connected to a capacitor to form an identical resonant tank.

To illustrate in details the functioning of the proposed system, a very simplified schematic of the primary circuit is given in Fig. 4.2. The circuit is made up of two identical conducting branches, each one consisting of a MOSFET transistor, a diode and a resistor. In branch number 1, the current is withdrawn by the DC

supply, Vcc, through resistor R1 and flows towards ground either through the diode D1 and the cascaded transistor T1, if transistor T1 is switched-on, or else through Zener diode DZ2. Equally, in branch number 2, the current is withdrawn by the same supply through resistor R2 and goes to ground either through diode D2 and the cascaded transistor T2, if transistor T2 is switched-on, or through Zener diode DZ1.

The circuit is symmetric being R1 = R2, R3 = R4, D1=D2, Dz1=Dz2, and T1 = T2, hence there should be no voltage difference between the terminals of the resonant *LrCr* tank connected to the transistors drains. But, in the practice the weak asymmetries and background noise in the tank start progressively mounting current and voltages oscillations. The asymmetries and noise act in conjunction with a positive reaction, obtained by cross-connecting the gate terminal of each transistor to the anode terminal of the diode that probes the conducting state of the other transistor in the opposite branch.

To help the injection and sustainment of the oscillations in the tank, a supplementary way for the current is arranged in the circuit by linking through a choke inductor the central tap that separates the two halves of the *Lr* coil to the DC supply. To limit the peak currents the inductance of the choke is chosen much greater than that of the coil forming the resonant tank.

The circuit reaches a steady state in which the transistors work in push-pull mode by switching on and off upon the polarity alternation of the sinusoidal voltage across the capacitor *Cr*. To protect the transistors the system also includes, not shown in Fig. 4.2, snubber circuits to limit the voltage between the drain and source terminals during switching-on and off transients.

A deep insight in the functioning of the system can be gained looking at the typical voltage waveforms that characterize the steady state operation of the circuit. To this end the circuit shown in Fig. 4.2 has been simulated using several different configurations. Table I reports the parameters that specify the hardware configuration that has been realized to carry out experiments. The waveforms that characterize the steady state functioning, namely, the voltage

across Zener diode DZ1, the voltage across the MOSFET transistor T1 (voltage between drain and source terminals *Vds*), the current in diode D1, and the voltage across the capacitor *Cr*, are shown in Fig. 4.3. In Table 4.1 are summarized the most important data referring to the main adopted electronic parts.

R1, R2 = 33 Ω	3 W resistor
R3, R4 = 10 kΩ	¼ W resistor
Ld = 1 mH	Ferrite core inductor
Lr = 1 µH	In air inductor
Cr = 350 nF	Cr Voltage 400 Vcc, 250 Vac
T1, T2 = IRFP250n	Continuous drain current 30 A. Gate to source voltage ±20 V. Drain to source breakdown voltage 200 V.
DZ1, DZ2 = bzx89c10	DZ1, DZ2 zener voltage = 10 V
D1, D2 = MUR860	D1, D2 ultrafast rectifier. Average rectified forward current 8 A. Peak repetitive reverse voltage 600 V. Maximum reverse recovery time 60 ns.

Table 4.1. Main part list adopted in the Royer oscillator.

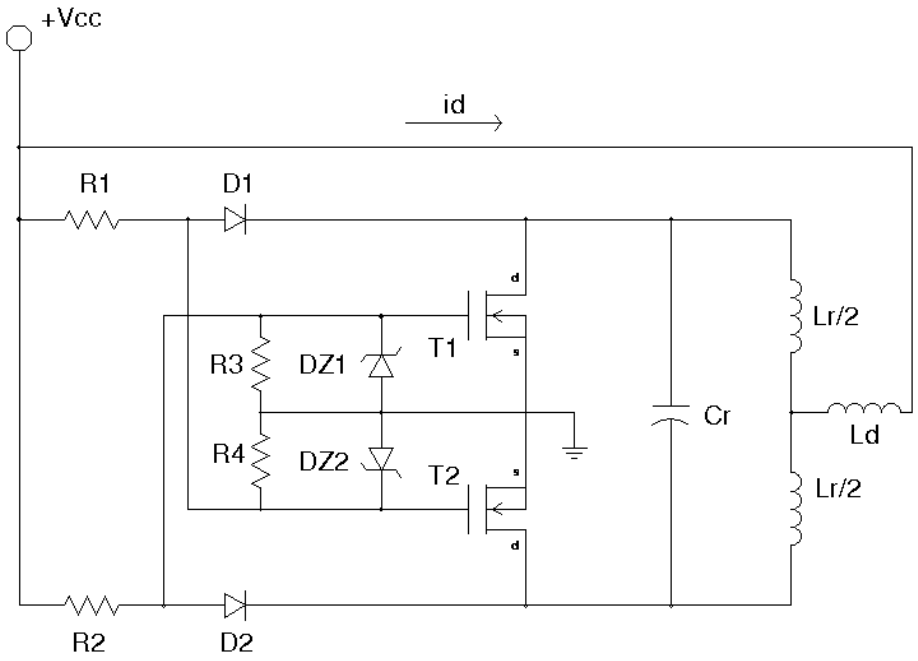

Fig. 4.2 Simplified layout of the primary circuit of the system. The layout does not show the snubber circuits necessary for power MOSFETs protection during switching on and off transients.

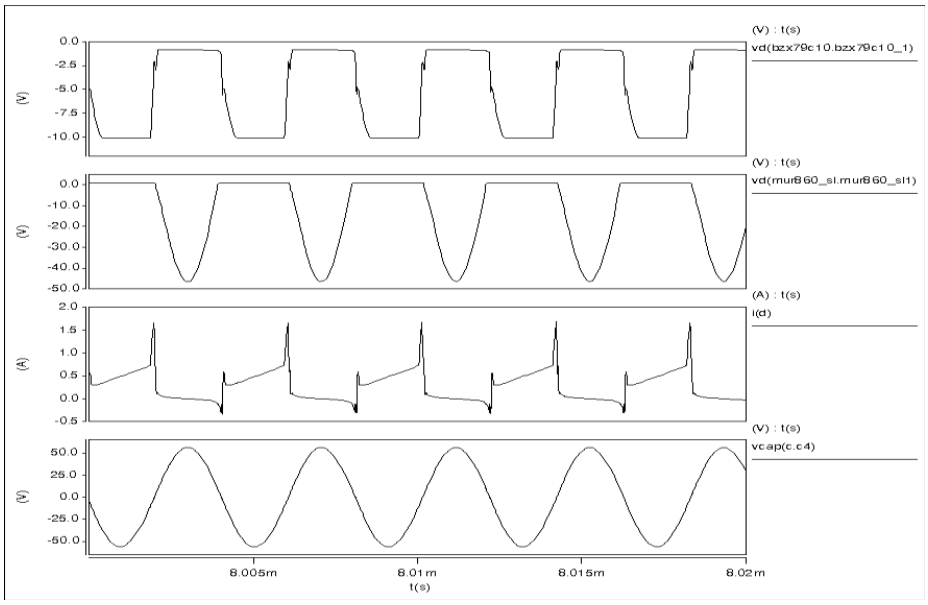

Fig. 4.3 Voltage waveforms characterizing the steady state functioning of the circuit. From top to down, voltage across Zener diode DZ1, between drain and source terminals of MOSFET transistor T1, current in diode D1, and capacitor Cr, can be recognized.

The research started with the electronic project, with the help of Saber Sketch environment, and the subsequent creation of a prototype in order to conduct an experimental study. During these studies a path starting from a general situation has been followed. In this scenario, has been proposed a prototype devoid of concrete application, which aim is only to investigate the feasibility of the project. A WPT system has been arranged, trying an effective possibility to transfer energy from one point to another without the need for physical connections. At this stage it is not yet been designed a specific application, but characterization measures were just made, aimed at comprising the system. This procedure made it possible to understand the strengths, limitations and shortcomings of the architecture conceived. In this way the foundations were laid for the essential structure optimization, optimization, aiming a triple aspect: the first concerning the understanding of the system and of the physical principle. The second related to a system tuning itself for itself, without a particular mission for the system itself. The third such an optimization, for a variety of applications, from personal interests, community or indicated by companies or simply related to the specific theme of research and industry.

Now will be shown different prototypes, first a resonant-type induction system designed to investigate on physical principles and understanding limitations and improvements needed. Then different applications will be presented. Circuits, assemblies, systems and whatnot are artisanal, aimed for the search itself.

4.1 Two coil test setup.

A prototype of the proposed power transmission system has been realized and a number of experiments have been carried out. The prototype utilizes a couple of twin coils made up of five circular copper windings and characterized by a diameter equal to 14 cm to assure the coupling between primary and secondary circuit.

For test purposes a measuring station consisting of a laboratory power supply (Kenwood PD18-30), two digital multimeters (Agilent 34401A), a digital

oscilloscope (Tektronix TDS210) and variable power resistors with slide-type wirewound, has also been set up. The power resistors connected to the secondary circuit have been utilized as load during the tests. The experimental set-up is shown in Fig. 4.4.

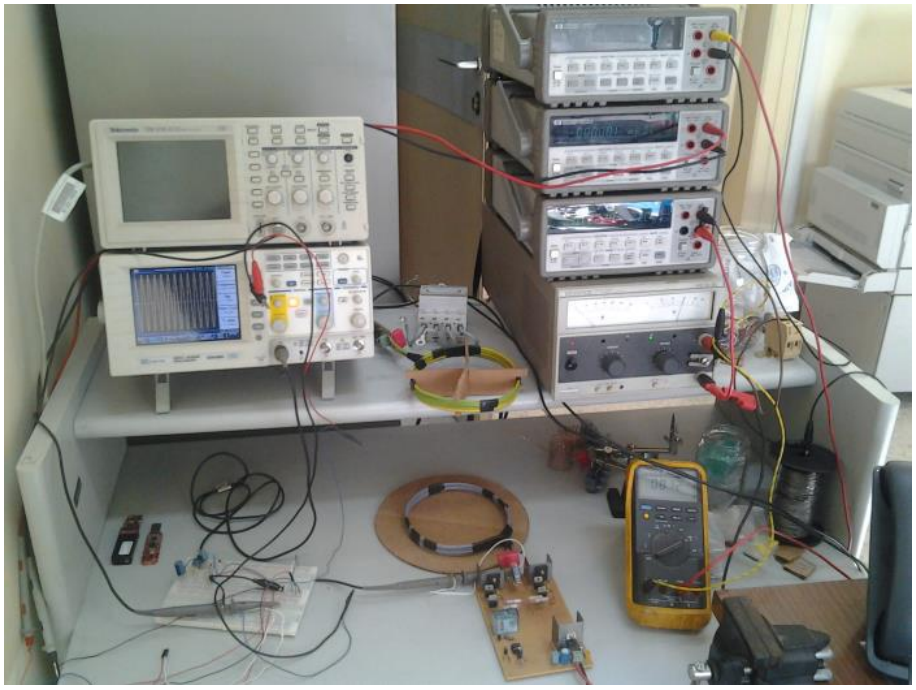

Fig.4.4 – Experimental setup utilized to evaluate the power transmission system.

Different scenarios have been explored in order to highlight how the transmitted power depends on the distance and mutual position of the coils, and on the load value.

Power versus distance measurements have been performed moving the secondary coil progressively away from the primary one. The experiments have been performed having at the secondary a resistive load, characterized by 20 Ω resistance. Power measurements have been obtained taking the ratio between the square value of the rectified voltage measured across the load and the load resistance.

Fig. 4.5 shows the transmitted power for different values of the distance between the coils, that are kept parallel to each other and with their center

aligned. It denotes that the resonant inductive technology is suitable for power transmission upon short distances.

Taking the ratio between the power absorbed by the primary circuit and that delivered to the load the efficiency curve given in Fig. 4.6 is obtained.

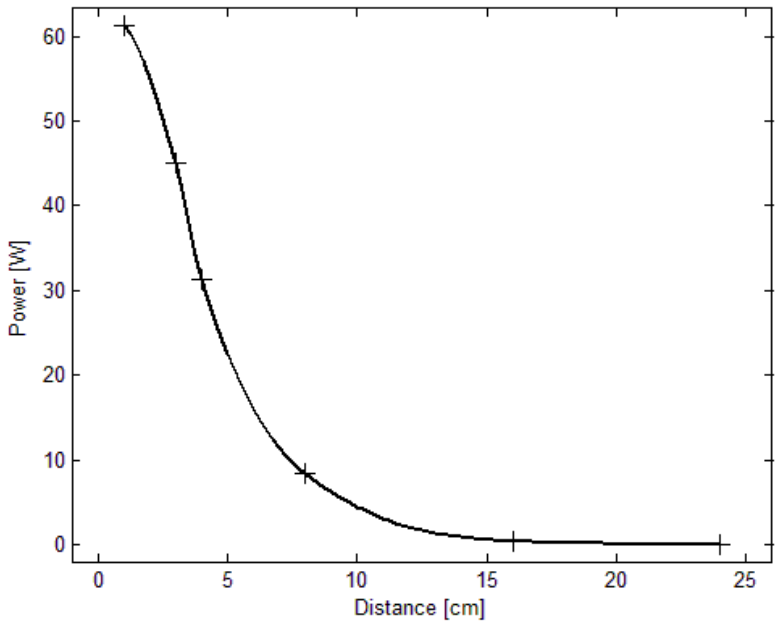

Fig. 4.5 – Power transmitted to the secondary circuit to feed a 20 Ω resistor as a function of the distance between coils.

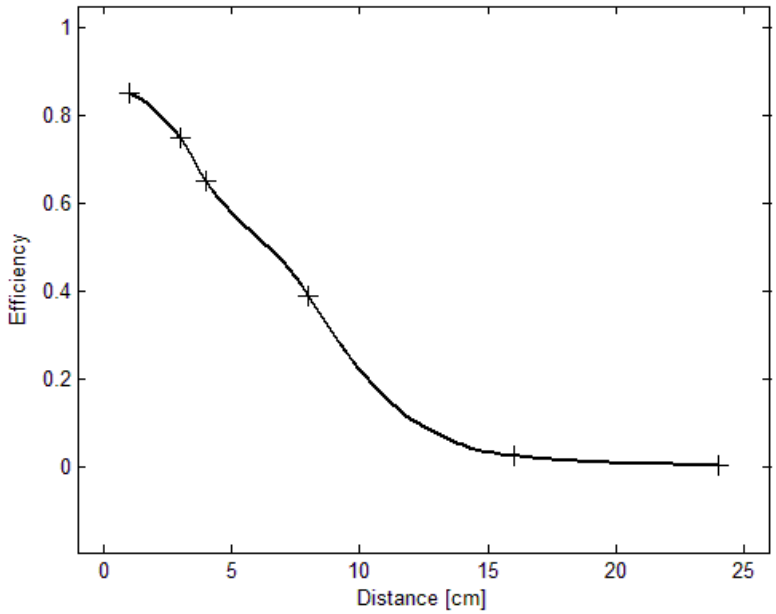

Fig. 4.6 – Efficiency as a function of the distance between the coils, measured in the presence of a 20 Ω resistor load.

The experiments have been repeated in the presence of a load characterized by 200 Ω resistance, that requires less power with respect to the 20 Ω load. In this case the transmitted power shows different values for the same distances between the coils. The graphic given in Fig. 4.7 is typical of a resonance phenomenon, that in this configuration clearly appears because of the minor loading effect on the resonant tank built around the secondary coil. In this specific test, the transmitted power shows a maximum for a distance equal to 8 cm, in correspondence of which the efficiency of the power transmission system is about 32%.

The power demand of the remote equipment is essentially specified by the load resistance. For high power demands the transmitted power monotonically decreases upon the distance; it is therefore convenient to have the secondary coil close to the primary one, whereas for low power demands, involved by higher load resistance circuits, a finite short distance between the coils can also be tolerated.

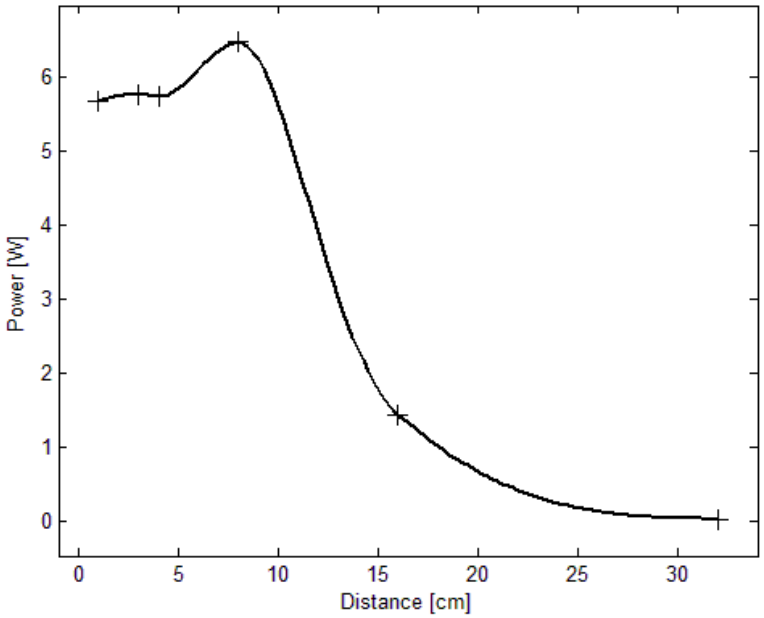

Fig. 4.7 – Power transmitted to the secondary circuit to feed a 200 Ω resistor as a function of the distance between coils.

The operating frequency depends on the capacitance, inductance and resistance parameters of the system, but also on the distance between the coils. In fact, altering the geometry of the system determines changes of the auto and mutual inductances of the coupled circuits. The oscillatory architecture anyway automatically settles to an operating frequency that grants the maximum power transmission for that configuration. Fig. 4.8 shows the operating frequency as a function of the distance between the coils, measured when the secondary circuit is loaded by a 200 Ω resistor. A roughly explanation of the aforementioned diminution of the operating frequency has to be found in the relative inductance increment seen at the primary circuit, caused by less flux cancellation due to the lengthened distance between it and the secondary coil.

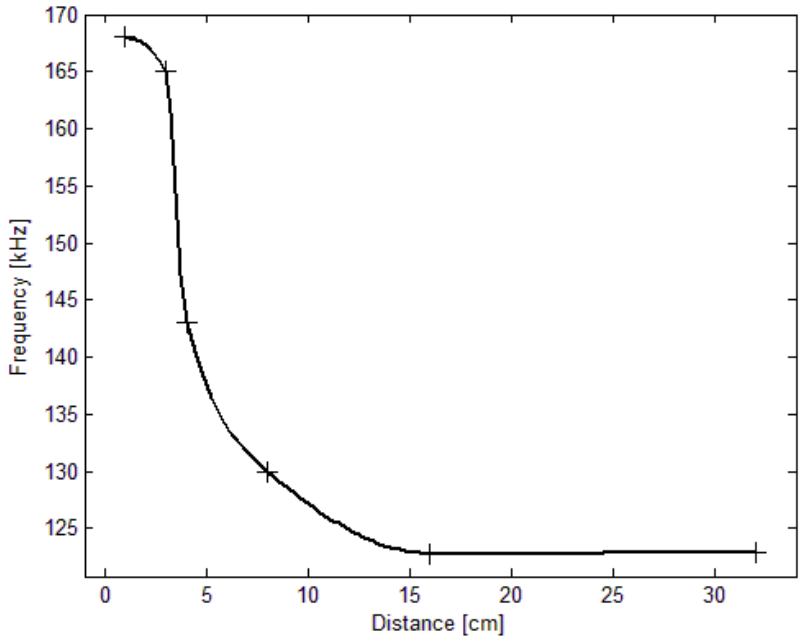

Fig. 4.8 – Operating frequency as a function of the distance between the coils. Measurements have been performed when the secondary circuit is loaded by a 200 Ω resistor.

Measurements have been repeated keeping the axis of the planar coils parallel but misaligned; the alignment mismatch is expressed in term of distance between the axis orthogonal to the planes hosting the coils. In these tests the two coils are kept perfectly parallel at a distance between the respective planes equal to 12 cm. Starting from perfect axial alignment conditions, the secondary coil has been gradually moved away in order to have its axis parallel but at a distance from the axis of the primary coil. The results are shown in Fig. 4.9.

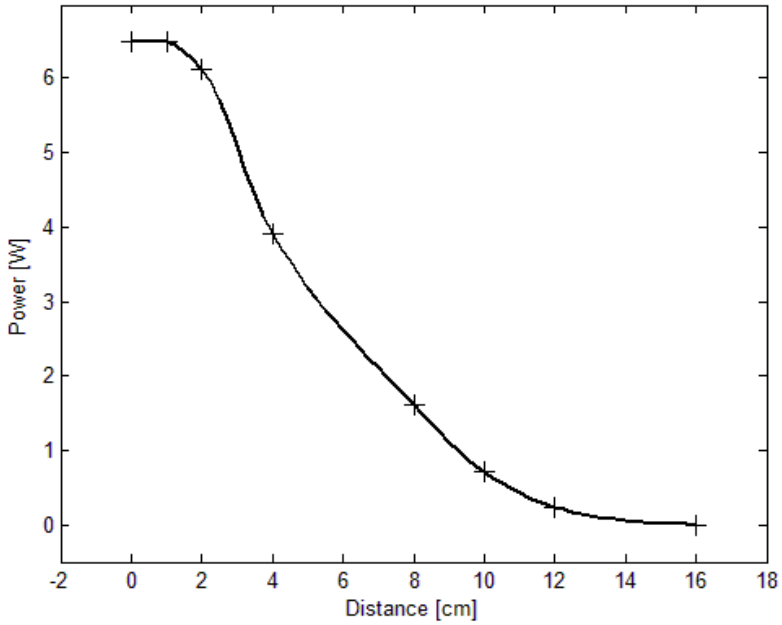

Fig. 4.9 – Effects of misalignment on the power transmission system: the planes hosting the primary and secondary coils are at a distance equal to 12 cm.

The results of several experimental tests on a prototype have been also presented in order to highlight (i) the efficiency of the power transfer mechanism and its dependence upon the distance between the coils, (ii) the effects of misalignments between the coils, (iii) the possibility of power transmission by means of orthogonally positioned coils.

In this work, is reportedly the path conducted during the various stages of research, and study the details of a specific problem concerning low power loads powering issues, of the order of tens of Watts. These loads are sensors, batteries, small appliances, different objects, often applied and used in the field of measurements and for which it may be convenient, or at the very least, interesting the ability to power them without wired solutions, removing or cooperating with the battery present, possibly aboard the system or device.

4.2 Inductive power transmission for wireless sensor network supply.

Wireless sensor networks are today more and more widespread. Along with the installation of more and more networks, a number of new standard documents has also been produced to update the regulation concerning data communication between sensors and data collectors. Differently, less attention has been paid to the different modes of powering the local sensors. At present, the energy required for local sensors functioning is essentially battery provided, despite the battery supply is often recognized as a critical aspect of remote sensing. In fact, the periodical battery replacement is sometimes non-strategic and troublesome, especially for those sensors which have to be installed in difficult to reach sites, or are integrated into medical implantable devices. In the abovementioned circumstances, battery-less sensors appear to be attractive, both from a pragmatic point of view, because of the strategic role they can play in critical scenarios, and from an innovation-oriented point of view, because of the novelty that wireless power transmission can add to a new groundbreaking remote sensors technology. Wireless power transmission technologies are capable of supporting battery-less sensor functioning. In the next, first the main issues related to alternative remote devices powering solutions are plainly discussed, then, a resonant-based induction power transmission system for supplying a sensor network is also presented.

4.2.1 Wireless sensor network.

A sensor network consists of a set of devices, deployed in a certain environment, by means of which it is possible measuring one or more physical quantities of interest, such as temperature, pressure, humidity, etc., in several different points of the surrounding area. The devices that are charged of the sensing task, i.e. the sensors, are generally active devices that also include the capability of transmitting data, either by means of cable connections or wirelessly, to a remote data collector. As a matter of fact, wireless sensors are more and more often preferred to cabled sensors since they allow fast installation and easy

reconfiguration of the network; the last feature being greatly valued by customers. A sensor network utilizing devices that are not plugged to the electrical grid constitutes a wireless sensor network (WSN).

WSNs can be regarded as wireless personal area networks (WPAN), wireless local area networks (WLAN), or even wireless metropolitan area networks (WMAN) according to their extension and the adopted communication protocol.

Specifically, a WSN that works as WPAN covers short distances, namely few meters, and are usually used within small size system; it is ruled by the IEEE 802.15 standard, which thoroughly defines the communication protocol. To cover areas greater than WPAN, a WSN has to be instead configured as a WLAN, which can offer a typical coverage range equal one hundred meters; the communication protocol is defined into IEEE 802.11a, b, g, n standard documents. Finally, a WSN has to be designed as WMAN in order to cover wide areas, ranging up to 10 km, according to IEEE 802.16 standard document. The attractiveness of WSNs is mostly due to the absence of cable connections, which eases network configuration changes, as well as network extensions through the adjunct of new sensor nodes. The aforementioned possibility can be exploited to optimize network usage, for instance by providing redundancy to increase reliability of nodes that occasionally operate in critical conditions. It is worth noting that to avoid connections to the grid, wireless sensors are powered by means of embedded batteries, that provide the power for the functioning of both sensors and complementary hardware for processing and data transmission operations. But, the use of batteries means limited energy autonomy, as well as performance limits in terms of data rate, network reliability, and sensors availability. As an example, the most frequent sensing nodes fails are due to the absence of energy supply, rather than to hardware problems or physical damages.

Moreover, the necessary replacement of the exhausted batteries represents a relevant weak-point of WSNs: in several applications it reveals to be non-strategic and/or troublesome, especially for those sensors which have to be

installed in difficult to reach sites, or are integrated into medical implantable devices.

In the following, the main attention is paid to wireless sensor networks that can be classified as WPAN, i.e that extend within a limited volume. The main goal is showing that, in the future, wireless power transmission technologies will likely be capable of supporting battery-less sensor functioning.

4.2.2 Remote devices powering issues.

The basic WSN topology is the star network, made up of a single *coordinator* and multiple *end devices*. The *coordinator* is a full function device (FFD): it is in charge of allocating network addresses, holding binding tables, receiving data from all *end devices*. The *end device*, i.e. the sensor, on the contrary, is a reduced function device (RFD): it is busy in monitoring and/or control functions, and regularly transmits data to the *coordinator*. An *end device* cannot directly send data to other *end device*s, it can send data only to the *coordinator* which cares on the occasion for forwarding to the intended recipient. Star networks are very simple to implement but are suitable to cover only limited distances; nonetheless their characteristic message latency is often long since the *coordinator* can communicate with one *end device* at time.

Advanced networks use one or more *routers*, that, like any *end device*, are capable of performing monitoring and/or control functions, as well as of operating as data transceivers. In the presence of a *router*, an *end device* does not need to be in radio range with the *coordinator*, the number of nodes of the network can be considerably increased and more topologies such as tree and mesh network can be developed. The degrees of freedom accomplished permit to tailor the network topology to the environment where the monitoring task has to be performed.

Two main alternatives can be distinguished to energize remote devices that are disconnected from the mains, namely by means of battery or by wireless power transmission.

In the most recent years batteries technology has become a hot topic, that has seen relevant investments and efforts aimed at realizing and delivering long-lasting batteries, the main goal being prolonging battery life to reduce the replacement frequency. The chief efforts in this field have concerned the definition and implementation of energy/power management approaches to be integrated in smart battery systems; a typical example is the battery employed in portable computers. Smart batteries include an on-board microcontroller, the firmware of which consists in algorithms that successfully allow to avoid energy misuse at the expense of increased complexity and costs.

In particular, to prolong battery life of terminal nodes of WSNs, sleep/wake-up mode strategies have been proposed and are nowadays extensively adopted. The implementation of a sleep/wake-up mode usually requires that the *coordinator* sends a wake-up signal to the *end device*. The *end device* lays in sleep mode most of the time, during which it draws a very low current (nanoamperes), but sufficient to collect and store a wake-up signal. The *end device* wakes-up periodically and checks for wake-up signals: if a pending signal is detected the *end device* enters in active mode, otherwise it returns in sleep mode. As soon as it enters active mode, the *end device* performs the measurement of the physical parameters, transmits the measured data to the *coordinator*, and finally returns in sleep mode. The aforementioned strategy allows to prolong battery life thanks to the substantial reduction of power consumption during sleep mode time intervals; note that *end devices* hold in sleep mode for most of the time.

The undesired side-effect of sleep/wake-up mode strategy is the significant increment of message latency, which can reveal for several application a bottleneck. The message latency can be reduced through the use of *routers* in the network; but *routers* are, like the coordinator, more power consuming and

generally need supply by the mains, since they have to keep the receiver in the ON state continuously.

Prolonging batteries lifetime is not a definite solution to the issues of powering WSNs, since even for long lasting batteries cyclical checks and replacement actions are necessary to guarantee reliability and availability operation of WSNs. Therefore, despite noteworthy advancements have been achieved in prolonging battery life, at present, the use of embedded batteries is still unwelcome in some monitoring applications: the battery replacement is in fact applicable only in those scenarios in which sensing nodes are accessible, while there are many applications of practical interest in which battery replacement is extremely critical, such as: medical monitoring, structural monitoring, surveillance of restricted environment hazardous to human, and micro-robot applications.

Moreover, the use of batteries is connected to environmental issues, being used batteries special wastes that have to be properly treated in order to perform recycling and reduce environmental impact.

Recently, wireless sensor networks harvested by ambient energy (WSN-HEAP) have also been proposed. The underneath technology, at the state-of-art, is utilized in systems demanding little power. Unfortunately, these systems typically deploy an extra back-up battery to support power peaks or intervene in case of any other power unavailability to grant regular operation. For back-up batteries all the aforementioned considerations can be repeated: they suffer of deterioration, require cyclic checks, need occasionally replacements, etc.; HEAP technologies are just a partial reaction to remote devices powering issues.

Recently, WPT is emerging as a promising technology to address the energy constraints in a WSN. By using a WPT technology, the goal of realizing wireless sensor networks that are not battery dependent seems achievable. Actually this technology is suitable to provide power to the end devices of short range WSN, even in the cases in which they cannot be easy accessed and shows to be much

more robust that energy harvesting systems, as well as capable of providing higher power rates.

Thanks to the use of wireless power transmission solutions, the energy supply is no more limited by battery capability. Also, the role of useful power management strategies can be redefined according to the new scenario and the optimal usage of the new available facility. So, in a sleep/wake-up protocol, the sleep time of *end devices* can be significantly reduced thanks to the continuous availability of a

power source. By reducing the sleep time, the data rate can increase, and the bottleneck related to the latency related to message delivery removed. As a consequence, the use of WSNs can be enabled for many other applications where a faster transfer data is required. WSNs exploiting WPT technology can be designed in order to enhance other performance factors e.g. related to safety, reliability,

availability, etc.

4.2.3 ZVS Royer oscillator for WSN powering.

A primary coil is energized through the injection of a current obtained by means of a DC-fed power inverter. The current oscillates in the coil, which is inserted in an oscillator architecture, and sustains a magnetic field in the neighboring environment. Each *end device* withdraws energy from the magnetic field by concatenating with an own coil a portion of the magnetic flux.

The electromotive force excited by the time varying magnetic flux, which is available at the terminals of the coils deployed by *end devices* is typically converted from AC to DC by means of a full rectifying bridge complemented with a smoothing capacitor.

To improve the transmission efficiency and widen the coverage area a capacitor is connected to the primary coil to form a resonant circuit. Similarly, capacitors are connected to any secondary coil to form resonant structures, all tuned at the same resonance frequency. In fact, two or more resonant objects of the same

resonant frequency exchange energy efficiently, while dissipating little energy in extraneous off-resonant objects.

The circuitry necessary to implement the aforementioned resonant induction mechanism employs a zero voltage switching (ZVS) push-pull inverter. In particular, a modified version of a classical ZVS inverter, adapted to operate in resonant conditions, and known in the literature as ZVS Royer oscillator, is adopted. ZVS oscillators represent well-assessed solutions and are adopted in low-power/high-frequency converters, as those utilized to recharge laptop and cell-phone batteries, as well as in high power low frequency supplier for induction heating ovens. They have a relatively simple architecture and use a minimum number of power components, which are the expensive part of the circuit.

Moreover, differently from other DC/AC inverters that use controlled power switches, in these kind of inverters power transistors turn on and off at zero voltage, thus minimizing stress and power losses, which, especially for high frequency operating conditions, is a very attractive feature.

The circuit is described in Fig. 4.10 by means of a schematic layout. It includes a central tapped inductor that physically realizes the front-end coil, responsible of the resonant inductive coupling.

The two halves of the central tapped inductor must be identical, since any asymmetry in the component would make the transistors work in unbalanced conditions leading to undesired increments of stress and energy loss. To obtain a resonant structure a capacitor *Cr* is parallel connected to the coil to form a tank.

The resonant tank is driven by two *MOSFET* transistors, T1 and T2, that alternatively conduct: one during the half positive voltage wave across capacitor *Cr*, the other during the negative one. Each transistor includes a freewheeling diode, not shown in Fig. 1, that bypass the drain-source channel and allows a reverse current to flow in the transistor as approaching the switch-off point. The transistors are also complemented by snubber circuits that limit power dissipation at switching on. Although in theory ZVS inverters have no

need of snubbers, in practical realization their use is always recommended to take into account unbalances due to structural asymmetries, or occasional unbalances, which are a common phenomenon in power switching devices.

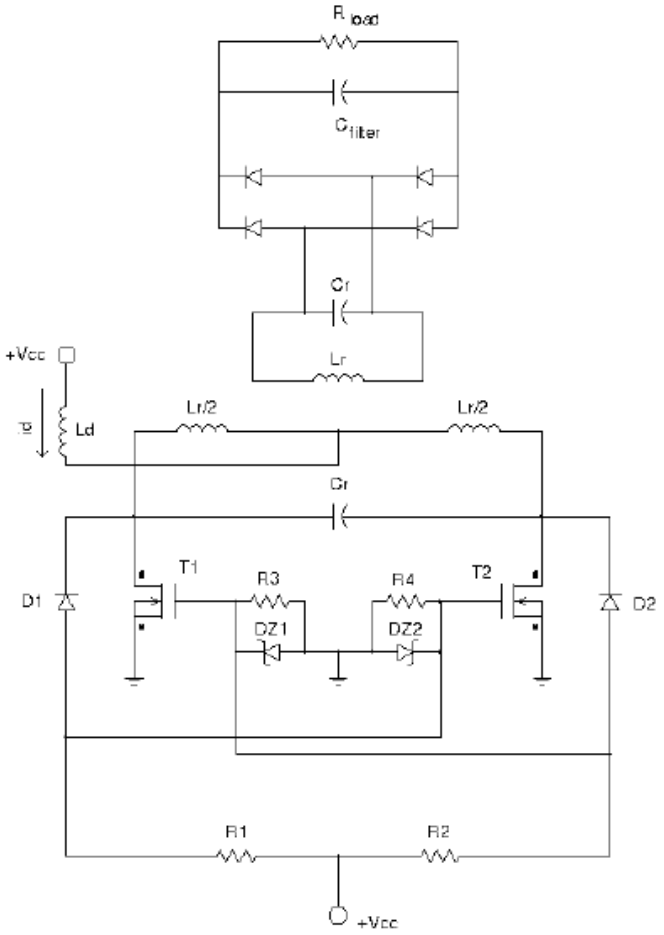

Fig. 4.10. Schematic layout of the proposed circuit employing the zero-voltage switching Royer oscillator. The secondary circuit is coupled to the primary one and hosts a full rectifier bridge to convert AC power to DC.

In order to assess the feasibility of the proposed solution, a number of preliminary tests have been carried out on a small WSN.

4.2.4 a wireless powered WSN prototype.

The network adopted in the tests was engaged in indoor temperature and battery voltage sensor monitoring. It exploited *Zigbee* protocol and consisted of the following hardware and software components:

- an automatic measurement station made up of a portable PC, equipped with a sensor monitor application software tool;
- one USB emulator board;
- three target boards.

Each target board includes: a dedicated 2.4 GHz Zigbee network processor, connected to a microcontroller via serial peripheral interface, two LEDs indicators (red and green lights), and an I/O interface with 5 GPIO lines.

The application software runs on the microcontroller, and allows retrieving temperature and battery level measurements; in detail, data from the temperature sensor and battery checker are digitized by an on-board analog to digital converter and forwarded through the local bus to the microcontroller. The USB emulator board grants serial to USB connection and allows one of the three target boards to act as network coordinator, i.e. as gateway in the communication between the other two target boards and the automatic measurement station.

The coordinator, i.e. the couple USB emulator and target board, is connected via USB port to the measurement station; the USB connection assures both the power supply to the coordinator and allows data from the remote target boards (end devices) to be forwarded to the PC.

In the experiments, the battery of the two target boards playing the role of end devices has been removed, and they have been supplied by means of an external resonant induction power transmission system. In particular, the two sensors have been supplied by equipping them with two power receiving systems, made up the a receiving resonant structure and a full rectifier bridge. To adapt the energy received by means of the resonant coupling mechanism to the parameters required by target boards, a precision voltage regulator (TL431 Texas Instrument shunt regulator) has been exploited. The regulator makes available a stabilized voltage supply adjustable within the range (2.5 – 36) V. According to the target boards requirements, an output of 3.0 V has been programmed. The

regulator is also capable of satisfying the current requirement by the target board, which is equal to 35 mA, being it capable of providing continuous current up to 100 mA.

Concerning the functioning of the target boards, the red LED of the one acting as coordinator is always ON to indicate that a valid network is established. Instead, the green LED remains ON in the target board configured as coordinator, whereas it blinks at 1 Hz in the boards configured as end devices. If a further sensor is adjoined in the network, the device begins to periodically send temperature and battery voltage data to the network coordinator. The sensor monitor software installed upon the PC receives data from the coordinator, and shows them through a graphical interface, which also reproduces the network topology.

To better illustrate the capability of the proposed solution, several tests have been performed on a very simple star configuration.

The adopted measuring station consists in a Kenwood PD18-30D laboratory regulated dc power supply, two Agilent 34401A digital multimeters and a GW instek GDS-820C digital oscilloscope.

The first tests have been carried out in the presence of the best coupling scenario, which is obtained by aligning the center of the coils along the same axis. In this setup, the secondary coil is moved away from the primary coil but having care that the concatenated magnetic flux satisfies the energy request by the remote target board. Since the secondary coil also produces a magnetic field, there is the possibility of supplying a second resonant coil positioned on the same axis at a greater distance from the active source, as shown in Fig. 4.11.

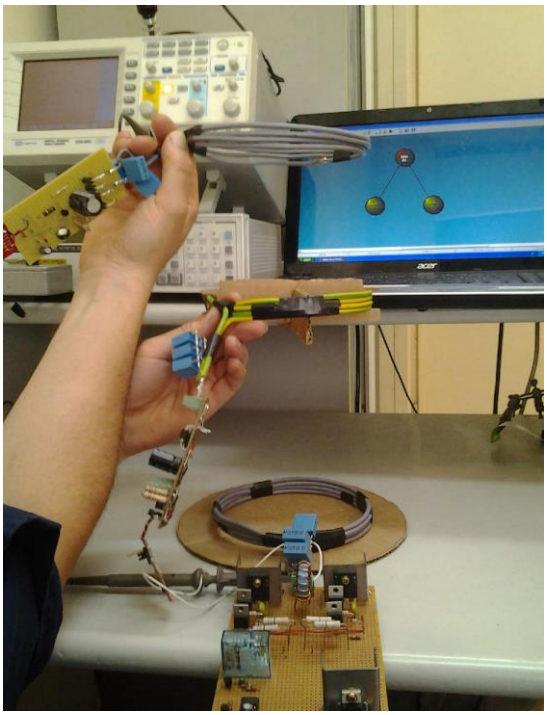

Fig. 4.11. Configuration with two target boards: their auxiliary coils to pick up the necessary power are aligned on the same axis.

This configuration has successfully worked when there were 25 cm between the active source and the first *end device* and 35 cm between the same active source and the second *end device*.

Fig. 4.12 shows instead a different configuration of the transmitting and receiving coils. Here, because of off-axis positioning the available distance reduces with respect to the above considered scenario: anyway, the experiment has shown that coupling can still be obtained at a distance equal to 20 cm.

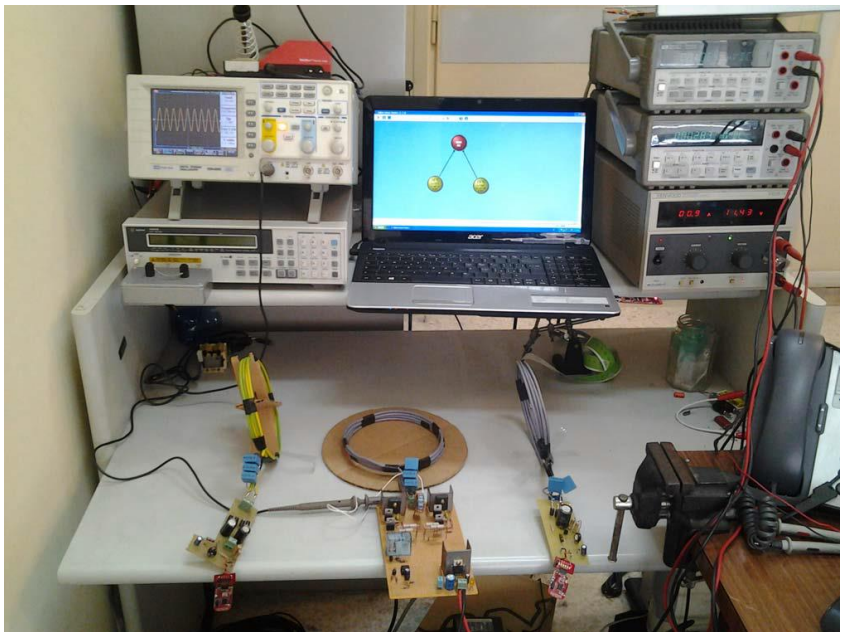

Fig. 4.12. Configuration with orthogonally positioned coils.

Similarly, as shown in Fig. 4.13 the power supply approach also works in the presence of coplanar positioning of the coils.

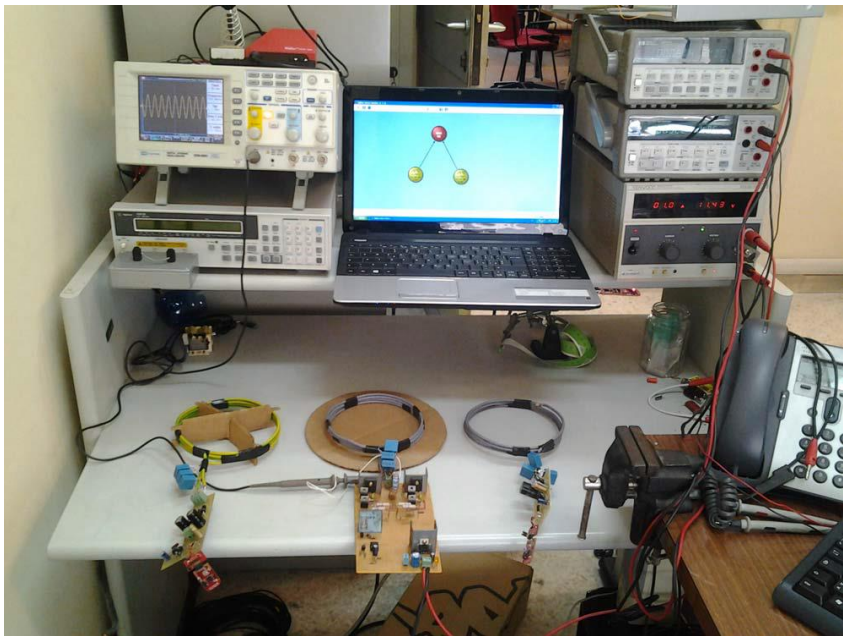

Fig. 4.13 Configuration with coplanar positioned coils.

In Fig. 4.14 the screen shot of the sensor monitor graphic interface, for the WSN configured as a star network to monitor indoor temperature and battery voltage

of the *end devices* is shown. The *coordinator* is represented by a red circle and the two *end devices* by yellow circles.

The links between coordinator and *end devices* are shown by arrows from *end devices* to the *coordinator*. For each *end device* the temperature, personal area network address, absolute time, and battery voltage of the last transmitting data are reported. The data were updated at a rate equal to 10 s. The test lasted several minutes during which there were no out-of-service events.

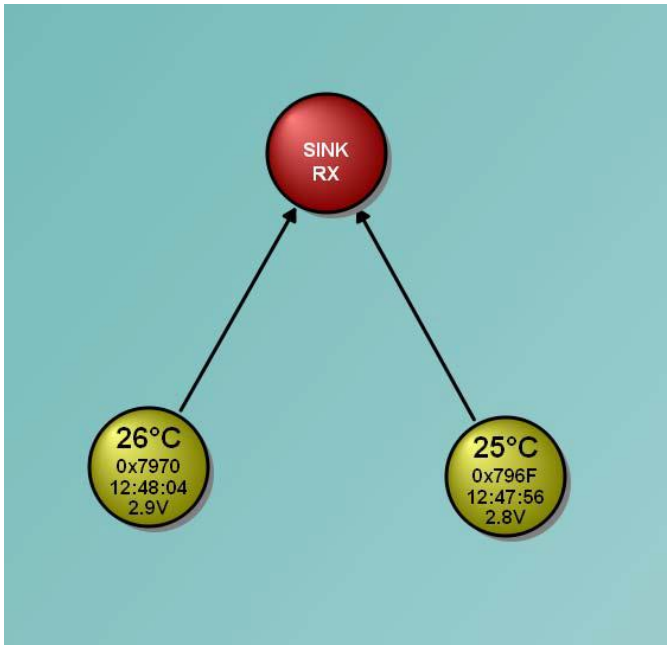

Fig. 4.14. Screen shot of the eZ430-RF2480 sensor monitor graphical interface for the WSN realized in the experimental activity.

The results of a preliminary study aimed at demonstrating that in a not very far future wireless power transmission technologies will be capable of supporting battery-less sensor functioning have been presented. In the considered configurations the active source that wirelessly energizes the remote active sensors was at short distances from the sensors, anyway, the transmission distance can be improved. In particular, a significant increase can be obtained by using a power supply system in the primary circuit capable of handling more power. In the presented system the adopted MOSFET transistors and capacitors

in the primary circuit limited the rated power, because of their maximum voltage operating limits. By deploying a more powerful source larger voltages and currents can be supported, and, consequently, larger field magnitude should be generated. Nonetheless different frequency choices, coupling configurations, and optimum coils design have to be considered, since all the aforementioned factors can improve power transmission by means of magnetic induction.

4.3 Heterogeneous load powering.

Anywhere a primary electrical source is not available, batteries seem to be the only way to allow the use of stand-alone electrical facilities. Unfortunately, there are some issues related to the use of batteries such as the necessity of regularly checking their charge status and, eventually, proceeding to their replacement, as well as of caring for their treatment as special waste at the end of their lifecycle that have to be faced; actually the delayed replacement of exhausts batteries is the primary cause of unavailability of the services offered by stand-alone devices. Rechargeable batteries just mitigate the aforementioned issues, since they require periodical interventions likewise to perform recharging, that, nonetheless, can be as troublesome as their replacement in several situations. Wireless power transmission approaches smoothly fit batteries recharging applications. In particular, by means of suitable solutions it is possible to recharge batteries without invasive operations, such as removal and reinstallations, but letting the batteries on board of the supplied device. In this paragraph, a wireless power supply system suitable to recharge general purpose NiMH batteries and Li-ion mobile phones cells, as well as the auxiliary wireless sensor systems, is presented. Details related to an experimental set-up aimed at highlighting the feasibility of the proposed approach are plenty given.

The majority of electrical facilities are usually connected to the mains in order to retrieve the power required to function. The connection to the grid grants, in theory, unlimited energy availability and high reliability in terms of continuity of the energy provision. Anyway, for several applications cable connections are

either technically impossible or inconvenient or even dangerous. In these cases the use of suitable battery supply systems is claimed for. A typical example is that of portable appliances that cannot be constrained by cable connections. The use of auxiliary batteries is also precious to react to the short time power interruptions of the mains caused by faults, or ordinary maintenance operations. The adoption of batteries as buffers, in fact, guarantees the availability of short-term energy by ensuring the power supply even if the primary source is momentarily unavailable. Anyway, some issues related to the need of regular replacement and special treatment at the end of their lifecycle discourage their utilization.

Recently new systems based on innovative wireless power transmission technologies are under examination as very interesting and attractive solutions, alternative to the use of batteries, to avoid conventional cable connections between power source and devices.

Wireless power transmission can be realized, as described, by means of several mechanisms, in particular coupling mechanisms are instead very often proposed for short distance and low power links set ups. They are gaining more and more attention as interesting solutions to be adopted to innovate several systems. In the recent years a lot of efforts have been done to increase the performance of pioneering wireless power transmission systems, based on coupling mechanisms, both in terms of coverage range and efficiency. The cutting-edge technology exploits the magnetic coupling between auxiliary identical self-resonant structures, one complementing the power transmitter, the others the receiver appliances. These resonant structures are realized by means of conducting loops, windings or helicoidal coils, and are characterized by sizes much lesser than the wavelength of the magnetic field they are intended to produce. Thus, the available power, associated to the magnetic component of the near field, is restrained in the neighboring of the system, and the power radiation, which would imply energy losses, is avoided.

In this work the main attention is dedicated to the use of wireless power transmission approaches to perform the recharge of NiMH batteries, which are widely utilized by a number of portable equipment, such as flash cameras, remote control joysticks, clocks, torches, etc, as well as of rechargeable Li-ion batteries that supply modern cell phones. Since battery recharging operations often require some monitoring and control operations, the proposed approach also considers the opportunity of contemporaneously supplying a multifunction sensor system, equipped with a microcontroller to perform on-site processing.

4.3.1 The contactless recharging

A battery supply needs regular checks that are indispensable to grant a reliable functioning. Nonetheless, after a limited time period, the battery has to be either recharged or replaced; both operations imply an additional cost required by the system to operate. With special regard to the replacement case, it is worth noting that this task involves not only caring in advance for the availability of spares, but also for the necessary actions to properly treat the exhaust batteries, which represent special waste. The replacement can be delayed by using rechargeable batteries that, however, admit a limited number of recharges and at the end need to be replaced as well.

The use of embedded batteries is definitively discouraged in monitoring applications that use sensors sealed in plastic enclosures, which limit or make even risky maintenance operations, or that are installed in difficult to reach sites, where battery replacement is difficult or expensive. The case of implanted medical devices represents an important example of both the aforementioned situations. Also, battery exploitation is just nearly tolerated in military operations to power on weapons deployed in critical logistic scenarios, where either electricity provision is unavailable or weapons are grid disconnected for safety reasons, or else to supply ancillary sensors that perform periodically checks of the main battery.

Anytime plugging to the grid is not convenient the use of batteries can be circumvented by wireless power transmission approaches. As it is shown in the following Sections, systems exploiting coupled circuits to transmit power within very short distances are typically considered to reach this goal. The coupling is made possible by means of coils at the front-end of a primary and one or more secondary circuits at the terminals of which the necessary power to recharge the batteries is retrieved thanks to the coupling mechanism.

4.3.2 Arrangements for heterogeneous load setup.

At the state of art three different types of resonant WPT system can be distinguished, according to the use of two, three or four coupled structures, essentially consisting in coils occasionally loaded with capacitors. The system that use two coils offers the best efficiency but the narrowest coverage. The use of a third coil allows the extension of the distance between the primary and secondary circuits, without complicating the architecture of the whole system too much. To attain further extension of the coverage range, the system can employ four mutually coupled resonant structures, at the expense of the overall efficiency.

Generally, a system to supply battery rechargers and/or sensor systems for monitoring and control operations needs a DC power supply to energize the primary circuit and transmit power through magnetic couplings to one or more neighboring secondary circuits. To this end the primary circuit has to produce a magnetic flux, which is attained by means of coils. Specifically, the circuit can profitably work on the principle of relaxation oscillations that assures for the frequency of the signal the adaptation to the natural resonant frequency of the system. In detail, a part of the magnetic flux produced by the primary circuit is concatenated by the coils of the secondary circuits, each of which in conjunction with a capacitor forms a resonant structure tuned, at design stage, on the common operation frequency of the system. A full bridge rectifier complemented with a low pass anti-ripple filter on the side of the secondary

circuits adapts the parameters of the received power in order to supply the loads.

For the considered set up two loads, namely a voltage/current controlled battery recharger and an active sensor system, have been considered. The two loads can be fed according to two alternative strategies: the first one requires the use of one primary transmission circuit with a resonant structure and one secondary circuit with its own resonant structure to which both loads are connected in parallel, Fig. 4.15. The other strategy instead requires so many resonant structures and secondary circuits as the number of loads to be fed, Fig. 4.16. The second solution involves more hardware but offers two relevant advantages:

- the possibility of moving the different loads, now fully independent from each other, not having to share the point of common coupling.
- the possibility of moving one of the two loads much faraway form the source, because one of the load can benefit of the major potentialities in terms of coverage range of a system with three resonant structures.

Specifically, thanks to the cascaded deployment of the resonant structures, the one farthest from the source can be positioned at a distance at which it could not be supplied by the same source in the absence of an intermediate resonant structure. Moreover, at design stage, it is always convenient to set the most power demanding load closer to the source where the intensity of the magnetic field is higher and more power can be picked up, and the less power demanding ones faraway.

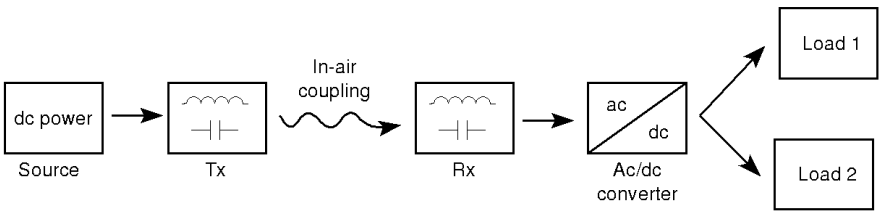

Fig. 4.15: Block diagram of the wireless power transmission system with one receiving resonant structure.

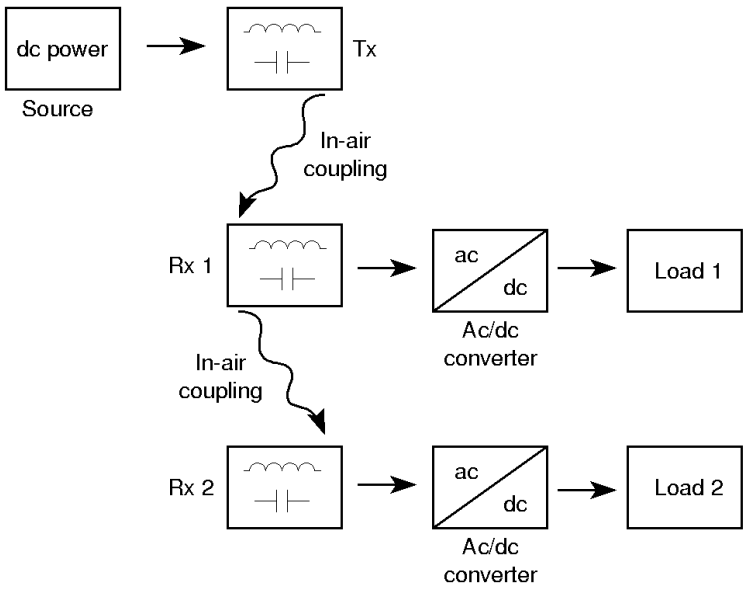

Fig. 4.16. Block diagram of the wireless power transmission system with two receiving systems.

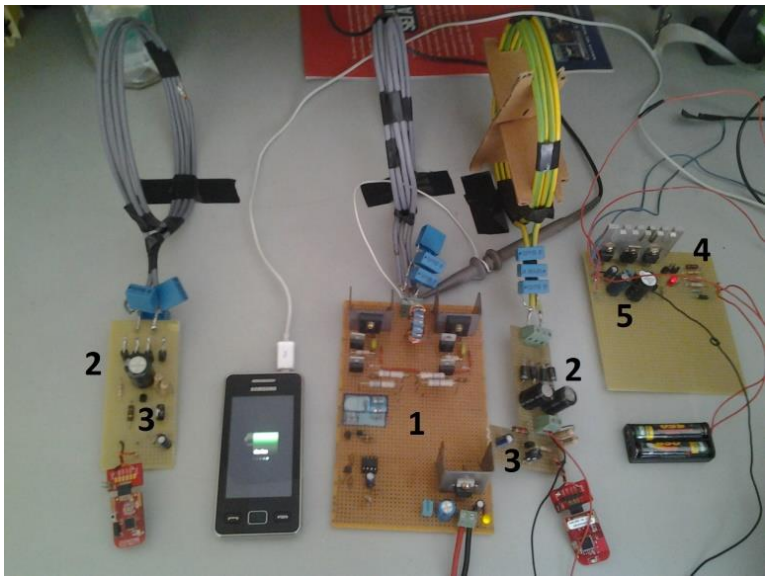

Fig. 4.17. Experimental setup comprising a variety of user devices.

The proposed experimental set up is shown in Fig. 4.17. It includes a push-pull inverter (1), a couple of full bridge rectifiers, one for each secondary circuit (2), two voltage regulators for sensors systems supply (3), one battery recharger

circuit for NiMH batteries (4), and one voltage regulator for Li-ion batteries equipped with a universal serial bus (USB) interface to connect to widespread gates available on several cell phones (5). To test the set up a DC power supply Kenwood PD18-30D, two digital multimeters Agilent Technologies 34401A, and a digital storage oscilloscope GW Instek GDS-820C, have been utilized. The push-pull inverter, employed to excite the resonant structure for power transmission, is very close to the aforementioned in previous section of this chapter. It is made up of two identical conducting branches, each one consisting of a MOSFET transistor, a diode and a resistor. Snubber circuits and free-wheeling diodes necessary for power MOSFETs protection during the switching transients are not shown in the diagram but have been included in the circuit. The frequency of operation of the coupled circuits is set upon 100 kHz by regulating inductance and capacitance parameters. The major advantage in the use of a relaxation oscillator consists in its inherent self-tuning capability, which assures a natural tracking of the maximum power transmission condition. In fact, a DC/AC inverter driven to operate at an assigned frequency, without auxiliary systems implementing articulated feedback control logics, would exhibit poor efficiency due to unavoidable detuning effects related to parametric variations, mainly due to changes in system configurations: the changes of the geometrical configurations imply modifications of the mutual inductances that would determine changes in the resonant frequency, making it deviate from the operating one.

The available power picked up by secondary circuits needs conversion in order to be utilized to supply ordinary loads. In particular, for DC loads such as batteries rechargers and remote sensors, the conversion involves both rectification and voltage level stabilization. To this purpose the proposed system uses at the secondary side a full bridge rectifier and low pass capacitive filter. Specifically, the full bridge rectifier is realized by means of 4 fast diodes FR302; the low pass anti-ripple filter is realized by means of an electrolytic capacitor.

Due to the high operation frequency of the system, ripple effects are easily cancelled by means of a not expensive low capacitance component.

4.3.3. Energy parameters according to different loads.

In order to supply the sensors system, which is characterized by low power demand and peak currents, the secondary circuit includes the programmable Zener diode system TL431. The considered component dissipates very low power, offers an input range up to 30 V, and makes available at the cathode terminal a stable output V_k = 3.1 V, which is proportional to the output reference voltage of the Zener system V_r = 2.5 V according to (4.9):

$$V_k = V_r\left(1+\frac{R_{adj}+147\Omega}{1k\Omega}\right) \tag{4.9}$$

Thanks to this choice the power supply can be granted both at very short distances where the voltage regulator input raise towards the full scale input, and at relatively large distances until the input voltage falls beneath 3.1 V.

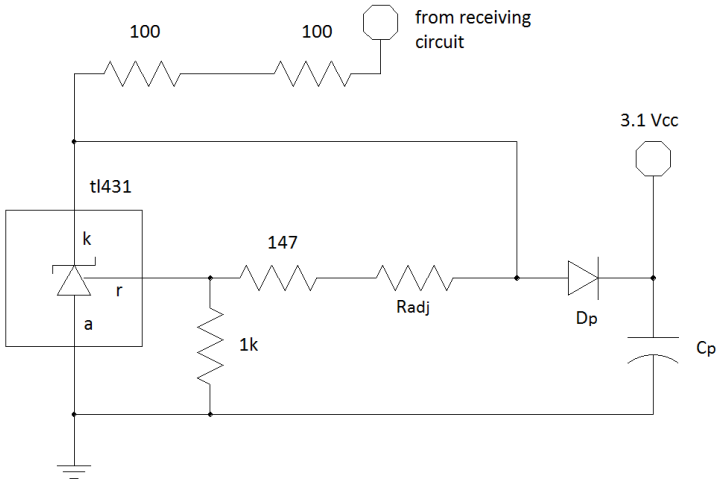

Fig. 4.18. Voltage regulator for monitoring and control hardware.

The output stage of the regulator, made up of the diode D_p and capacitor C_p, can compensate for peak power demands, which are inherent in the regular functioning of the sensors, as well as for voltage swells consequent to resonant structures movements, which regularly occur if the parts of the system are movable. Nonetheless, diode D_p also prevents harmful current backfiring that could occur in the case of momentarily input voltage interruptions.

4.3.4 Recharging system and power supply

One of the secondary circuits is intended to recharge Nickel-Metal-Hydride (NiMH) batteries, therefore it has to work as a stable current source. The layout of the battery recharger is shown in Fig. 4.19. It uses a Darlington TIP121 transistor polarized by the injection of a current in the base region. The current aimed at battery recharging is derived from the emitter terminal of the Darlington transistor, and flows through one of four different resistors selected by means of a switch. The current is limited by the feedback effect acted by transistor bc547 that intervenes as soon as the voltage drop across the selected resistor exceeds 0.6 V; the Darlington source diminishes its output current because a relevant part of the current directed to its base terminal is drained by transistor bc547.

Transistor bc557 is instead utilized to control the light emitting diode and indicates the presence of in-progress recharge operations.

Diode 1n4004 grants protection in case the battery is wrongly connected to the recharging circuit, i.e. with opposite polarity with respect to the right one.

The DC input to the recharging system is conditioned by voltage regulator 7812, not shown in the layout, that limits to 12 V the delivered voltage and avoids voltage swells that can occur whenever the coupled resonant structures are moved very close to each other.

The choice of the appropriate resistor to regulate the current intensity, suitable to perform the recharge operation, depends on the type of NiMH battery and, specifically, on the capacitance of the internal accumulators. According to the

common rule of thumb it has to be equal to 10% of the current that can be figured out from the specified battery capacitance, usually expressed in milliampere-hour.

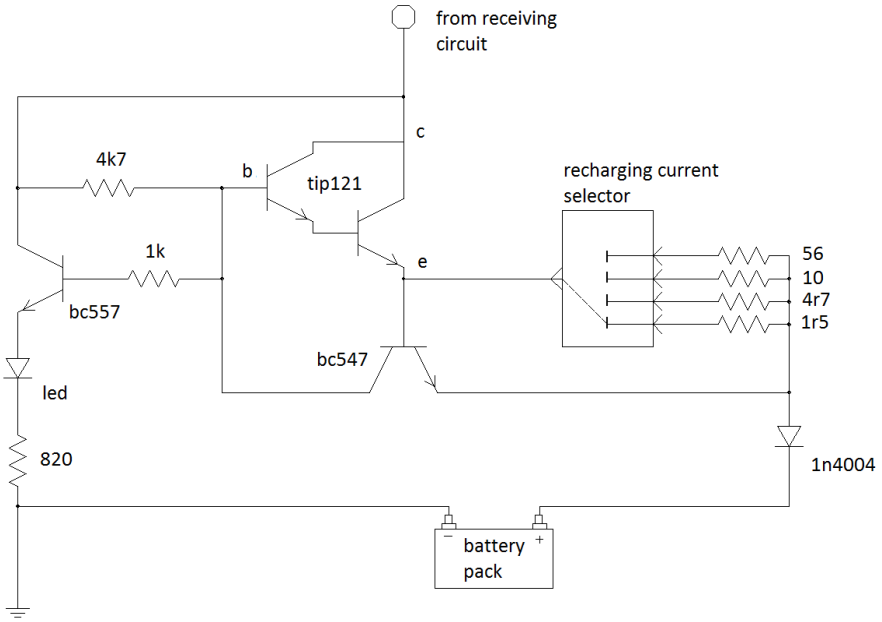

Fig. 4.19. Layout of the battery recharger.

For Li-ion batteries widely employed in cell-phones and commonly recharged through a universal serial bus (USB) connection, a stable DC voltage equal to 5 V and the capability of managing current intensities up to 0.7 A have been provided by means of a USB gate adaptor driven by voltage regulator 7805.

The proposed experimental set up has been tested in different operative scenarios, in which it power has been wirelessly transmitted to one or more loads and utilized to perform batteries recharging or activate a sensor system.

In the first experiments, a single load made up of two serially connected NiMH batteries, each of which characterized by 1.2 V nominal voltage and 850 mAh capacity, has been considered. According to the manufacturer specifications the batteries of the aforementioned type require, at zero charge level, a current intensity equal to 85 mA for 16 hours in order to be fully recharged. Thus, before executing the test the load has been emptied of any residual charge by keeping

it connected to a 100 Ω resistor until the measured current was less than the resolution of the adopted multimeter (1 mA). Then the load has been connected to the terminals of the recharging system, and subjected to a full charge. During the charging operation the injected current has been equal to 60 mA, which is slightly less than the suggested one, and involves a proportionally longer recharging time. The distance between the primary and secondary coils has been equal to 7 cm and the recharging system has been supplied at a constant voltage equal to 7 V, that has assured adequate power transfer to the load. The values of the main parameters measured during the recharging tests are summarized in Table I. As can be deduced by the data in Table I, wireless charging operations imply more power losses with respect to commercial battery chargers, since the power absorbed by the proposed recharging system is almost 6 W, i.e. efficiency is lower than 20 %.

TABLE 4.2. VALUES OF THE PARAMETERS IN RECHARGING TESTS.

Supply Voltage [V]	Received Voltage [V]	Supply Current [mA]	Recharging Current [mA]	Coils Distance [cm]
7.0	**17.1**	**830.2**	**60.2**	**7**

Further tests have been carried out in order to verify the behavior of the experimental set up, already shown in Fig. 4.17. when there are two separate secondary coils one of which serving two different loads. Note that the primary coil is in the middle between a fixed secondary coil on the left, which picks up power and provides it to an active sensor system, and a movable coil on the right, which captures and delivers power to two different loads for batteries recharging operations. The two loads connected to the movable coil consists in two different recharging circuits: the first one is intended to recharge a cell phone battery via USB port, the second one is instead designed to recharge NiMH batteries. During the test, the fixed coil for the zig-bee sensor has been placed at a distance equal to 15 cm from the primary coil, and the functioning of

the load has been monitored throughout the led indicating the presence of the power supply. The movable coil instead has been gradually moved away from the primary coil starting from 2.5 cm up to 18 cm. The test has shown that the recharging circuit for NiMH batteries, which requires a higher voltage to operate, does not guarantee sufficient current if the distance of 15 cm is exceeded. The maximum power absorption of the whole system is obtained for the shortest distance between the movable coil and the primary one, and it is equal to 21 W. It has been observed that the power absorption gradually decreases upon the increasing of the distance between the primary coil and the movable one, and the power absorbed at a distance equal to 15 cm is 15.4 W. Table II gives the values of the parameters measured during the test. In particular, the rows in Table II report: the distance between the primary and the movable coil, the DC voltage and current that supply the push pull-inverter, the DC voltage picked up at the output of the rectifier cascaded to the movable coil, the DC voltage picked up at the USB port terminals, and the DC current injected in the NiMH batteries.

TABLE 4.3. PARAMETERS MEASURED DURING THE TEST WITH MORE LOADS CONNECTED TO TWO DIFFERENT SECONDARY COILS

Distance [cm]	**2.5**	**5**	**10**	**15**	18
Supply Voltage [V]	**14**	**14**	**14**	**14**	14
Supply Current [A]	**1.8**	**1.5**	**1.3**	**1.2**	1.1
Received Voltage [V]	**37.3**	**30.1**	**20.2**	**10.5**	6.3
USB Voltage [V]	**4.988**	**4.988**	**4.973**	**4.973**	4.953
NiMH Recharging Current [mA]	**57.0**	**56.8**	**56.2**	**47.1**	3.01

4.4 A possible solution for wireless drone battery recharging.

Unmanned Aerial Vehicles (UAVs), also called drones, have been being proposed for an increasing number of applications where measurements and or images have to be made or taken autonomously from a determined height.

Drones like helicopters use vertical oriented rotors to lift and navigate forward. Thanks to the use of modern flight controllers, they often can fly autonomously. Namely, the user can mark target points on a map to which the helicopter is driven by the software controller without any other interventions of the user. Once on the target, the helicopter performs the intended task, such as landing, catching aerial photos, or releasing loads. But, in order to be fully autonomous the helicopters should be also capable of recharging the on board batteries, as it is required to complete long lasting missions, without requiring any external interventions.

Common factor among all the applications is the need of determining the right tradeoff between pay load and endurance, since increasing batteries capacity means reducing payload. For instance, with about 450 g of payload, a helicopter can have an autonomous flight endurance of about twenty minutes. This implies that missions must be shorter than 15 minutes and at landing a human being must be available for battery charging if a new take off must have place.

A helicopter equipped with a suitable hardware that allows autonomous recharge by simply landing on a given platform is presented. The front-end of the on-board recharging circuit is capable of linking the time varying induction flow, produced by a circuit integrated in the landing platform, and converting the power associated to the magnetic field from AC to DC in order to recharge the helicopter battery.

For various applications instead, aerial vehicles should be capable of autonomously connecting to a recharging station. Unfortunately, the most common approaches proposed for autonomous recharge lack of sufficient reliability: light vehicles often undergo fails because of the difficulties at connecting to the recharging station. The fails are due to the poor capability of

the vehicle of precisely landing on the recharging platform in order to assure the electrical contact of the pins to the terminals of the on-ground battery recharger. Large size copper terminals are deployed to increase the probability of successful connection, thus facing the risk of battery terminals short-circuits in the case of wrong landings. In order to allow more precise landing a suitable platform featured with a passive centering system has been proposed in together with an on board vision system that drives the control system in landing.

In any case the power transmission is entrusted to a galvanic contact between copper terminals. In the practice it has been experienced that all solutions requiring electrical contact between the on-board hardware and the ground source can also fail or undergo temporary breakouts because of dust or corrosion due to chemicals spoiling the ground contacts, and mechanical vibrations during the stopover.

Power transfer systems that allow overcoming the aforementioned problems and performing battery recharging without electrical plugging, or any other locked connection to the energy source are today the focus of attention of many scientific proposals concerning ground and aerial unmanned vehicles.

The most of these systems exploit coupled circuits to transmit power within very short distances. The first circuit, in the following named primary circuit, is installed immediately beneath the landing pad of the ground platform. It sustains a time varying magnetic induction flow by means of which the electrical power is transferred to the user as in an air core transformer. The other circuit, in the following referred to as secondary circuit, links the aforementioned flux and retrieves the electrical power demanded by the load. It is worth noting, however, that the secondary circuit is installed on board of the helicopter and represents an additional weight that could reduce the maximum payload of the vehicle.

As a consequence, the real problem is: how to optimize the power induction system design and how to obtain the best tradeoff between maximum payload and easiness in landing.

In the next paragraph, the proposed recharging system as well as the specific solution for its installation on-board of a helicopter are shown. Some tests both at the design and development stage are presented.

4.4.1 adapted system for drone battery recharge

In order to avoid the need of electrical plugging for battery recharge, the power transfer system exploits magnetic induction coupling between a primary circuit integrated in a landing platform on the ground and a secondary circuit on board to the helicopter.

Generally, in an induction based power transmission system the primary circuit produces a time varying magnetic flux, which is typically attained by injecting an alternate current into one or more coils. The use of more coils is typically exploited to increase the power transmission capability of the system at the expense of the complexity of the whole architecture. For instance battery recharging stations could use more primary coils deployed beneath a pad and/or within vertical walls surrounding the landing zone.

Sometimes, due to complex structures, and/or non-rigid configurations of the overall system, it is convenient to take particular care in the design of the primary circuit. Specifically, it is opportune taking advantage of resonance conditions, that make the system operate at a natural operation frequency: the alternate currents rising into the coupled coils can thus assure even in the presence of an unstable geometrical configuration and occasional parameters variations the maximum power transfer.

In fact, in the case of autonomous recharge of drones, the geometry of the whole system during the recharging operations is not accurately known, since it

depends on the position in which the helicopter lands, which can also vary in time due to setbacks.

The ground platform hosts the primary circuit connected to a virtually everlasting energy source, for example the main electrical grid.

Actually, the proposed system uses a primary coil, in which a resonant current originates a magnetic field to excite a corresponding current in the secondary coil; resonant conditions are arranged by introducing capacitors in the circuitry. The primary circuit is directly connected to the external energy source and exhibits an interface including one single coil positioned beneath the landing pad of the ground platform.

The magnetic flux produced by the primary circuit is partially concatenated by the coil of the secondary circuit, which is connected to capacitors to form a resonant structure.

The coil is mounted on board to the helicopter and connected to the recharging channel of the battery. The connection passes through a full bridge rectifier complemented with a low pass anti-ripple filter on the side of the secondary circuit for adapting the parameters of the electrical power and recharging the battery. The secondary circuit has to be compliant with several important requirements related to size, and weight, for not impeding the regular operations of the vehicle.

The full bridge rectifier can be realized by means of 4 fast diodes, while the low pass anti-ripple filter by means of an electrolytic capacitor. Due to the high operation frequency of the system, ripple effects are easily cancelled by means of a not expensive low capacitance component.

Often, recharging circuits require a control channel for the power channel utilized to perform the recharge. In order to supply the control channel, which is characterized by low power demand and peak currents, the secondary circuit could include a programmable Zener diode system. Zener diodes dissipate low power, offer large input ranges, typically up to 30 V, and make available at the

cathode terminal a stable output voltage, proportional to the output reference voltage of the Zener system.

The output stage of the Zener system is made up of a diode and a capacitor and can compensate for variations in the power demands. These variations are inherent in the regular functioning of the control hardware, as well as for voltage swells consequent to resonant structures movements, which could occasionally occur because of an external stimulus due to wind or mechanical vibrations.

The design of the power channel is different according to the battery type to be recharged. For instance if it is intended to recharge Nickel-Metal-Hydride (NiMH) batteries, it has to work as a stable current source.

The choice of the appropriate configuration to regulate the current intensity, suitable to perform the recharge operation, depends on the type of NiMH battery and, specifically, on the capacitance of the internal accumulators. According to the common rule of thumb it has to be equal to 10% of the current that can be figured out from the specified battery capacitance, usually expressed in mAh.

Differently Li-ion batteries, nowadays widely employed in cell-phones and commonly recharged through a universal serial bus (USB) connection, require a stable DC voltage and the capability of managing current intensities up to fractions of amperes. These requirements can be satisfied by means of a USB gate adaptor driven by a suitable voltage regulator.

4.4.2 The proposed system.

At design stage several configurations of the recharging system have been first evaluated from an analytical point of view and then simulated by means of a design tool (Saber Sketch).

For the primary coil an helical with a diameter equal to 30 cm and including N = 4 turns characterized by a cross section equal to 3 mm^2 has been considered. To estimate its inductance, L, an in-air single layer model has been adopted, according to (4.10):

$$L = \frac{\left(aN^2\right)}{22.9a + 25.4h} \tag{4.10}$$

being *a* the radius of each turn and *h* the height of the helical, obtaining the value 8.96 µH. For the secondary coil characterized by radius 7 cm, cross section 2.5 mm2, and height 1.1 cm the same model provides an inductance value equal to 4.16 µH.

The resonant frequency of the primary circuit has been determined by connecting in parallel to the coil a 660 nF capacitor, obtaining a value equal to 65.6 kHz. In order to tune the secondary circuit at the same frequency a 1.42 µF capacitor is needed.

Since the drone can land in several different positions, characterized by misalignments between the axis of its own coil and that of the primary coil, a circular coil with a diameter much larger than that of the secondary coil has been considered.

Thanks to this choice, even in case of relevant misalignments, the secondary coil is always completely contained in the area of the primary one.

The prototype mounted and tested is shown in Fig. 4.20. The circuitry of the system has been mostly realized according to the specifications given before. In detail, the helical has been made up wrapping four times twisted insulated copper wires, each wire characterized by a cross section equal to 1.5 mm^2. For the other parts of the system, the components available on the shelf have been used, so that the values of some components have been slightly different from those considered at design stage.

For the prototype set up at development stage, measurements performed by means of a digital impedance-meter, have given for the primary coil a 9.95 µH inductance, and a 5 mΩ resistance values, whereas for the secondary coil a 4.01 µH and a 25.68 mΩ. The measured frequency has been 60.5 kHz, which is almost 10 % less than the one considered at design stage. This is mostly due to the large

uncertainty, almost 20 % of the low cost capacitors utilized to build the resonant structures. A dissipative load connected to the secondary coil, in the best case, collects about 20 W.

Fig. 4.20. Prototype mounted and tested at development stage.

The secondary circuit of the proposed recharging system is going to be mounted on board of the Unmanned Aerial Vehicle shown in Fig. 4.21. Moreover, further suitable hardware is going to be designed and realized in order to cope with the specific requirements to be satisfied for performing the recharge operation. The UAV is a quad-rotor manufactured by AIR DRONE SRL. The drone allows to install different kind of sensors and processing units up to a maximum suggested payload of 450 g. At maximum payload the drone endurance is limited to 15 min using 2x5000mAh 4s batteries.

The drone uses the NAZA-M V2 flight controller and needs correct weight balancing to perform at best. The Naza-M V2 has different Built-In Functions: Multiple Autopilot Control Mode, Enhanced Fail-safe, Low Voltage Protection, S-Bus Receiver Support, PPM Receiver, Support Independent PMU Module and 2-axle Gimbal Support. The Naza used is composed by four parts: the Main Controller (MC), the GPS module, the Power Module Unit (PMU) and the LED module.

Above all it is possible to add a waypoint navigation system in order to simplify fly missions. Both the GPS accuracy and the integrated Intelligent Orientation Control (IOC) function of the helicopter determine the precision in reaching the target. In outdoor environments, the integrated GPS module can be used for a complete autonomous flight: take off, navigation and landing. Anyway, though NAZA V2 it is possible to fly indoor without GPS assistance, the system is not able to autonomously perform these tasks in indoor or GPS-denied environments.

The Naza-M V2, can be configured for a Quad-rotor I4, X4, it has an Electronic Speed Control (ESC) with a 400 Hz refresh frequency. The working voltage range are: for the MC: 4.8V~5.5 V and for the PMU: 7.4 V~ 26.0 V.

The power consuming in normal condition is about 0.6 W (0.12 A @5 V), and 1.5 W (0.3 A @5 V) in case of maximum speed. The flight performance are expressed as: Hovering Accuracy (Gps Mode) about Vertical: ± 0.8m Horizontal:± 2.5 m; Max Yaw Angular Velocity 200°/s; Max Tilt Angle 35°; Ascent/Descent 6 m/s, 4.5 m/s.

Fig. 4.21. The helicopter equipped with the prototype induction based recharge system.

4.5 Transcutaneous wireless energy transmission: battery recharge for implanted pacemaker.

The number of implanted medical devices such as pacemakers, artificial hearts, and nerve stimulators is rapidly increasing with the continuing advancements of biomedical technologies.

Pacemakers are electronic biomedical devices necessary for the treatment of specific cardiovascular diseases. Energy provision required by the pacemaker to operate is usually granted by means of long lasting batteries, that anyway require periodical checks and substitution. Wireless energy transfer to medical implants is therefore desirable, since it offers a non-invasive way to recharge batteries of implanted devices. It could allow to delay surgery for substitution. In this section the proposed system shows that transcutaneous energy transfer can be attained by coupling the electronics of the implanted hardware with an external energy source. In particular it supplies a primary coil, which is positioned at contact with the chest of the patient, with an alternate current to produce a magnetic flux; the latter enfolds a secondary coil, which is instead implanted in the human body in the proximity of the pacemaker, and allows to retrieve the energy to recharge the implanted battery. To limit the eddy currents that would be induced in the titanium case of the pacemaker and could produce undesired heating and/or malfunctioning, the proposed system utilizes a magnetic shield; the shield is also useful to avoid that the aforementioned parasitic coupling worsens the energy transfer efficiency.

Batteries usage is a very debated topic. Many scientists maintain that batteries are unavoidable for biomedical devices and therefore support research efforts aimed at miniaturization and efficiency increments; their goals are small size long lasting batteries that make surgery the least invasive one. Many others believe that the use of battery-powered devices has to be more and more often discouraged, especially if the battery replacement appears troublesome or invasive, as it is for implanted medical devices whose replacement needs surgery. They favorably look at wireless energy transmission approaches that

can allow remotely powering of biomedical devices and thus to avoid surgery for regular substitution of the battery of the implanted device, or else of the device as a whole.

For pacemakers high energy density and prolonged longevity embedded batteries are typically employed. Depending on their operation mode and related frequency of stimulation, the batteries of pacemakers can last up to seven years. Nonetheless, in the course of the battery lifetime, patients undergo to regular check-ups, during which the battery life could be extended by means of intermediate recharge operations. In fact, if the pacemaker was preventively equipped with the necessary hardware to retrieve the energy spanned by an external source, the recharge could be attained without any surgery, but just by means of a few hours treatment during which an active coil is positioned upon the chest of the patient.

At present the use of radio frequency systems to radiate energy from an external source to the implanted battery has been already proposed in the literature. Similarly transcutaneous energy transmission that exploit magnetic induction principles have been also considered. Some contributions published in the scientific literature demonstrate throughout careful numerical analyses how the performance of an energy transmission system depends on the selected frequency and can be improved by shielding the pacemaker with a foil characterized by high magnetic permeability.

In the following an experimental approach is instead adopted to investigate the feasibility of a wireless energy transmission system to recharge the implanted battery. To this aim a prototype is built up and several experiments with different system configurations are carried out in order to both analyze its performance in quasi-real operating conditions and highlight how coils positions affect the energy transfer efficiency. Also, the important role of the magnetic shield is examined throughout the experiments.

4.5.1 Rearranged system for transcutaneous energy transfer.

Due to the complex structure, and above all the non-rigid configuration of the system, the circuit that drives the primary coils is designed in order to take advantage of resonance conditions, that allow the adaptation to a natural resonant frequency of the system for the alternate current rising into the coils.

Specifically, the magnetic flux produced by the primary circuit is partially concatenated by the coil of the secondary circuit, which is connected to a capacitor to form a resonant structure. A full bridge rectifier complemented with a low pass anti-ripple filter on the side of the secondary circuit adapts the parameters of the electrical power in order to supply the load, or, as it is in the case of the pacemaker, recharge the battery.

Actually, the proposed system uses a primary coil, in which an alternating current originates a magnetic field to excite a corresponding current in the implanted secondary coil, and maximizes the efficiency by pursuing resonant conditions that are arranged by introducing in the circuitry capacitors.

The primary system is directly connected to the external energy source and exhibits a body interface including one single coil to be applied to the outer surface of a cutaneous layer on the chest of the patient. It is locked to the chest of the patient using adhesive tape or other appropriate supporting material. The secondary coil is instead implanted in the body of the patient, in the vicinity of the pacemaker separated from it by a magnetic shield that prevents pacemaker heating and coupling interference. Nonetheless, the secondary coil has to be compliant with several important requirements related to size, weight, and above all biocompatibility. The secondary coil of the proposed system has to grant a constant power demand of 2.5 W, that is sufficient to recharge the battery in a reasonable time.

Fig. 4.22 shows a diagram of the primary circuit adopted to inject the alternate current into the LC structure to sustain the power transmission. The circuit is made up of two identical conducting branches, each one consisting of a MOSFET transistor, a diode (MUR860) and a 220 Ω resistor. Each MOSFET is

complemented with a dedicated snubber circuit and a free-wheeling diode (by398) that assure protection during the switching transients. The central tapped inductor made up of 0.5 µH twin inductors, parallel connected to the capacitor, represent the front-end coil that is coupled to the secondary circuit of the system. The 20 µH inductance connected to the central tap of the coil limits inrush currents from the DC supply at MOSFET switching.

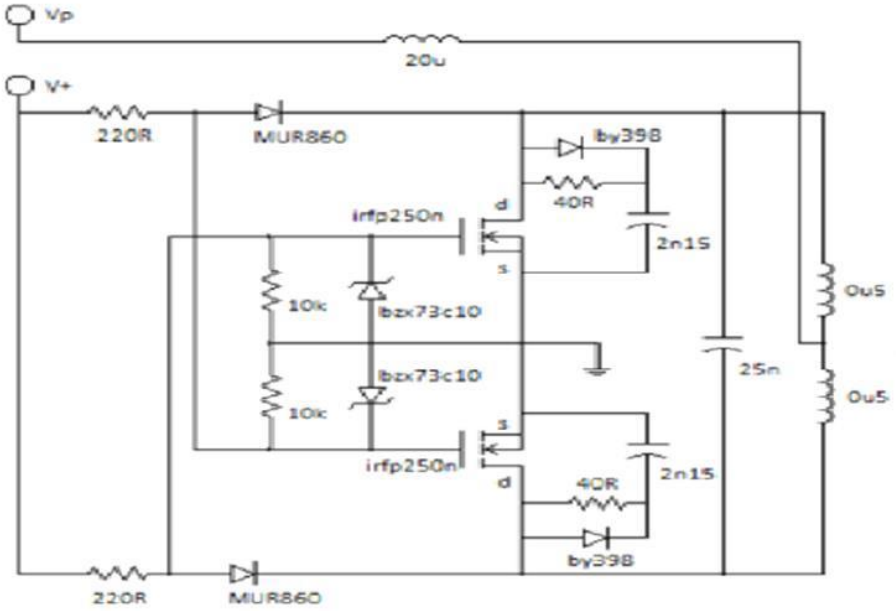

Fig. 4.22. Layout of the primary circuit including the resonant structure that sustains the magnetic flux to perform the energy transmission.

The primary circuit works as an inverter transforming the energy provided by the DC supply into AC energy. Specifically, the inverter oscillates at the resonant frequency that characterizes the LC structure: at steady state the MOSFET transistors work in push-pull mode by complementary switching on and off upon the polarity alternation of the sinusoidal voltage across the capacitor. The voltages and currents in the LC structure are characterized by a natural resonant frequency, that can be observed when the primary circuit is unloaded. In loaded conditions the resonant frequency changes because of the mutual coupling.

At design stage a resonant frequency equal to 88 kHz has been chosen for the system; consequently the inductances, capacitances, and distances between the coupled structures that affect the mutual coupling have been coherently selected. The major advantage in the use of this kind of oscillator consists in its inherent self-tuning capability, which assures a natural tracking of the maximum power transmission condition. An inverter driven to operate at a given frequency, without auxiliary systems implementing articulated feedback control logics, would exhibit poor efficiency due to unavoidable detuning effects related to parametric variations, mainly due to changes in the system configuration. In fact, the changes of the geometrical configurations imply modifications of the mutual inductances that would determine changes in the resonant frequency, making it deviate from the operating one. The available power picked up by the secondary circuit needs to be transformed into DC power in order to be utilized to supply ordinary loads. The conversion involves both rectification and voltage level stabilization. To this purpose the proposed system uses at the secondary side a light solution made up of a rectifier and an anti-ripple capacitor as low pass filter. The rectifier is a full bridge circuit realized by means of 4 fast diodes FR302, whereas the low pass anti-ripple filter consists of a cheap electrolytic capacitor. Ripple effects are characterized by a frequency equal to 176 kHz and are easily cancelled by means of the capacitor. Specifically, at the resonant frequency f = 88 kHz, the capacitance of the anti-ripple capacitor is chosen according to (4.11):

$$C = 1.2 \frac{I_l}{f V_r} \tag{4.11}$$

in which, I_l is the load current, V_r is the amplitude of the residual voltage ripple and 1.2 represents a constant that includes a 20% margin.

Typically the use of identical LC structures at the primary and secondary sides, meaning that the two front-end coils have the same geometry, the same self-

inductance, and are connected to identical capacitors, assures the best working conditions. Unfortunately for the considered application, the secondary circuit has to be implanted together with the pacemaker, thus its design has to satisfy additional constraints that is not convenient to retain for the primary circuit design.

For the primary coil a circular geometry is chosen and optimized in order to obtain sufficient intensity for the magnetic induction at the center of the distant secondary coil. The primary coil is realized with a copper wire conductor characterized by cross-section equal to 1.5 mm^2, wrapped around a cylinder without overlaps for a number of turns equal to 10; the width of the coil along the longitudinal direction is equal to 15 mm (Fig. 4.23). The inductance measured by the Agilent 4263B LCR impedance meter, at 100 kHz is 7.28 μH.

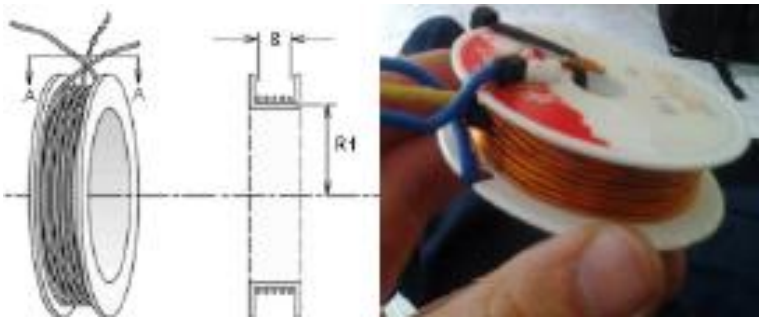

Fig. 4.23. Primary coil design and prototype.

The secondary coil is realized taking into account the constraints related to position and size. In fact the coil has to be placed in the same cavity of the body hosting the implanted device. In particular, the elliptical spiral type geometry shown in Fig. 4.24 is adopted. The coil is glued on a plastic support and it is characterized by the following average parameters: outer semi-major axis 22 mm, inner semi-major axis 14 mm, outer semi-minor axis 16 mm, inner semi-minor axis 8 mm, coil planar width = 8 mm. The elliptical geometry allows the deployment of a sufficient number of turns, maximizing the surface area enfolded by the induction field. Due to the different geometry and inductance of

the secondary coil with respect to the primary coil, it is not possible to use capacitors characterized by equal values of capacitance. The capacitor connected to the secondary coil is chosen in order to let the two structures resonate at the same target frequency.

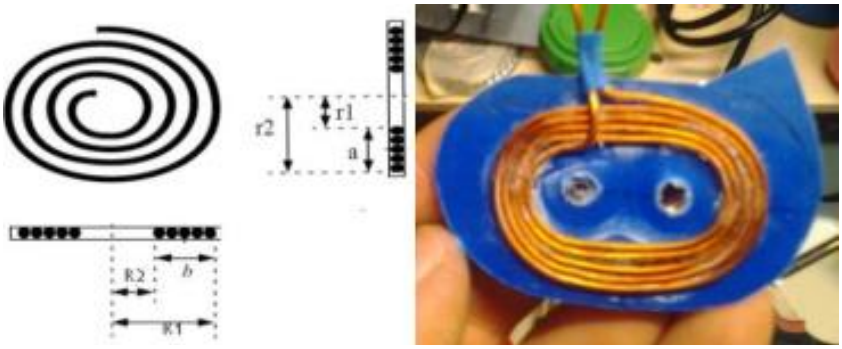

Fig. 4.24. Secondary coil design and prototype.

In the realization of the prototype it is also necessary to accurately measure the inductance exhibited by the secondary coil during the effective operating conditions. The measurement has to be carried out when the secondary coil is positioned on the outer top surface of the pacemaker and is separated from it by a ferromagnetic shielding layer. The shield is necessary to avoid that the magnetic flux induces eddy currents in the titanium frame of the pacemaker.

4.5.2 eddy currents

It is believed, below, useful to show in more detail what are the effects and principles that govern the presence of parasitic currents, also called eddy current, inside conductive materials. Typically, when designing magnetic circuits for transformers or inductors, eddy currents effect turns out to be not useful and productive for the application itself, as such a current seat of dissipation and noise; for this reason the classic assessments of the phenomenon in question are typically framed in terms of disadvantage and elimination of the phenomenon. In other cases, such as those relating to sensors and transducers, but not like this, what we try to do is exploit this phenomenon as intentionally causing

sensor operating principle the eddy currents, avoiding the implementation of all those constructive methods suitable for their limitation and using these currents to produce a variation of the field , which can be observed and measured.

Eddy current induced within the conductive material core of inductors, transformers and, in this case, the pacemaker, result in the power dissipation in the core itself, which is commonly referred to as Eddy current loss.

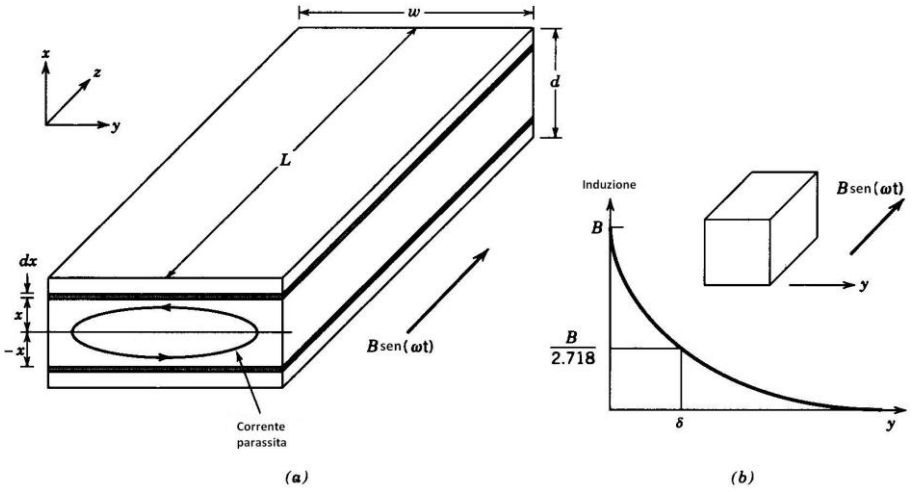

Fig. 4.25 – (a): eddy currents induced in a subtle element of conductive material as a result of the induction field with law B (t).
(b): decay of the induction field B with reference to depth y material.

The most immediate effect of this phenomenon, is an increase in core temperature and, consequently, of all parties to intimate contact, especially the windings are arranged around the periphery.

With reference to figure 4.25 (a), consider a conductor surrounded by a uniform field of induction and time-variant sinusoidal law:

$$\delta = \frac{1}{\sqrt{\pi f \mu \sigma}} \tag{4.12}$$

$$B(t) = B \cdot sen(\omega t) \tag{4.13}$$

Assume that the dimension *d* is less than the thickness of penetration δ, previously defined by the relation (4.12). In this way it can be considered that

the eddy currents induced are not due to reduction in the field of induction B in the material. Assume that the conducting material, such as a sheet used in electromechanical constructions, have a conductivity σ.

If you were to treat other material, simply put a different conductivity value, without which those proceedings lose of generality. Now consider a path of infinitesimal thickness dx, placed, as shown in the figure, at the abscissa x and-x, track, in the corresponding xy plane of the conductor. The flow entirely concatenated from that surface, may be represented by the following relation

$$\phi(t) = 2xwB(t) \tag{4.14}$$

According to Faraday's law, this time-variant flux will cause an induced voltage *v(t)* inside of the electrical circuit so identified, characterized by the same law, and can be expressed as:

$$v(t) = 2xw\frac{\partial B(t)}{\partial t} = 2wx\omega\cos(\omega t) \tag{4.13}$$

At this point, the infinitesimal circuit resistance of the circuit can be calculated, with depth *L*, thickness *dx*, and length *2w*.

$$r = \frac{2w\rho_{nucleo}}{Ldx} \tag{4.16}$$

With reference to these elementary quantities, appropriately identified, the instantaneous power dissipated in elementary circuit can be calculated. With reference to Ohm's law, it is obtained:

$$\delta p(t) = \frac{v^2(t)}{r} \tag{4.17}$$

By integrating this quantity on the entire volume, the average total power P_{cp} dissipated in time for effect of eddy currents induced, is obtained.

$$P_{cp} = \left\langle \int \delta p(t) dV \right\rangle = \left\langle \int_0^{d/2} \frac{\left[2wx\omega B\cos(\omega t)\right]^2 L dx}{2w\rho_{nucleo}} \right\rangle = \frac{wLd^3\omega^2 B^2}{24\rho_{nucleo}} \tag{4.18}$$

Note that in the previous report the symbol $\langle\ \rangle$ indicates the average over time.

Finally it is possible to calculate the specific power dissipated due to the eddy currents induced per unit volume, as the following way:

$$P_{cp,sp} = \frac{d^2\omega^2 B^2}{24\rho_{nucleo}} \tag{4.19}$$

Note that the power dissipated inside the material is a square function of the thickness *d* and, therefore, to limit the effect of such dissipation, practice suggests to limit this thickness by adopting lamination stack. Note, however, that a considerable thickness, like that of an object the size of a pacemaker, introduces a high amount of loss in material, which is considered as the only disadvantage for the application.

Besides the specific losses are once again, related to the square of the frequency. For this reason, to shield an object from the field, it is necessary to introduce materials that are immune to the eddy currents. The choice falls on the use of materials made through ferrite powders appropriately sintered and compacted, grouped in thinness sheets. These are characterized by high resistivity, Eddy current losses induced effect is greatly reduced.

The main effects of eddy currents in the titanium would consist of heating and supplemental undesired loading that would reduce the energy transmission. For the prototype a ferrite enclosure, made up of four 0.225 mm foils is employed to

surround and shunt the magnetic flux sustained by the primary circuit. Table 4.4 shows the inductance of the coil of the secondary circuit measured in different operating conditions; in the presence of the ferrite shield no appreciable changes between the value measured with and without the presence of the titanium pacemaker are observed. The presence of the ferrite shield also prevents the temperature increments of the titanium case due to heating produced by eddy currents. Conversely, it can be appreciated how the absence of the magnetic shield involves a 45% diminution of the inductance.

Test type	[μH]
In-air coupling	**1.09**
Secondary coil metal case and no ferrite layer	0.59
Secondary coil metal case and a single ferrite layer	0.75
Secondary coil metal case and 4 ferrite layers	**1.08**
Secondary coil and no metal case and a single ferrite layer	1.16

Table 4.4. Secondary coil inductance: the use of ferrite shields mitigate the presence of the titanium medium.

4.5.3 performance assessment

In order to assess the performance of the proposed prototype an experimental set up including: a primary circuit with a push-pull inverter and a resonant LC structure (1), a secondary system with a resonant LC structure and a full bridge rectifier (2), a power resistor for emulating a load (3), a pacemaker (4), a DC laboratory power source (5), and further measurement equipment (6) has been arranged (Fig. 4.26).

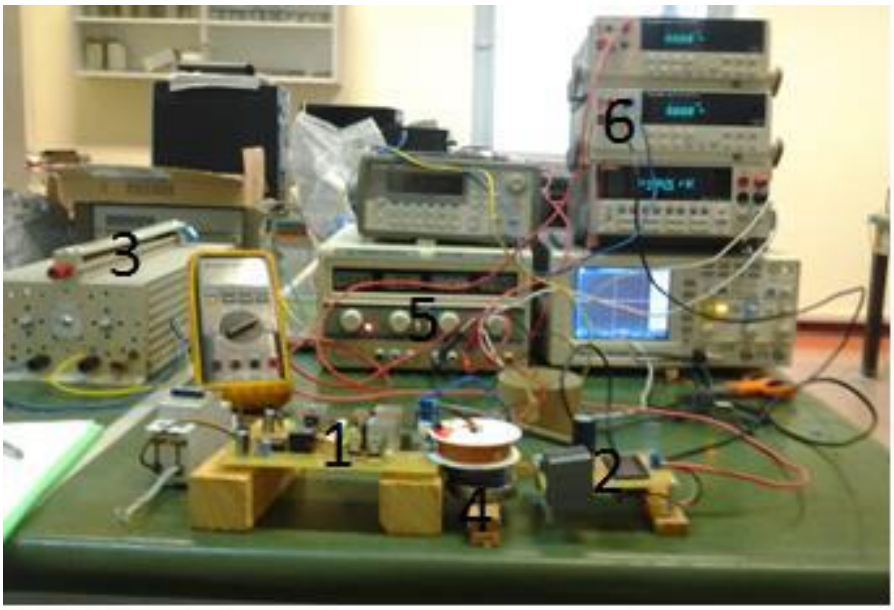

Fig. 4.26. Experimental setup including the main parts of the proposed system and the instruments adopted during the prototyping stage.

Although for the specific application the distance between primary and secondary coils is very short, the axial alignment between the two coils cannot be well verified and granted. In fact the implanted device, although fixed by stitches, can move a little around the implanted point. The physician cannot locate with sufficient accuracy without the help of radio imaging systems the exact position of the implanted secondary coil. To assure energy transfer the system has to grant acceptable performance even in the presence of axial misalignments, undesired tilt angles, and excessive distance.

Hereinafter, the results of a number of experimental tests highlight how the system behaves in the presence of the aforementioned system shortages. The tests are carried out by supplying the system at constant voltage equal to 15 V and progressively varying the parameters that identify the configuration under test. The transmission distance is equal to 17 mm, corresponding to the distance for a device that is correctly implanted. To emulate the 2 W power absorption of the battery during recharge, a 19 Ω resistive load has been connected at the output of the recharger circuit.

Axial misalignment

In these tests, keeping constant to 17 mm the distance between the primary and secondary coil, the primary coil is moved along the minor axis of the receiving elliptic coil, starting from a perfect alignment condition, and the power dissipated on the test resistor is measured Fig. 4.27.

Similarly, under the same test conditions mentioned above, the primary coil is moved along the major axis of the secondary elliptic coil and the power dissipated on the test resistor connected to the battery recharger is measured Fig. 4.28.

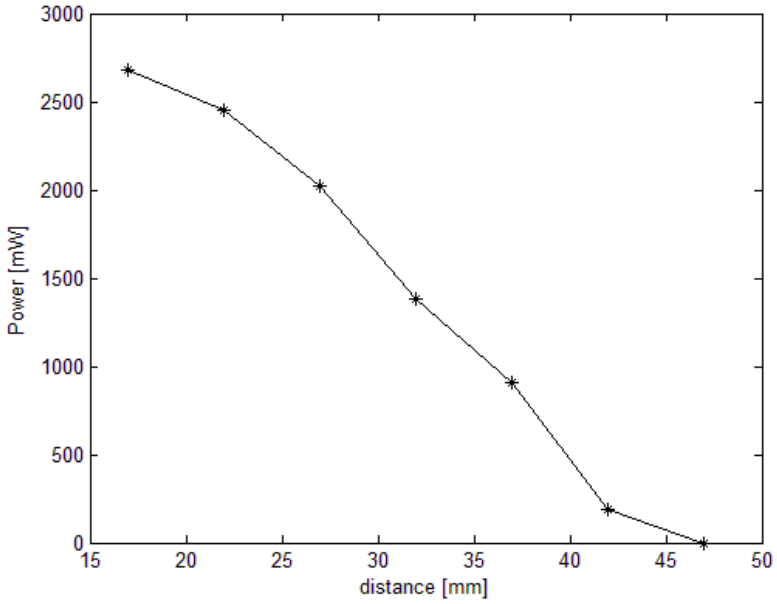

Fig. 4.27. Power absorbed by the resistive load connected to the recharger versus misalignment distance; the primary coil moves in the direction of the minor axis of the ellipse.

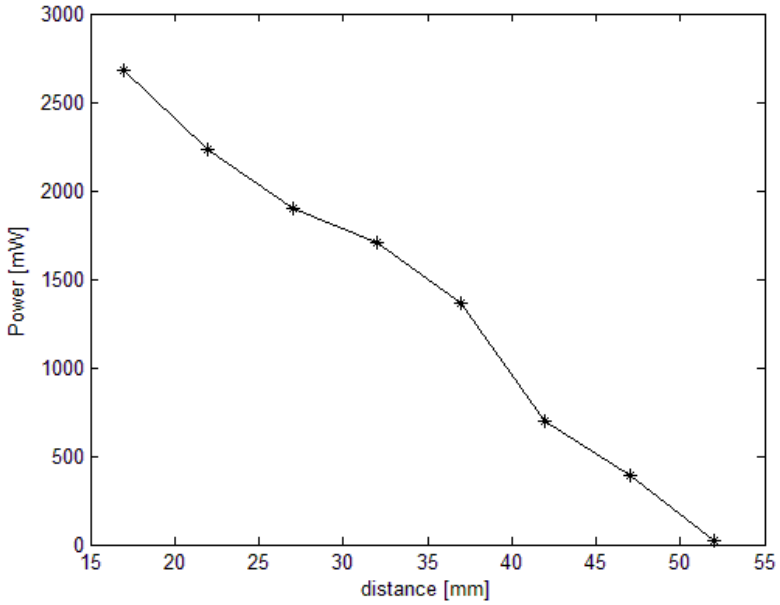

Fig. 4.28. Power absorbed by the resistive load connected to the recharger versus misalignment distance; the primary coil moves in the direction of the major axis of the ellipse.

Tilt angle

The primary coil is also gradually rotated, keeping its center aligned with that of the secondary coil, up to a maximum tilt angle equal to 25 degrees. The results obtained in this test are shown in Fig. 4.29.

Excessive distance

In these tests the primary coil is progressively moved away from the secondary coil, which should be set at 30 mm from it, until the power transferred to the load is below 10% of the necessary power Fig. 4.30. During these tests, no tilt angle and perfect axial alignment are considered.

In all tests the overall efficiency at a distance equal to 17 mm is equal to 7%. Fig. 4.31 shows the trend of overall efficiency measured during the tests related to excessive distance between primary and secondary coils.

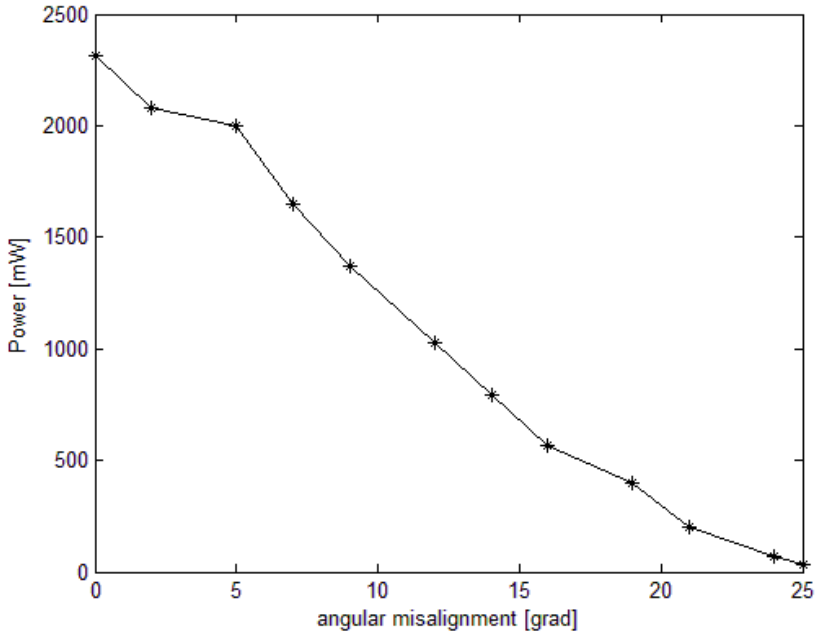

Fig. 4.29. Power absorbed by the resistive load connected to the recharger versus tilt angle up to a maximum of 25 degrees.

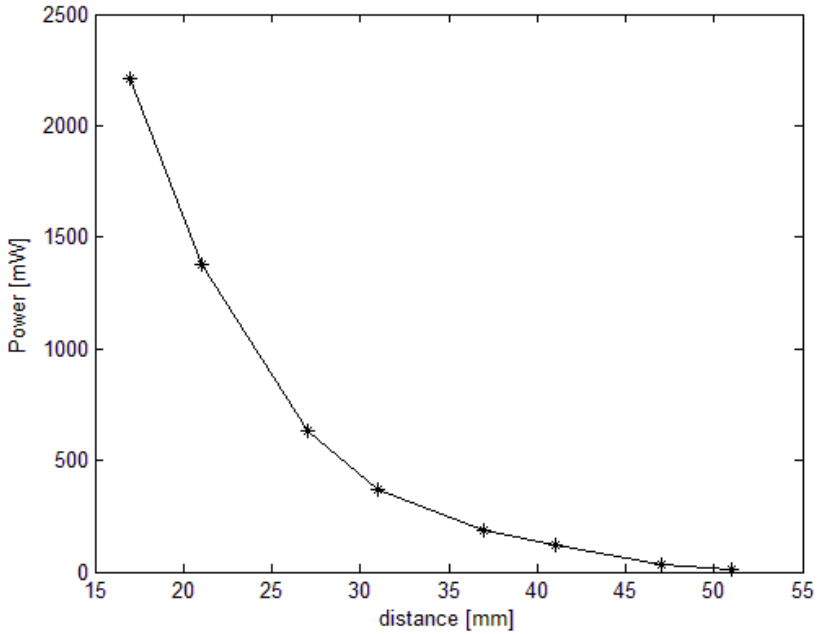

Fig. 4.30. Power absorbed by the secondary coil versus distance.

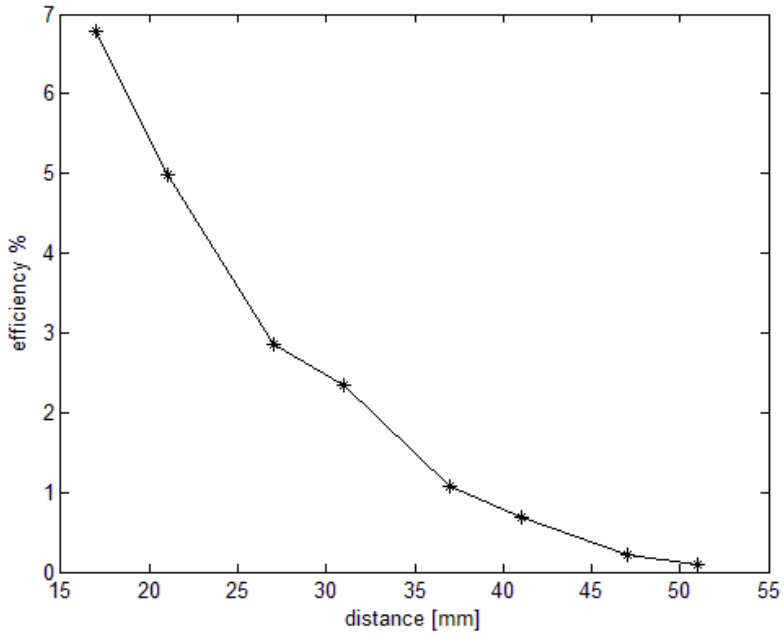

Fig. 4.31. Overall efficiency measured for increasing distance between primary and secondary coils.

4.6 Resonant mutually coupled system for ground monitoring application.

Information on soil moisture are of paramount importance for numerous engineering studies, given the close correlation between the mechanical properties of soils with their water content. For hydraulic and geotechnical engineering, monitoring and direct measurement of water content, along with other conditioning factors of slope stability, constitute an indispensable stage for understanding and preventing triggering mudslides and therefore provide a useful contribution to knowledge in various stages of management of a slope. Infiltration mechanisms depend on several factors, such as the structure of the subsoil, the boundary conditions and characteristics of hydraulic conductivity of soils that constitute it. For these reasons, frequent monitoring is required. For the use of water resources, soil moisture monitoring is the starting point for a proper management of the resource, often insufficient for irrigation and always in competition with civil and industrial uses. A careful management involves on the one hand a limitation of waste and the other a water use optimization. Also in road engineering is useful knowledge of moisture content of soils for aspects related to the susceptibility of the mechanical behavior of building materials. In the study of environmental problems, for example related to hydrogeological situations, often requires monitoring the spatial distribution of the volumetric water content and the definition of preferential water flow. Methods for measurement of water content in the soil are varied, the best known are the TDR time domain reflectometry, ERT electrical resistivity tomography and EMI electromagnetism. In this paper, the authors propose a first phase of definition and development of a system for the measurement of electric conductivity of soil through EMI technique. The attention is focused on the physics of the problem and the definition of the architecture of the system, verifying the effectiveness of the device in the presence of various soil configurations. Later stages of processing and interpretation of the information gathered and analysis of waveforms collected are left to future developments.

4.6.1 EMI technique.

The method is based on the response generated from the ground, following the stress induced by a primary electromagnetic field (c.m.p) produced by an alternating current flowing through a primary coil (P). Once generated, the c.m.p is present above and below the Earth's surface. The c.m.p component that penetrates into the subsoil, can meet electrical conductive buried objects. In this case, through the motion of charge present at each point of the object, electrical currents are produced. These currents are called Eddy currents. They are directly proportional to the apparent conductivity (C.E.a) of the conductor, measured in mS/m. The underground Eddy currents, also produce a magnetic field (c.m.s), directly proportional to the induced currents that created it. Therefore, the c.m.s and its geometric components, quadrature and phase, are conductivity characteristics of geological structures investigated. On the surface, the c.m.s. combines with the primary one, the resulting field is concatenated with a secondary winding (S). This magnetic field is detected and recorded by the secondary coil. The differences between the primary magnetic field and the resulting magnetic field, detects the presence of conductive objects into the ground and allow to obtain information about their geometry and their electrical properties. The apparent electrical conductivity is calculated as phase difference between the primary magnetic field and the secondary magnetic field. The interpretation of phase difference leads to the determination of the conductivity value of the subsoil of the concerned area. The measurement uses the phenomenon of electromagnetic induction, which generates a secondary electromagnetic field into the ground, the intensity of which depends on the physical characteristics of the soil itself. With the same primary electromagnetic field entered in the subsoil, the intensity of the secondary will be the higher the higher the conductivity σ of the soil. In addition, secondary electromagnetic field intensity also depends on the distance between P and S, and the frequency of the signal. The resulting field, detected and recorded by S, measured two components, one in quadrature and one in phase, compared to the field

produced by the coil P. Using the quadrature component, is possible to determine the electrical conductivity of the soil volume. The relationship between the magnetic field and the primary one, depends on whether the two coils are placed in vertical or horizontal configuration. Those H_s and H_p induction fields supported by primary and secondary coils, it is possible to prove that the apparent soil conductivity is proportional to their relationship according to equation (1):

$$\sigma_a = \frac{4}{w\mu_0 r^2}\left(\frac{H_s}{H_p}\right) \tag{4.20}$$

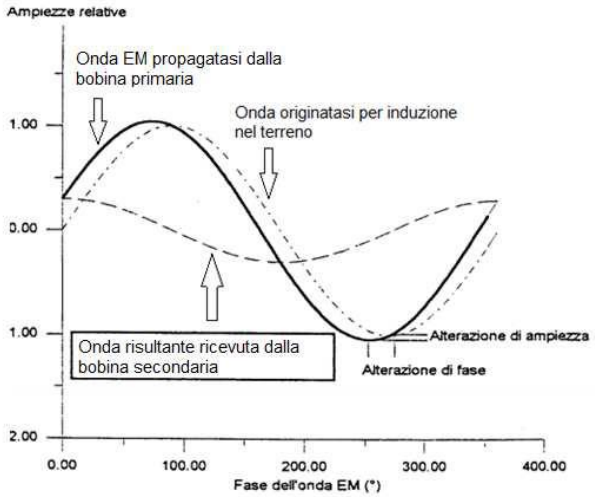

Fig. 4.32. Composition of the resulting wave as field effect produced by the sensor and reaction product from the ground due to the eddy currents induced.

4.6.2 Ground monitoring.

The physical phenomena at the basis of mutual coupling between solenoids are well known in the scientific literature. examples of systems that use mutually coupled coils are multiple and recurrent cases suggest power and measurement transformers, sensors and transducers. On the other hand also the resonance phenomenon is well-known. In measuring systems often make use of the words sensitivity and noise immunity. Specifically to appreciate small changes in measuring, you want the measuring device is very sensitive. On the other hand

you also want that the measuring device is sensitive only to variations of the object under test and is not influenced by external factors that could disguise and confuse the information itself. In other words, you want the device is immune against those named, disorders or lack of information sources. As well known by means of physical laws describing electromagnetic phenomena, a solenoid set in a time-varying magnetic field, shows an induced electromotive force proportional to the derivative of the flux concatenated, and the coefficient of proportionality is a function of the number of turns of the solenoid. Therefore, in reference to the application, in the receiving coil are induced electromotive forces of different nature and therefore unwanted. For these reasons, have a system that is only sensitive to inputs of interest and not able to collect different inputs from desired ones, appears to be desirable. For this purpose, the phenomenon of resonance allows to reach the goal. Making the system consisting of resonant coupled coils, is possible to obtain high sensitivity and noise immunity. The high sensitivity is ensured by the fact that the system has a coefficient of amplification, ideally infinite, in practice very high, only at resonance frequency. So it is sufficient a small amplitude stimulation at that precise frequency to trigger high induced electromotive forces. Noise immunity is guaranteed by the fact that, unless the noise is tuned exactly at the resonant frequency, or moves a little around it, it is automatically filtered by the system itself, as it is not sensitive to sources tuned at a different frequency than the resonance.

4.6.3 two coupled coils setup.

In this first hypothesis, the test has been focused on defining a first approach, based on an architecture that uses two coils in vertical configuration. These are a primary coil, which traveled from an alternating current produces a time-varying primary magnetic field and a secondary coil that concatenates with part of the magnetic field from these resulting, sum of primary magnetic field and secondary magnetic field.

Focusing on the physics of the problem, in the absence of conductive ground, the field detected by secondary winding, is perfectly in phase with the field produced by the primary coil, but is mitigated by an amount that depends on the distance between the two coils. In this case the secondary coil is crossed by field lines produced by the primary coil, that are able to concatenate it.

In the presence of a conductive floor, because of induction phenomena, the concatenated field from the secondary coil, presents alterations than the previous case. Approaching the primary coil to the ground, the primary field, induces eddy currents, directly proportional to the apparent soil electrical conductivity. These currents produce a magnetic field that is directly proportional to the currents that produced it. Therefore, the secondary magnetic field, and therefore also its geometric components of phase and quadrature, are a function of apparent soil electrical conductivity investigated.

The resulting field, sum of the primary field and the secondary one, is, what is to be chained by the secondary coil. It differs from the primary magnetic field in amplitude, phase and direction. Through the information thus collected in indirectly possible to estimate the apparent soil electrical conductivity.

With further detail, in the primary coil is injected a sinusoidal alternating current, with pulse ω and intensity I_p. This current is responsible for the primary magnetic field, which concatenates, in addition to the primary coil itself, in part through the secondary winding, and in part through the ground.

Due to the presence of conductive carriers into the soil, it will be the induced electromotive forces at same pulse but with phase delay relative to the primary magnetic field. As a result, soil induced eddy currents are responsible for a secondary magnetic field shifted a quantity Φ with respect to the primary magnetic field. This displacement depends on the electrical properties of the soil.

The total phase difference between the primary and secondary field, is derived from the sum of the two phase delays. The combination of the primary field and subfield is called resulting field this field is harvested from the secondary coil.

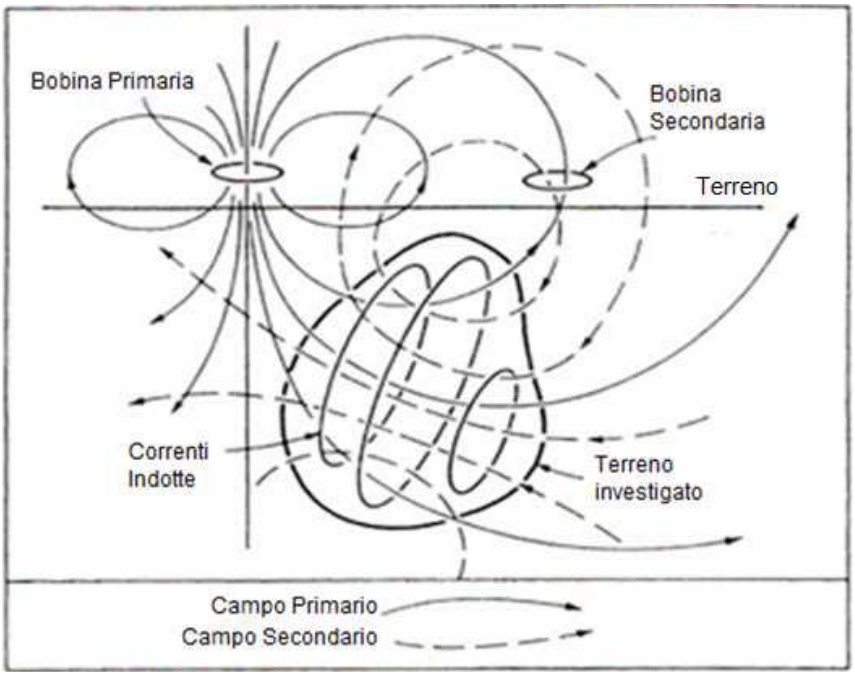

Fig4.33. Fild line composition for two coupled coil setup. The secondary coil detect the filed reaction in soil presence.

The primary field H_p, generated by the sinusoidal current I_p that circulates in the primary coil, can be expressed by the equation (4.21):

$$H_p = kI_p = kI_p sen(wt) \tag{4.21}$$

Where k depends on the geometry of the coil.

The electromotive force induced in soil, or in a conducting body immersed in it is given by:

$$e_s = -M\frac{dI_p}{dt} = -wMI_{po}\cos(wt) = -j\frac{wMH_p}{k} \tag{4.22}$$

This electromotive force, produces Eddy currents inversely proportional to the resistance R_s and inductance L_s, as follows:

$$i_s = \frac{e_s}{r_s + jwL_s} \tag{4.23}$$

This current produces a secondary H_s magnetic field, superimposed on the primary Hp, which can be seen from the secondary coil.

$$H_s = -\frac{kjwMH_p}{k(r_s + jwL_s)} \tag{4.24}$$

with

$$Q = \frac{wL_s}{r_s} \tag{4.25}$$

By combining the previous equations is obtained (4.26):

$$H_s = -\frac{kMH_p(Q^2 + jQ)}{kL_s(1+Q^2)} \tag{4.26}$$

Secondary field is then in advance of an angle between 90° and 180° with respect to the primary. This phase shift is equal to 180° when nothing resistivity. Otherwise the value tends to 90°. The amplitude of the quadrature phase component is therefore a measure of resistance. It can be shown that if the distance between primary and secondary windings is large, compared to the diameter, then the electrical conductivity σ by a homogeneous and isotropic conductive space is given by:

$$\sigma_a = \frac{H_s}{H_p}\frac{4}{w\mu_0 s^2} \tag{4.27}$$

4.6.4 three coupled coils setup.

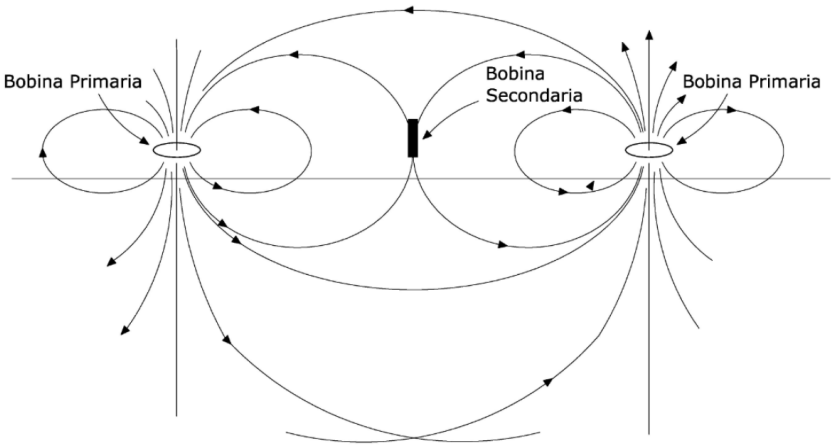

Fig. 4.33. Three coils setup with no soil presence. The half orthogonal coil concatenates only with soil field reaction.

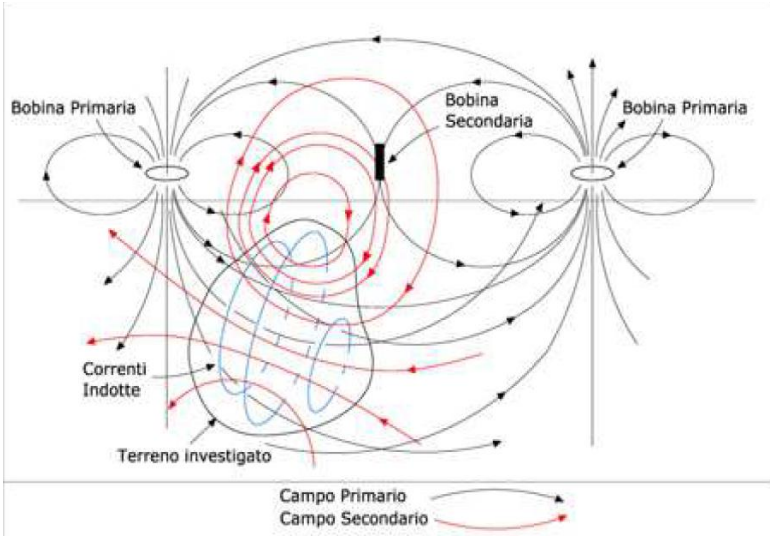

Fig. 4.34. Three coils setup with soil reaction presence.

At this stage, the authors propose a different system configuration, in reference to the number and arrangement of the coils. The primary coil is a pair of series-connected coils vertically disposed. These two coils are responsible for the primary magnetic field. The secondary coil is placed centrally in relation to the primary coils, in horizontal position and thus, orthogonal to the primary coils. In

this way, the geometry prevents the secondary coil may be sensitive to primary field. In fact, it can only collect the secondary field, generated as a result of the reaction induced in soil from the primary magnetic field. With this configuration, in the absence of soil, or soil dielectric, there is no voltage across the secondary coil. For this reason, the effect of the primary field on the secondary winding is cancelled. With this configuration, the secondary coil is sensitive only to the secondary magnetic field produced by the land, unlike the previous point application, for which the secondary coil is sensitive to a resulting magnetic field, combination of primary magnetic field and the magnetic field produced by the soil reaction.

4.6.5 two coils and three coils compare

In this section, the authors have prepared a prototype of the system discussed in point A, which uses two coils. The first generates the field and the second who picks it up. The two coils are cylindrical spiral wound, the geometry is guaranteed by plastic supports of the same size. The distance between the two coils is equal to 50 cm. The primary coil is made of 1.5 mm^2 insulated cable and consists of 30 turns, diameter 13 cm and 10 cm length. The secondary coil counts 200 turns, with insulated copper wire by 0.5 mm^2 from the same geometric dimensions.

The system can be described as an in air transformer, devoid of ferromagnetic core. The secondary coil is part of a parallel RLC resonant circuit. The resistance R is related to connecting wires, while the capacity C is obtained by means of a decades variable capacitor. The power source is a function generator, whose signal is sent to a power amplifier, which has as load the RLC resonant system. The system is supplied with a sinusoidal signal at a resonance frequency, of 16850 Hz.

The secondary coil is connected to an oscilloscope, then on a high impedance load. Tests showed that: the difference between absence of ground conductor, and presence of ground conductor, translates into a change in phase and

amplitude of the detected signal on the secondary winding extremely small; therefore in this configuration it is possible to obtain a very limited sensitivity.

Fig 4.35. Two coils setup arrangement during test and prototyping operations.

With the three coils configuration, without conductive soil, across the secondary coil no signal is detected, being parallel to the field lines. In the presence of conductive soil, is considerably measured a waveform attenuated in amplitude than that measured on the primary coils and phase delayed. With this configuration it is possible to detect more easily the presence of conductive soil.
To verify, in principle, the functionality of the proposed method, the coil system was slid on a voluntarily damp ground. There has been a change in the amplitude and phase of the signal detected across the secondary coil, at least, suitable for a subsequent processing and interpretation of the information contained within.

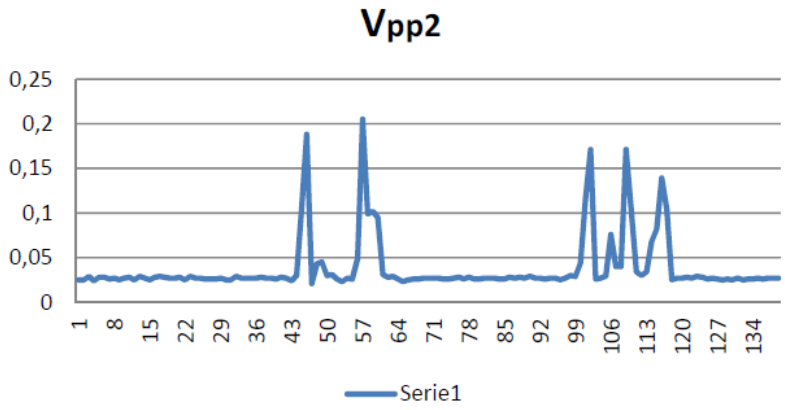

Fig. 4.36. Voltage measured across the sensing coil while moving the system on different soil conditions.

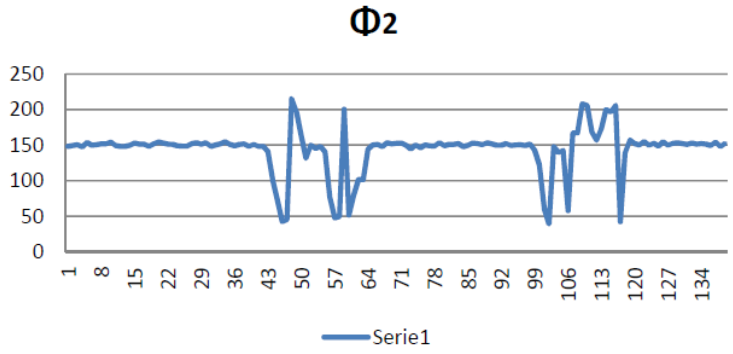

Fig 4.37. Phase shift on the sensing coil, with reference to primary coil phase, moving the system on different soil condition.

4.7 A mid-range four coil proposal.

In this paragraph are analysed various relevant parameters for a resonant 4 coils system, in particular looking at how some of these parameters affect the performance of the entire system and the performance of the connection. Theoretical calculation of the performance, which will be compared with experimental results obtained for two coils are used theories: "Reflected load theory" and "Coupled mode theory". These methods, compared lead to the same set of equations.

4.7.1 A practical four coil coupled system.

Are now shown several four coils systems calculating efficiency, referring to different geometries, different distances, in order to understand the strengths and weaknesses of the system. Analyzing a first case in which resonant coils are about 16.8 cm in diameter and the exciters of 5.2 cm. All coils are made with copper windings, their dimensions are shown in table 4.7.

	BOBINE 1 e 4	BOBINE 2 e 3
DIAMETRO BOBINE (cm)	5.2	16.8
DIAMETRO CONDUTTORE (mm)	0.64	0.87
NUMERO DI AVVOLGIMENTI	2	4
SPAZIO TRA GLI AVVOLGIMENTI (mm)	0.1	0.26

Tab. 4.7: geometrical parameter of the four coil system.

Resonant coils have an estimated inductance at about 5.25 µH and an estimated 29 pF parasitic capacitance. Then the resonant frequency is equal to 12.88 MHz. To ensure that the energy transfer is efficient, exciters coils are placed within larger ones, which are the real responsible for energy transmission. To further improve the transmission power, capacitor may be connected in parallel to the coils exciters, so tune the 4 coils on the same frequency. Note section and cable

length, the estimated resistance of the coils can be calculated and thus the merit factors.

Results are: Q_1 = Q_4 = 172 e Q_2 = Q_3 = 591.

In the following coupling factors k_{13}, k_{14}, k_{24} have been neglected. The ones calculated are instead, k_{12}, k_{34}, equal to 0.09.

The coupling factor of resonant coils can be estimate by means of the (4.28) for coplanar geometry.

$$k(x) \cong \frac{r_p^2 r_s^2 \cos\alpha}{\sqrt{r_p r_s}\left(\sqrt{x^2 + r_s^2}\right)^3} \qquad (4.28)$$

Where r_p and r_s are respectively the primary and secondary coils radius, α is the angle between the two coils and x the distance between the centres of the same.

This expresses the coupling coefficient as a function of the radius r of the coils and the distance x between them. Figure 4.38 shows how this decay very rapidly with increasing distance and reaches a value close to zero when this is approximately 50 cm.

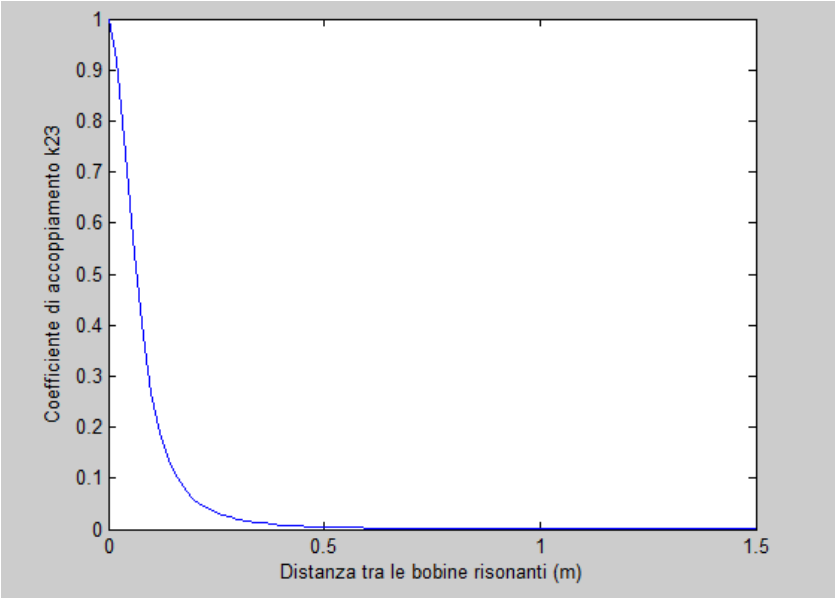

Fig. 4.38: Coupling factor varying the distance.

If the exciter coil is energized to resonance pulsation, and a 100 Ω load is connected to the receiving one, using the above equations the efficiency of the system can be obtained.

Figure 4.39 shows as the efficiency takes maximum value when the two resonant coils are placed at a distance of about 35 cm. At this distance, a four coils system, has a theoretical efficiency of about 50%.

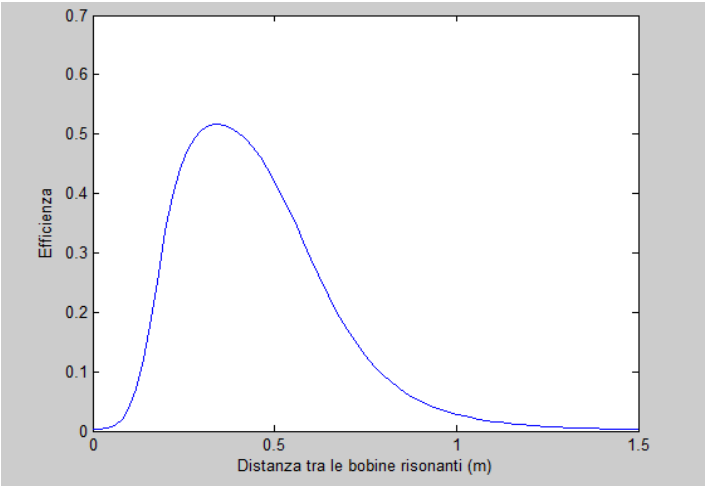

Fig. 4.39: Effyciency for a four coil system.

A four coil system is preferable when the energy transfer must take place at a determined distance. In the case of intimate distance two coils systems are more efficient.

For a two coils system with radius 16.8 cm, made with copper conductors, efficiency varies with distance as shown in Figure 4.40. Such a system is efficient only for short distances, on the contrary is the case of four systems.

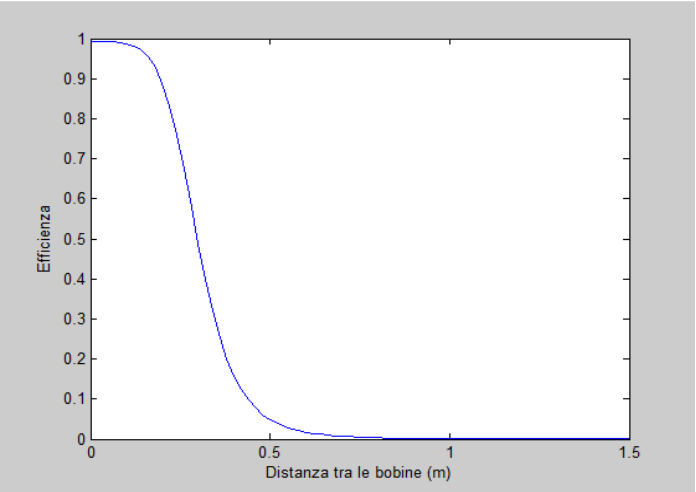

Fig. 4.40: Efficiency for a two coil system.

So two coils systems are desirable for short distances applications.

Therefore a WPT system that has to work for distance lass than 30 cm is more efficient if done with only two coils. For longer distances, the same size, the best choice is a four coil system.

To further increase the optimal distance of transmission, it is necessary to increase the size of the system, in particular, by acting on the radius of the coils. Considering a system geometrically increased, we examine the case of coils with a diameter of 12 cm and exciters resonant coils with a diameter of 40 cm.

By increasing the size of the coils the value of inductance increases and thus the resonant frequency decreases. The resonance frequency of the system is 5.08 MHz. Table 4.6 lists the other parameters. As can be seen the merit factor is increased and this improves the performance, although it tends to make the system more frequency selective and thus more difficult to tune.

	BOBINE 1 e 4	BOBINE 2 e 3
DIAMETRO BOBINE (cm)	12	40
DIAMETRO CONDUTTORE (mm)	0.7	1.5
NUMERO DI AVVOLGIMENTI	2	4
INDUTTANZA (μH)	0.896	13.426
FATTORE DI MERITO	143	688

Tab. 4.6: Parameters for a four coil system.

In this test is used a identical load to the previous example. The determination of coupling coefficients is performed in a similar manner. It is expected that using larger coils, a peak of the efficiency value at a greater distance is obtained. This is ensured when the two coils are placed at a distance of about 85 cm. The trend of efficiency as a function of distance is shown in Figure 4.41.

It is recalled that, in addition, the distance can be highly improved by decreasing the frequency of the system, or what is the same, increasing the wavelength.

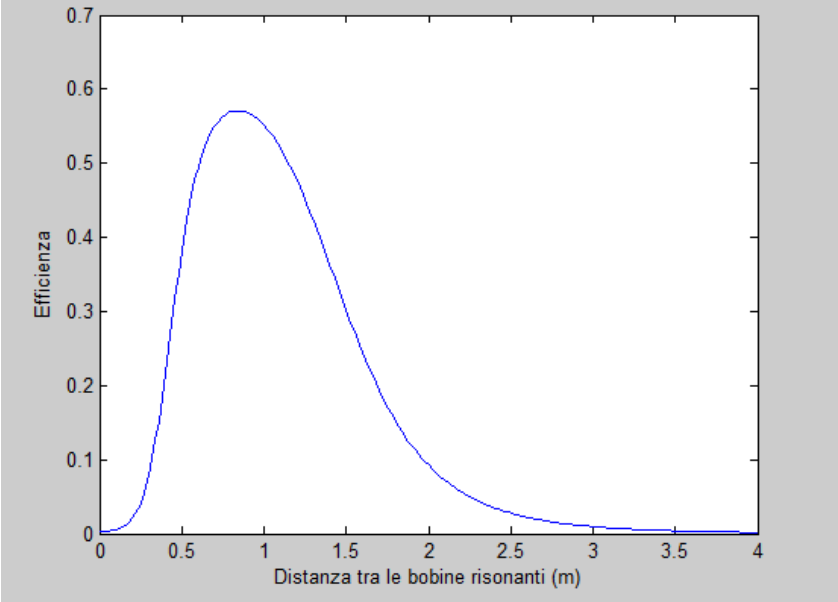

Fig. 4.41: efficiency for a fuor coil system.

To obtain a lower resonance frequency, it is necessary to increase the value of the capacitor or inductor. The first can be increased by connecting a capacitor in parallel to the coil, obviously the capacitors to be connected at two resonant coils must be identical so the resonance frequencies remain the same for both. Although from a theoretical point of view this may be a good solution, when implemented a great precision in the choice of the value of the capacitors is required. To increase the inductance can be operated on the winding number increasing it. This creates a dual effect, in fact, besides the inductance, also acts

on the coil resistance. An increase in resistance and a decrease in the work frequency, can lower the merit factor, reducing efficiency. Figure 4.42 shows the plot of efficiency as a function of distance, for 4, 8 and 16 coils systems. It can be seen that the maximum value decreases as the number of turns, and then obtained to greater distances. Increase the number of windings may also be inappropriate in terms of size and therefore cannot be used for certain applications.

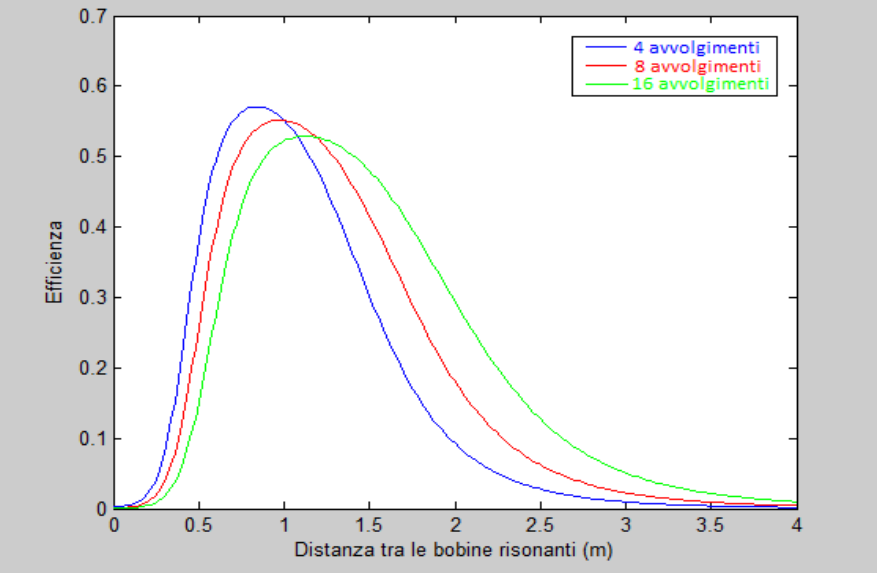

Fig. 4.42: Efficiency for multi coil systems.

Ultimately, the windings case characterised by sufficiently large diameters is presented. The size of the system are shown in table 4.7.

	BOBINE 1 e 4	BOBINE 2 e 3
DIAMETRO BOBINE (cm)	20	80
DIAMETRO CONDUTTORE (cm)	0.3	1
NUMERO DI AVVOLGIMENTI	2	8
SPAZIO TRA GLI AVVOLGIMENTI (cm)	0.5	3

Tab. 4.7: Dimensions of the adepted coils.

The system is more efficient for greater distances than previous cases, this is due mainly to the increase in the size of the windings. Although this system is efficient in applications not within striking distance, its use may be difficult because of the special geometry, and specifically, because of substantial size. In the literature are not present, explicitly, notions about the design of the devices of the type mentioned, nor are available analytical models that well approximate the actual behaviour of windings characterised by these dimensions. In reference to the calculation of the inductance and the parasitic capacitance, it is necessary to combine analytical procedure to a series of analysis and experimental validation, being the data obtained via modelling, distant from reality. Factors influencing the quality of equations described above and employed, are many and it is complicated both mention that quantify the burden on the overall result. Anyway, definitely one of the factors that most influence the result is the steady state equivalent resistance that the conductor shows at high frequencies. The problem appears even more emphasized by the special shape, characteristic of the conductor. In fact, both in reference to the skin effect, both for purposes of simplicity, but also for technical reasons such as the need to dissipate the heat produced by the high currents often copper pipe conductors cables are employ. That is why the calculation of equivalent resistance, which greatly influence the final value of the merit factor, does not appear so straightforward and simple. These analytically calculated values lead, therefore, to have merit factors much bigger that the expected. The efficiency plot as a function of the distance between the coils is shown in Figure 4.43. Although the maximum efficiency in reality takes smaller values, the efficiency peak is achieved for longer distances than previously analyzed. The maximum efficiency is achieved when the distance between the coils is 2.15 metres.

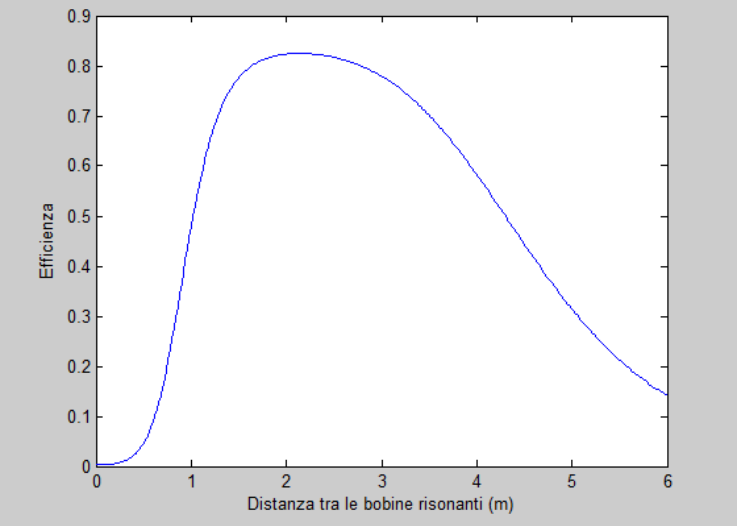

Fig. 4.43: Efficiency for a four coil system.

Conclusions:

In this work were reviewed various issues concerning the supply of electrical and electronic equipment in presence of not wired physical scenarios have been reviewed. Possible solutions have been examined, in particular, the WPT solution one. Different technologies have been analysed, with particular attention to resonant inductive type, examining applications and study approaches, as well as the pros and cons.

Different prototypes have been studied, time after time, simulated designed and manufactured; these prototypes made possible the use of several methods of characterization. Finally an application, based on the same technology, for sensing purposes, specifically ground monitoring, has been optimized.

List of publications:

[1] L. Angrisani, G. d'Alessandro, M. D'Apuzzo, M. D'Arco, 'Wireless Power Transmission Technology for Contactless Recharging and Batteryless Supply,' Journal of Energy Challenges and Mechanics, Volume 1 (2014), issue 4, article 2; available on line: http://www.nscj.co.uk/JECM/JECM1-4.html.

[2] Baccigalupi, G. d'Alessandro, M. D'Arco, R. Schiano Lo Moriello, 'Least square procedures to improve the results of the three-parameter sine-fitting algorithm,' june 2015, volume 4, numero 2, p 100-106.

[3] L. Angrisani, G. d'Alessandro, M. D'Apuzzo, M. D'Arco, 'Enabling induction and wireless power transmission technologies aimed at supplying remote equipment in critical logistic scenarios,' IEEE Workshop on Measurement & Networking, 7-8 Oct 2013, Naples, ITALY, pp. 184-188.

[4] L. Angrisani, G. d'Alessandro, M. D'Arco, D. Accardo, G. Fasano, 'A Contactless Induction System for Battery Recharging of Autonomous Vehicles,' IEEE Workshop on Metrology for Aerospace, 29-30 May 2014, Benevento, ITALY.

[5] L. Angrisani, F. Bonavolontà, G. d'Alessandro, M. D'Arco, 'Inductive power transmission for wireless sensor networks,' IEEE Workshop on Environmental, Energy and structural Monitoring Systems, 17-18 September 2014, Napoli, ITALY.

[6] Leopoldo Angrisani, Guido d'Alessandro, Mauro D'Arco, 'An experimental energy set-up for wireless battery recharging,' IEEE International Instrumentation and Measurement Conference I2MTC 2015, , 11-14 May 2015, Pisa, ITALY.

[7] Guido d'Alessandro, Mauro D'Arco, Michele Vadursi – "Measuring Transmission Line Parameters in the Frequency Domain". Atti dell'I2MTC International Instrumentation and Measurement Technology Conference. 6 – 9 Maggio 2013, Minneapolis (MN).

References:

[1] Q. Xi, Z. Gao, H. Wang, J. He, Z. Mao, M. Sun, "Batteries Not Included", *IEEE Microwave Magazine*, Vol.14, No.2, 2013, pp. 63-72.

[2] K. Na, H. Jang, S. K. Oruganti, F. Bien, "An Improved Wireless Power Transfer System with Adaptive Technique for Implantable Biomedical Devices," IEEE MTT-S International Microwave Workshop Series on RF and Wireless Technologies for Biomedical and Healthcare Applications (IMWS-BIO), 9-11 Dec. 2013, Singapore, pp.1-3.

[3] Al-Kalbani, M. R. Yuce, J. M. Redouté, "A Biosafety Comparison Between Capacitive and Inductive Coupling in Biomedical Implants", *IEEE Antennas and Wireless Propagation Letters*, Vol.13, 2014, pp. 1168-1171.

[4] Zhang, S. A. Hackworth, X. Liu, J. Sclabassi, M. Sun, "Wireless Power Transfer System Design for Implanted and Worn Devices", IEEE 35th Annual Northeast Bioengineering Conference 2009, 3-5 Apr. 2009, Boston MA, pp.1-2.

[5] R. Jegadeesan, Y. Guo, M. Je, "Electric Near-Field Coupling for Wireless Power Transfer in Biomedical applications", IEEE MMT-S International Microwave Workshop Series on RF and Wireless Technologies for Biomedical and Healthcare Applications (IMWS-BIO) 9-11 Dec. 2013, Singapore, pp.1-3.

[6] Q. Wang, H. Li, "Research on the wireless power transmission system based on coupled magnetic resonances," Electronics, Communications and Control Conference (ICECC) 2011, 9-11 Sep. 2011, Ningbo, pp.2255-2258.

[7] R. Xue, K. Cheng, M. Je, "High-Efficiency Wireless Power Transfer for Biomedical Implants by Optimal Resonant Load Transformation," *IEEE Transactions on Circuits and System*, Vol. 60, No. 4, 2013, pp. 867-874.

[8] L. Angrisani, G. d'Alessandro, M. D'Apuzzo, M. D'Arco, "Wireless Power Transmission Technology for Contactless Recharging and Batteryless Supply," Journal of Energy Challenges and Mechanics, Volume 1 (2014), issue 4, article 2; available on line: http://www.nscj.co.uk/JECM/JECM1-4.html.

[9] N. Kemal Ure, Girish Chowdhary, Tuna Toksoz, Jonathan P. How, Matthew A. Vavrina, and John Vian "An Automated Battery Management System to Enable Persistent Missions With Multiple Aerial Vehicles" *IEEE Transactions on Mechatronics*, DOI: 10.1109/TMECH.2013.2294805.

[10] Bhaskar Saha1, Edwin Koshimoto, Cuong C. Quach, Edward F. Hogge, Thomas H. Strom, Boyd L. Hill, Sixto L. Vazquez, Kai Goebel, "Battery Health Management System for Electric UAVs" IEEE Aerospace Conference, 5-12 March 2011, Big Sky, MT, USA, pp.1-9.

[11] Kurs, A. Karalis, R. Moffatt, J. D. Joannopoulos, P. Fisher, and M. Soljačić, "Wireless power transfer via strongly coupled magnetic resonances," *Science*, 2007, Vol. 317, No.5834, pp. 83–86.

[12] Karalis, J. D. Joannopoulos, and M. Soljačić, "Efficient wireless non-radiative mid-range energy transfer," *Annals of Physics*, Jan. 2008, Vol.323, No.1, pp. 34–48.

[13] Aristeidis Karalis, J.D. Joannopoulos, Marin Soljacˇic, "Efficient wireless non-radiative mid-range energy transfer", *Annals of Physic,* Vol.323, No.1, 2008, pp.24-48.

[14] W. Fu, B. Zhang, "Study on Frequency-tracking Wireless Power Transfer System by Resonant Coupling," IEEE Power Electronics and Motion Control Conference. IPEMC 2009, 17-20 May 2009, Wuhan, pp.2658-2663.

[15] Akira Oida, Hiroshi Nakashima, Juro Miyasaka, Katsuaki Ohdoi, Hiroshi Matsumoto, Naoki Shinohara "Development of a new type of electric off-road vehicle powered by microwaves trasmitted through air". ScienceDirect, *Journal of Terramechanics*. 44 (2007) 329-338.

[16] Y. Zhang, Z. Zhao, K. Chen, "Frequency Splitting Analysis of Magnetically-Coupled Resonant Wireless Power Transfer", Energy Conversion Congress and Exposition (ECCE), 2013, pp. 2227-2232.

[17] P. Sample, D. A. Meyer, and J. R. Smith, "Analysis, Experimental Results, and Range Adaptation of Magnetically Coupled Resonators for Wireless Power

Transfer," *IEEE Transactions on Industrial Electronics*, 2011, Vol.58, No.2, pp.544-554.

[18] L. Cannon, J. F. Hoburg, D. D. Stancil, and S. C. Goldstein, "Magnetic Resonant Coupling As a Potential Means for Wireless Power Transfer to Multiple Small Receivers," *IEEE Trans. Power Electron.*, 2009, Vol.24, No.7, pp. 1819–1825.

[19] Gregg E. Maryniak, "Status of International Experimentation in Wireless Power Transmission" *Solar Energy* Vol.56, No.1, 1996, pp 87-91.

[20] William C. Brown, "The History of Wireless Power Transmission," *Solar Energy*, Vol. 56, No.1, 1996, pp. 3-21.

[21] Lee, B. H. Waters, C. Shi, W. S. Park, J. R. Smith, "Design Considerations for Asymmetric Magnetically Coupled Resonators used in Wireless Power Transfer Applications" IEEE Radio and Wireless Symposium (RWS) 2013, 20-23 Jan. 2013, Austin TX, USA, pp. 28-30.

[22] L. Angrisani, G. d'Alessandro, M. D'Apuzzo, M. D'Arco, "Enabling induction and wireless power transmission technologies aimed at supplying remote equipment in critical logistic scenarios," IEEE Workshop on Measurement & Networking, 7-8 Oct 2013, Naples, ITALY, pp. 184-188.

[23] J. Kim, H. Son, K. Kim, Y. Park, "Efficiency Analysis of Magnetic Resonance Wireless Power Transfer With Intermediate Resonant Coil," *IEEE Antennas and Wireless Propagation Letters*, Vol.10, 2001, pp.389-392.

[24] Silvano Cruciani1, Tommaso Campi, Francesca Maradei and Mauro Feliziani. "Numerical Simulation of Wireless Power Transfer System to Recharge the Battery of an Implanted Cardiac Pacemaker", *Proc. of the 2014 International Symposium on Electromagnetic Compatibility (EMC Europe 2014), Gothenburg, Sweden, September 1-4, 2014.*

[25] Costanzo, M. Dionigi, F. Mastri, M. Mongiardo, "Rigorous modeling of mid-range wireless power transfer systems based on Royer oscillators," *IEEE Wireless Power Transfer* (WPT) *Conference* 2013, May 15-16, Perugia, Italy, pp.69-72.

[26] L. Angrisani, G. d'Alessandro, M. D'Arco, D. Accardo, G. Fasano, "A Contactless Induction System for Battery Recharging of Autonomous Vehicles," IEEE Workshop on Metrology for Aerospace, 29-30 May 2014, Benevento, ITALY.

[27] L. Angrisani, F. Bonavolontà, G. d'Alessandro, M. D'Arco "Inductive power transmission for wireless sensor networks," IEEE Workshop on Environmental, Energy and Structural Monitoring Systems, 17-18 September 2014, Napoli, ITALY.

[28] Yoichi Kurose, Eiji Hiraki, Akito Fukui, and Mutsuo Nakaoka, "Phase Shifted ZVS-PWM High Frequency Load Resonant Inverter for Induction Heated Foam Metal Type Dual Packs Fluid Heater", IEEE Industrial Electronics Conference IECON 2003, 2-6 Nov. 2003, Vol.2, pp.1613-1616.

[29] Alireza Namadmalan, Javad Shokrollahi Moghani, and Jafar Milimonfared, "A Current-Fed Parallel Resonant Push-Pull Inverter with a New Cascaded Coil Flux Control for Induction Heating Applications" *Journal of Power Electronics*, Vol. 11, No. 5, September 2011.

[30] UYaisom, W. KJmmgern and S. Nitta, "The Study and Analysis of The Conducted EMI Suppression on Power MOSFET Using Passive Snubber Circuits" 3rd International Symposium on Electromagnetic Compatibility, 2002 , pp.561-564.

[31] H. Waters, A. P. Sample, J. R. Smith, "Powering a Ventricular Assist Device (VAD) With the Free-Range Resonant Electrical Energy Delivery (FREE-D) System", *Proceedings of the IEEE*, Vol.100, No.1, 2012, pp.138-149.

[32] Jiang, P. Brazis, M. Tabaddor, J. Bablo, "Safety Considerations of Wireless Charger For Electric Vehicles – A Review Paper", IEEE Symposium on Product Compliance Engineering (ISPCE), 5-7 Nov. 2012, Portland OR, USA, pp.1-6.